UNIVERSIDADE ESTADUAL DE CAMPINAS

INSTITUTO DE QUÍMICA

DOUGLAS HIDEKI NAKAHATA

SYNTHESIS, CHARACTERIZATION AND BIOACTIVITY OF COPPER(II) COMPLEXES WITH N-HETEROCYCLES

SÍNTESE, CARACTERIZAÇÃO E BIOATIVIDADE DE COMPLEXOS DE COBRE(II) COM N-HETEROCICLOS

CAMPINAS
2016

DOUGLAS HIDEKI NAKAHATA

SYNTHESIS, CHARACTERIZATION AND BIOACTIVITY OF COPPER(II) COMPLEXES WITH N-HETEROCYCLES

SÍNTESE, CARACTERIZAÇÃO E BIOATIVIDADE DE COMPLEXOS DE COBRE(II) COM N-HETEROCICLOS

Master's thesis presented to the Institute of Chemistry of the University of Campinas as part of the requirements to obtain the title Master's in Chemistry in the area of Inorganic Chemistry.

Supervisor: Prof. Dr. André Luiz Barboza Formiga

THIS COPY CORRESPONDS TO THE FINAL VERSION OF THE MASTER´S DISSERTATION DEFENDED BY DOUGLAS HIDEKI NAKAHATA AND SUPERVISED BY PROF. DR. ANDRÉ LUIZ BARBOZA FORMIGA.

CAMPINAS
2016

Agência(s) de fomento e nº(s) de processo(s): CNPq, 131013/2014-9

Ficha catalográfica
Universidade Estadual de Campinas
Biblioteca do Instituto de Química
Danielle Dantas de Sousa - CRB 8/6490

N163s

Nakahata, Douglas Hideki, 1991-
Synthesis, characterization and bioactivity of copper(II) complexes with N-heterocycles / Douglas Hideki Nakahata. – Campinas, SP : [s.n.], 2016.

Orientador: André Luiz Barboza Formiga.
Dissertação (mestrado) – Universidade Estadual de Campinas, Instituto de Química.

1. Complexos metálicos. 2. Cobre. 3. Bioatividade. I. Formiga, André Luiz Barboza. II. Universidade Estadual de Campinas. Instituto de Química. III. Título.

Informações para Biblioteca Digital

Título em outro idioma: Síntese, caracterização e bioatividade de complexos de cobre(II) com N-heterociclos
Palavras-chave em inglês:
Metal complexes
Copper
Bioactivity
Área de concentração: Química Inorgânica
Titulação: Mestre em Química na área de Química Inorgânica
Banca examinadora:
André Luiz Barboza Formiga [Orientador]
Ana Maria da Costa Ferreira
Wdeson Pereira Barros
Data de defesa: 26-02-2016
Programa de Pós-Graduação: Química

BANCA EXAMINADORA

Prof. Dr. André Luiz Barboza Formiga (Orientador)

Profa. Dra. Ana Maria da Costa Ferreira (IQ-USP)

Prof. Dr. Wdeson Pereira Barros (IQ-UNICAMP)

A Ata da defesa com as respectivas assinaturas dos membros encontra-se no processo de vida acadêmica do(a) aluno(a).

Este exemplar corresponde à redação final da Dissertação de Mestrado defendida pelo aluno **DOUGLAS HIDEKI NAKAHATA**, aprovada pela Comissão Julgadora em 26 de fevereiro de 2016.

I dedicate this dissertation to the few, but inspiring people who told me to pursue my dreams and keep going forward.

Dedico esta dissertação às poucas, porém admiráveis pessoas que me disserem para perseguir meus sonhos e seguir em frente.

“Stand alone and fight for the things you want,
you are the only ***Warrior*** *for your life.”*

“Whatever happens, ***Life Goes On****.*
Keep looking ahead and moving forward.”

- Hiromi Uehara, pianist.

Acknowledgements

To my mother, Tereza, who gave me birth and cared that I could study and pursue my dreams. You taught how strong a human being can be in order to overcome the challenges and obstacles life eventually imposes on us. Thank you so much!

To Prof. Dr. André L. B. Formiga, for the opportunity to join his research group and for all his time dedicated to guide and teach me. To Prof. Dr. Pedro P. Corbi, for his constant support during the development of this dissertation.

To Prof. Dr. Wdeson P. Barros and Prof. Dr. Juliano A. Bonacin for their contribution to my work in my qualification exam.

To Prof. Dr. Ana Maria da Costa Ferreira for her great contributions in my dissertation bench.

To Prof. Dr. Wilton R. Lustri and Prof. Dr. Marcelo Lancellotti and their respective research groups for the development of the experiments of antibacterial and antifungal activities of some of the compounds synthesized in this dissertation.

To Prof. Dr. Alexandre Cuin for his collaboration with powder diffraction measurements.

To members (both current and former) of LQC: Carol, Daniel, Helen, Irlene, Luiz, Mariana, Naheed, Naíma, Renan, Renata and Sabrina and especially to Eduardo, Marcos and Sergio, for all their help, advices and patience during different stages of my learning.

To the members of LQBM, especially to Nina and Enoque for their friendship and for the shared evenings performing experiments. I also thank Marcos Alberto for our talks, advices and companionship during the Saturdays we were working in the lab.

To my great friends Ana Thereza, Bruno Morandi, Danijela, Kalil, Marcio, Pãmyla and Vera for their companionship, for making the work days in the lab. so enjoyable and for the great days of laughter, eating and playing games.

To the lab. technitian Cintia Saito for all her support and for setting an example of efficiency. To all technitians from the institute: Cláudia, Sônia, Renata, Priscilla, Milene, Paula, Anderson, Gustavo, Raquel, Fabi and Déborah for performing the analyses and for the trainings.

To all members of CPG, especially Bel, Gabriela, Isabela and Janaína, for assisting me during all stages of my master's course.

To my friends from UEPG, Ageo, Alan, Ana, Bruna, Dhésmon, Jéssica, Rafael, Rodrigo, Tanna e Valdirene, for the years of friendship and for all the days of laughter.

To Prof. Dr. André V. C. de Andrade, for all the years teaching me during my undergraduate studies and to Prof. Dr. Mariza B. Marques, Prof Dr. Sandra R. M. Antunes and Prof. Dr. Augusto C. Antunes (*in memoriam*), for their teachings and life lessons.

To the greatest pianist there is, Hiromi Uehara and "*The Trio Project*", whose compositions inspire me constantly and for fulfilling my dream of going to their live concert in August, 2014.

To UNICAMP and the Chemistry Institute for allowing the development of this project. To CENAPAD for the computational time.

To CNPq (grant 131013/ 2014-9) for the scholarship.

RESUMO

Neste trabalho, foram investigadas a química de coordenação e bioatividade de complexos de cobre(II) com N-heterociclos contendo imidazol ou tetrazol em sua estrutura. A estrutura cristalina dos ligantes mostrou que a presença de ligações de hidrogênio entre os anéis imidazólicos ou tetrazólicos possui uma grande contribuição na determinação do seu empacotamento. Dados de difração de raios X mostraram que a geometria quadrada planar é adotada pelos complexos contendo ligantes bidentados ou monodentados, com fórmulas de coordenação $[CuCl_2(L)]$ e $[CuCl_2(X)_2]$, L = impy, impm and impz e X = thim, respectivamente. Análises elementares e de espectrometria de massas concordaram com as estequiometrias propostas. Técnicas espectroscópicas mostraram que a mudança do número ou posição de átomos de nitrogênio em um anel pode resultar em mudanças significativas nas propriedades eletrônicas e vibracionais tanto dos ligantes isolados quanto dos complexos. Os ligantes impy, impm e impz não mostraram atividade sobre *E. coli* e *S. aureus*, enquanto seus respectivos complexos, $[CuCl_2(impy)]$, $[CuCl_2(impm)]$ e $[CuCl_2(impz)]$, foram ativos contra estas cepas (MIC = 17.8 $\mu mol \cdot mL^{-1}$), mas sem distinção entre os complexos e a cepa testada, o que pode ser relacionado à carga dos complexos após a hidrólise dos cloretos. Experimentos biofísicos indicaram que o complexo *trans* $[CuCl_2(thim)_2]$ interage covalentemente com o DNA, um possível alvo molecular dos complexos e também mostrou atividade antifúngica sobre *Trichophyton mentagrophytes*.

ABSTRACT

The coordination chemistry and bioactivity profiles of copper(II) complexes with N-heterocycles containing imidazole and tetrazole in their structures have been investigated. The crystal structures of the ligands showed that hydrogen bonding between either the imidazole or the tetrazole rings has an important effect on determining their packing. Based on X-ray diffraction data, square planar geometry was proposed for the complexes containing bidentate or monodentate ligands with coordination formulas $[CuCl_2(L)]$ and $[CuCl_2(X)_2]$, L = impy, impm and impz and X = thim, respectively. Elemental analysis and mass spectrometry results were in agreement with the proposed stoichiometries. Spectroscopic techniques showed that changing either the number or position of nitrogen atoms in a ring can result in significant changes in the electronic and vibrational properties of both the isolated ligands and the complexes. The imidazolic ligands impy, impm and impz showed no activity over *E. coli* and *S. aureus*, whereas their respective complexes, $[CuCl_2(impy)]$, $[CuCl_2(impm)]$ and $[CuCl_2(impz)]$, showed some activity towards these strains (MIC = 17.8 $\mu mol \cdot mL^{-1}$), but with no distinction between the complexes and the tested strain, which may be due to the charge of the complexes after hydrolysis. Biophysical experiments showed that the *trans* complex $[CuCl_2(thim)_2]$ interacts covalently with DNA, a possible molecular target for this complex, and it also showed antifungal activity over the *Trichophyton mentagrophytes* strain.

SUMMARY

Chapter 1

Introduction

1.1. Metals in Medicine

Several transition metals are present in biological systems and some of them are essential for life. Medicinal inorganic chemistry is the field of knowledge that uses the fundamentals of inorganic chemistry for the therapy or diagnosis of diseases.[1]

The development of new metal complexes for the treatment of diseases rose exponentially after the discovery of the bioactivity of cisplatin (see Figure 1.1. (a)), by Barnett Rosenberg. Rosenberg found that cisplatin is capable of inhibiting cell division in *Escherichia coli* (*E. coli*).[2,3] Cisplatin is currently used worldwide for the treatment of several cancers and it is estimated that half of all patients that undergo chemotherapy are treated with a platinum compound.[4] Patients diagnosed with testicular cancer and treated with cisplatin have above 90 % chance of long-term survival rates.[1,5,6]

The main mechanism of action of cisplatin involves the hydrolysis of the chloride ions and subsequent covalent binding of the $[Pt(NH_3)_2]^{2+}$ moiety to either guanine or adenine residues of DNA (more specifically to the N-7 atom of either nucleotides), via interstrand or intrastrand cross-links. These adducts interfere in the normal cell division process, thus leading to apoptosis.[5,7–9]

Besides platinum, the use of several other metals in different oxidation states, geometries and with different ligands has been explored and resulted in many complexes with promising bioactivity.[1,6,10,11]

Gold(I) complexes, such as auranofin (Figure 1.1. (b)), have been used clinically used for the treatment of rheumatoid arthritis, though they were eventually

substituted by organic molecules due to side effects. The mechanisms of action of such gold complexes are still not completely elucidated.[1]

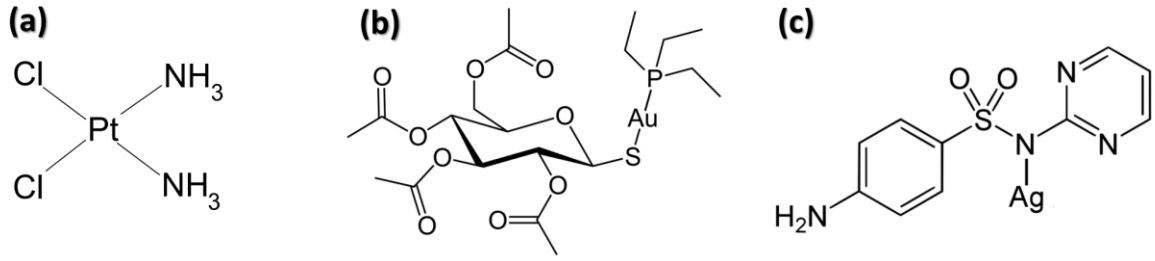

Figure 1.1. Chemical structures of (a) anticancer cisplatin (b) anti-rheumatoid arthritis auranofin and (c) antibacterial silver sulfadiazine.

Palladium(II) and gold(III) complexes are isoelectronic with the Pt(II) ion – d^8 electronic configuration – and have been investigated for the treatment of cancer, resulting in promising compounds, such as gold(III)-porphyrin[12] and gold(III)-dithiocarbamates complexes.[13]

Silver(I) compounds are widely reported as antibacterial agents. A clinical example of such a compound is silver sulfadiazine (Figure 1.1.(c)), used topically for the prevention of bacterial infection on burns. Silver ions have been reported to be bioactive via several mechanisms, including modification of mitochondrial structure[14] and interaction with biomolecules like DNA and enzymes involved in metabolism.[15]

Beyond these metals that have no reported biological function in organisms, essential metals have also been explored for the development of metallodrugs. Important examples include copper-based complexes. They have been investigated based on the fact that endogenous metals may be less toxic for normal cells than to cancer cells and on the fact that copper itself has antimicrobial effects.[16–18] More about copper (bio)chemistry and the use of its complexes for medicinal purposes is discussed on the next item.

1.2. Chemistry and biological aspects of copper

Copper is among the thirty most abundant elements in the earth's crust and it exists as two stable isotopes and nine radioactive isotopes. This element has played an important role in human history, as copper compounds have been used

extensively in a wide range of applications, including catalysis, agriculture as fungicides and as a pigment.[19,20]

Copper possesses a rich coordination chemistry. The most common oxidation states are I and II, the latter being the most abundant. Copper(I), of electronic configuration [Ar] $3d^{10}$, acts as a soft Lewis acid, so it forms complexes preferably with soft bases, such as phosphines and thiols. Cu(I) is easily oxidized to Cu(II) or it can disproportionate to Cu(0) and Cu(II). The copper(II) ion has a [Ar] $3d^9$ electronic configuration and it has a borderline acid character, which makes nitrogen, oxygen and chloride donors good ligands for Cu(II).[20–23]

As the other metal(II) ions from the first transition series, copper(II) forms complexes with a variety of coordination numbers, four, five and six being the most common (see Figure 1.2). However, the [Ar] $3d^9$ electronic configuration of Cu(II) is prone to the Jahn-Teller effect due to the degenerate e_g state (d_{z^2} and $d_{x^2-y^2}$ orbitals) an octahedral field would impose, leading to a variety of distorted structures.[19,22,24] This versatility of Cu(II) in forming coordination compounds results in more coordination complexes of this metal than of any other metal from the periodic table.[20,24]

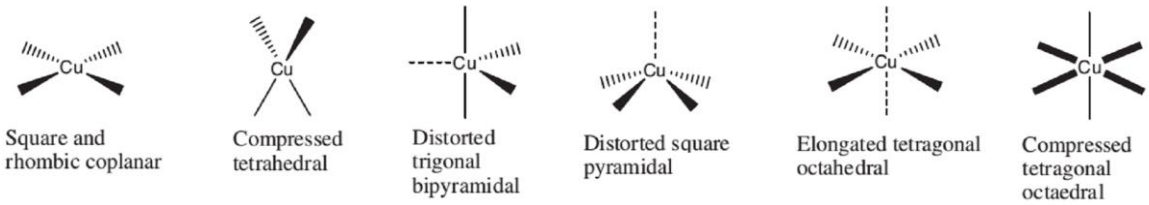

Figure 1.2. Examples of geometries of the most common coordination numbers adopted by copper(II) complexes. Adapted from reference [23].

The rich coordination chemistry of copper is also observed in nature. The presence of copper in biological systems dates to around 2 billion years ago, which is the time of rising oxygen levels in the atmosphere. This resulted in the overall oxidation of Cu(I) to the soluble and bioavailable Cu(II) ions. Concomitantly, the oxidative atmosphere resulted in Fe(II) oxidation to Fe(III), which is more insoluble due to the formation of $Fe(OH)_3$, which resulted in copper becoming more common in biological systems.[2,21,25]

Copper is an essential (trace) element in many organisms, as it is part of many enzymes.[23,26,27] The main ligands for copper in these cuproenzymes are the amino acid histidine, methionine and cysteine. The structural and redox versatility this metal possesses leads to a variety of enzymes with different functions, some of which are listed in Table 1.1.

Table 1.1. A small list of copper proteins and their functions. Adapted from reference [27].

Copper protein/ enzyme	Function
Electron transfer proteins	
Azurin	Electron transfer in respiration
Plastocyanin	Electron transfer in photosynthesis
Cytochrome c oxidase	Electron transfer in respiration
Oxidoreductases	
Ascorbate oxidase	Oxidation of ascorbate
Ceruloplasmin	Oxidation of Fe(II) to Fe(III)
Cu, Zn-SOD	Superoxide dismutation
Laccase, Tyrosinase	Oxidation of phenols
Nitrite reductase	Reduction of NO_2^- to N_2
Other	
Hemocyanin	Oxygen transport

Type I copper proteins usually have a role in electron transfer reactions. The copper center is coordinated to two histidine residues and to one sulfur from a methionine, in a trigonal planar geometry, with varying axial ligand. These proteins show a strong absorption around 600 nm, due to a charge transfer from sulfur to copper, which usually leads to a blue color. Thus, these type I enzymes are usually called blue copper proteins. Plastocyanin (Figure 1.3 (a)), an enzyme involved in electron transfer reactions in photosynthesis, is an example of a type I copper enzyme.

Type II copper centers in enzymes usually show a distorted square geometry, with the metal ion usually bound to nitrogen atoms from histidine residues, though oxygen donors are also observed. An example of enzyme from this class is Cu, Zn superoxide dismutase (see Figure 1.3 (b)). This enzyme was firstly reported in 1969 by Fridovich and McCord[28], the copper center is responsible for the dismutation of potentially harmful superoxide radical ions that result from metabolism, whereas zinc

plays a structural role. In this enzyme, the metal ions are bridged by an imidazolate ion.

Finally, type III copper containing enzymes show binuclear copper centers, with each metal bound by three nitrogens from histidine residues and coupled antiferromagnetically. These centers are found in some oxidases, such as tyrosinase, which participates in some steps on the conversion of L-tyrosine to melanin and in hemocyanin (see Figure 1.3 (c)). The latter is a protein responsible for oxygen transport in some invertebrate animals.[23,25,27]

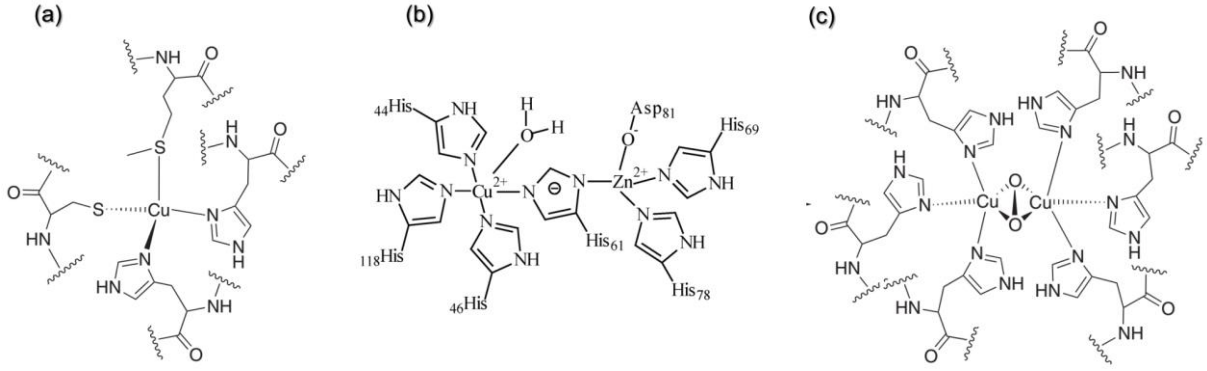

Figure 1.3. Active sites of copper(II)-containing proteins: **(a)** plastocyanin, **(b)** copper-zinc superoxide dismutase, **(c)** oxygenated form of hemocyanin. Adapted from references [27] and [29].

Ingested copper is mainly absorbed in the small intestine. Before entering the cells, the Cu(II) ions are reduced on their surfaces and transported across the cell membrane by the human copper transporter enzyme. Inside the cell, chaperones are responsible for copper trafficking, while glutathione and metallothioneins ensure that almost no free copper capable of redox cycling (and thus leading to cellular damage) is available. In the liver, copper is incorporated into ceruloplasmin, which contains six copper ions in its structure and acts as a ferroxidase. Excess copper is usually eliminated via biliary excretion.[17,23,30,31]

In the work by Rae et al., the authors showed that the cellular mechanisms of preventing oxidative damage by copper redox cycling are so efficient that the concentration of free copper in yeast cells is less than 10^{-18} mol·L^{-1}. By taking the cell volume into account, less than one free copper ion is present per cell.[32]

Contrary to the low sensitivity of human tissues to copper, microorganisms are much more susceptible to the toxic effects of this metal.[16,17,33] One of the first reports of the use of copper for the water sterilization dates 2200 B.C., from an ancient Egyptian medicinal text.[34]

The mechanisms of copper toxicity to microorganisms may involve the Cu(I)/ Cu(II) redox cycling, which is greatly avoided in human cells, as mentioned before. It is suggested that elevated copper concentrations leads to cell membrane damage via generation of free radicals, thus leading to leakage of intracellular components and to cell death. Copper can also interact with DNA via covalent or noncovalent (intercalation, groove binding and electrostatic) modes, depending on the structure of the ligand.[35] Oxidative DNA strand breakage may result, especially in the presence of reducing agents, which results in the generation of more Cu(I) and, consequently, of reactive oxygen species via a Fenton mechanism.[16,17,33]

However, non-Fenton chemistry has also been suggested as mechanisms of antibacterial activity of copper, and involves the Cu(I) ion. Copper in this oxidation state is absorbed by the cell. In anoxic conditions, the Cu(I) state is predominant and exhibits intense thiophilicity, which may disrupt key cytoplasmic iron-sulfur enzymes, resulting in disruption of bacterial metabolism.[21]

Currently, copper salts are extensively employed in agriculture. The use of copper salts as fungicides became more common with the use of a mixture of copper sulphate, lime and water called “Bordeaux mixture”, which is used to this date.[16,20] Metallic copper is used for the production of antibacterial door handles, bed rails, toilet seats, especially useful to prevent bacterial proliferation in hospitals.[34] Copper oxide nanoparticles were recently reported to be active over yeast with generation of reactive oxygen species and lipid peroxidation mechanisms.[36]

It is thus not surprising that other copper compounds, besides metallic copper and its simple salts, have also been investigated due to their antimicrobial activities. Copper(II) coordination complexes have been widely investigated not only for their antimicrobial properties[37–39], but also for their anticancer activities[18,23,40,41], for the treatment of Alzheimer’s disease, of diabetes, of inflammation processes.[39]

Copper(II) complexes containing ligands such as 2,2’-bipyridine (bipy) or 1,10-phenantroline (phen), shown in Figure 1.4, are widely reported as antibacterial, anticancer and antifungal compounds.[18,39] Copper complexes with substituted bipy

and phen and another anionic ligand (aminoacidates or acetylacetonate, for example) are examples of promising anticancer compounds of this metal and are patented under the name Casiopeínas. These compounds were also shown to be promising as anti-*Tripanosoma cruzi* agents.[42,43]

As the copper(II) ion, the *in vitro* activity of the complexes is usually related to their DNA binding, followed by its oxidative cleavage. Copper–phen complexes were first reported as artificial nucleases in 1979. The aromatic character of the phen ligand allows the intercalation of the complex in DNA, so that the reactive species are generated in close proximity of the target.[44,45]

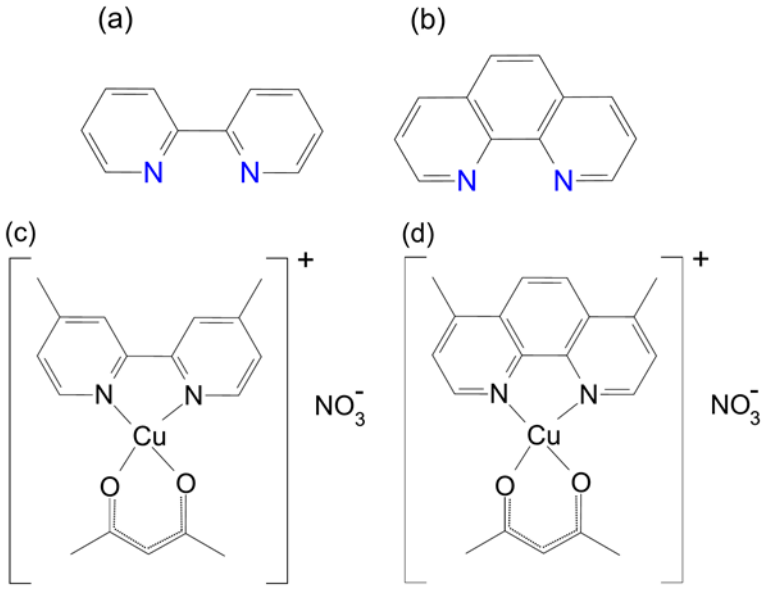

Figure 1.4. Chemical structures of (a) 2,2'-bipyridine, (b) 1,10-phenantroline (phen) and Casiopeínas (c) Cas III-ia and (d) Cas III-Ea.

Imidazole, benzimidazole and derivatives form promising antibacterial and antigunfal complexes with Cu(II). Thiosemicarbazones of imidazole and benzimidazole and their corresponding copper complexes were shown to be active against the yeast *Saccharomyces cerevisiae* and Gram-positive bacteria such as *Staphylococcus aureus* (*S. aureus*).[46] A copper complex of benzimidazole and L-arginine showed activity against both Gram-positive and Gram-negative bacteria.[38] The combination of imidazole and moxifloxacin led to a copper(II) complex active over *E. coli* and S. *aureus*.[47] These are just some examples of complexes with

potential antimicrobial applications and new examples are constantly being published in the literature.

The following section is dedicated to the discussion of the chemistry and biological and medicinal properties of some N-heterocyclic molecules studied in this work.

1.3. Chemistry and biological properties of N-heterocycles

N-heterocyclic molecules have long been explored as ligands in coordination chemistry. The borderline base character of nitrogen allows it to coordinate a several metals, thus leading to a variety of molecular architectures. Nitrogen is one of the most frequent donor atom for copper(II) complexes.[22]

Among the five-membered nitrogen-containing heterocycles, imidazole and tetrazole are vastly reported for the formation of compounds with promising properties. Imidazole is a five-membered aromatic heterocycle containing, in addition to a tertiary nitrogen, an imino group.[48] Histidine is an essential aminoacid that has the imidazole moiety. Imidazole is also structurally present in histamine, a neurotransmitter. Imidazole has an extremely important role in metalloproteins, as it acts as a ligand to bind metal ions to their specific sites, as illustrated in the previous section (Figure 1.3).

Many medications contain an imidazole moiety. Metronidazole, for example, is a widely used antibiotics which is in the list of the World Health Organization of essential medicines.[49] Imidazoles are employed as antifungal agents due to their their activity over the enzyme responsible for ergosterol synthesis in these organisms. Low levels of ergosterol in fungi result in fungal membrane disruption.[50] A recent report showed that imidazole is the seventh most frequent N-heterocycle present in the structure of U.S. approved drugs and benzimidazole is at the fifteenth position.[51]

Tetrazoles contain the maximally possible number of nitrogen atoms in a five membered-ring and have aromatic character.[52] It is less basic than imidazole and pyridine. Even though the tetrazole ring is not found in nature, it is now used as an isosteric (different functional groups that have similar physicochemical and biological properties) replacement for the carboxylic acid functional group in drug

development.[53] Tetrazoles have found applications in clinically used antibacterial and antihypertensive agents.[51]

Thiophene is not an N-heterocycle, but a sulfur-containing five-membered aromatic ring. This molecule is widely used as a building-block for drugs, as it is isosteric with benzene (also with pyrrole and furan). However, the presence of the sulfur atom makes it an electron-rich aromatic system, in a way that thiophene-based drugs may have a different metabolism than benzene derivatives.[54] Many commercial drugs already in use contain the thiophene moiety and many studies are currently performed to explore its bioactivity.[55]

Pyridine, pyrazine and pyrimidine are six-membered aromatic heterocycles and their derivatives are present in biomolecules or used as building-blocks in the development of new drugs. The pyridine ring is present in vitamins B_3 and B_6. Pyridine ranked second as the most frequent nitrogen heterocycles in U.S. Food and Drug Administration (FDA) approved drugs. This heterocycle is usually substituted at position 2, but even pentasubstitution of the ring is found in clinically used compounds.[51]

The pyrimidine ring ranked tenth in the same study.[51] Most of the pyrimidine drugs are substituted at position 2, probably due to the greater reactivity of this site. Pyrazine was not present at the top 24 nitrogen heterocycles of the FDA approved drugs[51], even though simple derivatives from this molecule are clinically used. As an example, pyrazinamide is used in combination with other drugs to treat tuberculosis.[56]

Different combinations of these heterocycles in a single structure may lead to ligands with interesting coordination chemistry and biological properties. The proposed molecules of study in this dissertation are shown in Figure 1.5.

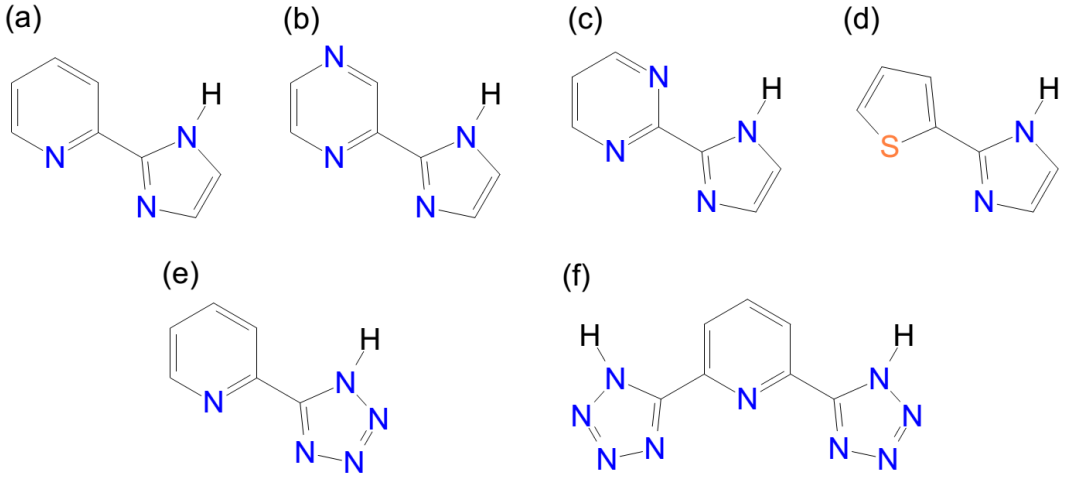

Figure 1.5. The ligands of interest of this dissertation. On the first row: 2-(imidazole-2-yl)heteroaryl ligands, where heteroaryl = **(a)** pyridine (impy), **(b)** pyrazine (impz), **(c)** pyrimidine (impm) or **(d)** thiophene (thim). On the second row: the tetrazolic **(e)** 2-(tetrazole-5-yl)pyridine (tzpy) and **(f)** 2,6-di(tetrazol-5-yl)pyridine (ditzpy) ligands.

1.4. Objectives and dissertation presentation

The objectives of this work are to synthesize imidazolic and tetrazolic N-heterocyclic ligands, study the influence of the different ligands on the chemical, structural and spectroscopic properties of their copper(II) coordination complexes and to test the bioactivity of the synthesized molecules over selected bacteria and fungi.

This text is divided in six chapters, including this Introduction.

Chapter 2 discusses the crystallographic data of three of the proposed ligands. Molecular structure and supramolecular interactions are discussed. Appendix A reports additional information on the usual spectroscopic characterization of these ligands and bond lengths and angles obtained from the structure determination.

Chapter 3 reports the synthesis and characterization, including crystal structure, of the novel copper complex $[CuCl_2(thim)_2]$ with one of the proposed imidazolic ligands that also contains thiophene (thim). Biophysical experiments were performed in order to evaluate the possible mode of interaction of this complex with calf-thymus DNA. Antifungal activity was evaluated by the disc diffusion method. Additional information about ligand characterization, spectroscopic data and bond lengths and angles of this complex can be found in Appendix B.

Chapter 4 reports a discussion on copper(II) complexes with impy, impz and impm ligands. Spectroscopic, diffraction and molecular modeling studies were performed to either assess their similarity in coordination mode or their differences in chemical properties, thus highlighting the effect of the ligand structure. Both the antibacterial and the antifungal activity of the complexes were evaluated. Additional spectroscopic data from the ligands, molecular modeling and crystal structures can be found in Appendix C.

Chapter 5 brings a general discussion on the chemical, crystallographic, spectroscopic and biological properties from the molecules studied in this dissertation, concludes this work and presents perspectives.

Chapter 2

Crystal structures of three N-heterocylic ligands: 2-(imidazole-2-yl)pyrazine, 2-(tetrazole-5-yl)pyridine and 2,6-di(tetrazol-5-yl)pyridine

The content of this chapter is an adaptation of an article in preparation by our research group, which includes the syntheses and characterization of several 2-(imidazole-2-yl)heteroaryl and 2-(tetrazole-5-yl)heteroaryl ligands.

My contribution to this work was partial spectroscopic and chemical characterization of the title ligands, obtention of single crystals from the title compounds of this chapter and description of their crystal structures. NMR and mass spectra of the title compounds are discussed in supporting information of this chapter (Appendix A), as these results have already been reported.[57–59]

2.1. Introduction

N-heterocyclic molecules have long been explored as ligands in coordination chemistry. The intermediate acid-base character of nitrogen allows it to coordinate a variety of metals, thus leading to a variety of molecular architectures.

Among the five-membered nitrogen-containing heterocycles, imidazole and tetrazole are vastly reported for the formation of compounds with promising properties. Imidazole is a diazole and heterocyclic containing both an amino and imino nitrogen groups.[48] This ring is found in nature in histidine (an essential aminoacid), in histamine and in many alkaloids. Tetrazoles contain the maximally possible number of nitrogen atoms in a five membered-ring and have aromatic character.[52] This ring is not found in nature, though they are studied as carboxylic acid isosters in drug development.[53]

Besides the coordinating ability of nitrogen of imidazoles and tetrazoles, these rings can be either protonated or deprotonated. Protonation results in the decrease of electronic density over all atoms within these rings, while deprotonation leads to the opposite effect.[52] This possible tailoring of electronic density by protonation deprotonation can be useful for the planning and development of coordination polymers and polynuclear complexes with applications in materials chemistry[60–62], bioinorganic[63] and catalysis[64].

Substitution of these molecules leads to a broad variety of ligands which can be systematically studied on their coordination properties. In particular, combining the imidazole and tetrazole rings with other N-heterocycles classically studied in coordination chemistry, such as pyridine and pyrazine, can lead to assymetric ligands with different properties from bipyridine and phenantroline, for example.

The synthetic procedures for the preparation of 2-substituted imidazoles or 5-substituted tetrazole molecules are quite diverse and well-established. In the paper by Voss et al, 2-substituted imidazoles are synthesized from nitriles, by a one-pot methodology.[59] The synthesis of 5-substituted tetrazoles has been recently reviewed[65] and highlights the classical method of Finnegan[66], which uses a proton-mediated synthesis and the cleaner method by Sharpless[67,68], which is mediated by zinc bromide. Characterization of the synthesized molecules in such articles is usually achieved by chemical and spectroscopical analyses.

However, characterization by diffraction is usually not reported due to the difficulty of single crystal obtention, so crystallographic data are not as vast. The evaluation of crystal structures allows the unambiguous determination of the molecular structure in the solid state and the obtention of information not as easily obtained by spectroscopic or chemical techniques, such as the types of intermolecular interactions and packing.

Moreover, the determination of crystal structures of a class of molecules allows the identification of hydrogen bonds patterns, as well as which type of aromatic-aromatic or π - π interactions governs crystal packing in these compounds. This is of fundamental importance for the rational development of supramolecular chemistry by tailoring and predicting novel crystal structures.[69]

In this work, we report the crystal structures and present a systematic discussion about the intermolecular interactions of one imidazole-substituted molecule, 2-(imidazole-2-yl)pyrazine, and two tetrazole-substituted molecules 2-(tetrazole-5-yl)pyridine and 2,6-di(tetrazol-5-yl)pyridine. These structures are among the first examples of crystal data available for 2-(imidazole-2-yl)heteroaryl and 2-(tetrazole-5-yl)heteroaryl molecules our research group is interested in.

2.2. Experimental Section

2.2.1. Materials and Methods

2-Pyridinecarbonitrile (99%), 2-pyrazinecarbonitrile and (99%), 2,6-pyridinedicarbonitrile (97%), and sodium azide (99%), aminoacetaldehyde dimethyl and diethyl acetals (both 99% purity) were purchased from Sigma-Aldrich. were purchased and Lithium chloride (99%) was purchased from Merck. Ammonium chloride (99.5%) was purchased from Synth (Brazil). All other reagents and solvents were used as received, without further purification.

Elemental analyses were performed on a Perkin Elmer 2400 CHNS/O Analyzer. The ^{1}H NMR spectra of the ligands were recorded in DMSO-d6, in a Bruker Avance III 500 MHz (11.7 T) spectrometer. Electrospray ionization mass spectrometry (ESI-MS) measurements were carried out using a Waters Quattro Micro API. The molecules were analyzed in a 1:1 methanol:water solution with addition of

0.10% (v/v) formic acid . Each solution was directly infused into the instrument's ESI source and analysed in the positive mode, with capillary potential of 3.00 kV, trap potential of 2 kV, source temperature of 150 ^{o}C and nitrogen gas for desolvation.

2.2.2. Synthesis

2-(Imidazol-2-yl)pyrazine (impz) This ligand was synthesized according to the procedure reported by Voss, et al.[59] 0.90 mL (10 mmol) of 2-pyrazinecarbonitrile, 10 mL MeOH and 0.38 mL (1 mmol) of a 30% solution of NaOMe in MeOH were added to a 100 mL round-bottom flask. The mixture was stirred for 30 minutes at room temperature. 1.45 mL (10 mmol) of aminoacetaldehyde diethyl acetal followed by 1.2 mL of AcOH were added dropwise to the mixture and stirred for 1 hour at 50°C. Afterwards, the mixture was left to cool at room temperature, 20 mL of MeOH and 5 mL of HCl 6 mol·L^{-1} were added and the resulting mixture was heated under reflux for 5 hours. The solution was evaporated to dryness, resolubilised in 15 mL of water and extracted with 3 × 5 mL of Et_2O, resulting in a deep brown solution. The pH was adjusted to 8-9 with a NaOH 2 mol·L^{-1} solution, then the volume was reduced to favor the product precipitation. The dark brown product was filtered and washed with Et_2O. To remove unwanted salt, the resulting powder was transferred to an Erlenmeyer. 20 mL of methanol were added and the system was heated to almost boiling. The hot solution was transferred to a flask and rotaevaporated to obtain the ligand as a dark brown powder. Yield 66 %. Anal. Calc. for $C_7H_6N_4$ (%): C 57.53; H 4.14; N 38.34. Found: C 57.63; H 4.16; N 38.14. ^{1}H NMR (500 MHz, DMSO-d_6): δ 7.176 (br s, 1H), 7.351 (br s, 1H), 8.606 (d, 1H, J = 2.5 Hz), 8.659 (dd, 1H, J = 0.5, 1.5 Hz), 9.252 (d, 1H, J = 1.5 Hz), 13.060 (br). MS (ESI-(+)) (*m/z*): calcd for $C_7H_6N_4$ $[M+H^+]^+$: 147.1, found: 147.1. Single crystals of impz were obtained by slow evaporation of a hot methanolic solution of this ligand to dryness.

2-(tetrazole-5-yl)pyridine (tzpy) This ligand was synthesized according to the procedure reported by Bond, et al.[57] To a three-neck round bottom bound were added 1.05 g (10 mmol) of 2-pyridinecarbonitrile, 1.43 g (22 mmol) of sodium azide, 1.18 g (22 mmol) of ammonium chloride and 0.31 g (7 mmol) of lithium chloride in anhydrous dimethylformamide (10 mL). This mixture was stirred for 10 h at 110 ^{o}C

under argon gas flux. After the reaction time, the suspension consisting of inorganic salts and yellow solution of the ligand was separated by filtration. The yellow solution was rotaevaporated to remove DMF and a yellow oil was obtained. To the oil were 50 mL of water and 0.75 mL of concentrated HCl, which led to the precipitation of a white solid. The product was isolated by filtration in a Buchner funnel, washed with cold water and dried under vacuum. Recrystallization in ethanol afforded white needles of the product. Yield 46 %. Anal. Calc. for $C_6H_5N_5$ (%): C 48.98; H 3.42; N 47.70. Found: C 48.70; H 3.25; N 47.31. ^{1}H NMR (500 MHz, DMSO-d_6): δ 7.654 (ddd, 1H, J = 1.0, 5.0, 7.5 Hz), 8.110 (td, 1.5, 8.0 Hz), 8.246 (d, 1H, J = 7.5 Hz), 8.817 (d, 1H, J = 4.5 Hz. MS (ESI-(+)) (*m/z*): calcd for $C_6H_5N_5$ $[M+H^+]^+$: 148.1, found: 148.1. Recrystallization of the initial powder in ethanol led to the formation of needles unsuitable for diffraction. After leaving the needles in contact with the ethanolic solution overnight, block-shaped crystals suitable for diffraction appeared.

2,6-di(tetrazol-5-yl)pyridine (ditzpy) This ligand was synthesized according to the procedure reported by Fleming, et al.[58] To a three-neck round bottom bound were added 1.20 g (10 mmol) of 2,6-pyridinedicarbonitrile, 1.45 g (21.5 mmol) of sodium azide, 1.10 g (21.5 mmol) of ammonium chloride and 0.30 g (7 mmol) of lithium chloride in anhydrous dimethylformamide (20 mL). This mixture was stirred for 10 h at 110 ^{o}C under argon gas flux. After the reaction time, the suspension consisting of inorganic salts and yellow solution of the ligand was separated by filtration. The yellow solution was rotaevaporated to remove DMF and a dark yellow oil was obtained. To the oil were 40 mL of water and 0.5 mL of concentrated HCl, which led to the precipitation of a white solid. The product was isolated by filtration in a Buchner funnel, washed with cold water and dried under vacuum. It was obtained as a white powder. Yield 33 %. Anal. Calc. for $C_7H_5N_9$ (%): C 39.07; H 2.34; N 58.58. Found: C 38.59; H 2.03; N 56.94. A discussion about ^{1}H NMR of this ligand is given in Appendix A. MS (ESI-(+)) (*m/z*): calcd for $C_7H_5N_9$ $[M+H^+]^+$: 216.1, found: 216.3. Crystallization of a small amount of this ligand was achieved by dissolving it in hot methanol (2 mL) and adding a few drops of water. The cooling of this mixture led to the formation of single crystals suitable for diffraction.

2.2.3. Single crystal X-ray diffraction

Data collection for all three molecules was performed with a Bruker Apex II CCD diffractometer with graphite monochromated Mo – K_α (λ = 0.71703 Å) or Cu – K_α (λ = 1.54178 Å) radiation. Accurate unit cell dimensions and orientation matrices were determined by least squares refinement of the reflections obtained by θ-χ scans. The data were indexed and scaled with the ApexII Suite [APEX2 v2014.1-1 (Bruker AXS), SAINT V8.34A (Bruker AXS Inc., 2013)]. Bruker Saint and Bruker Sadabs were used to integrate and for scaling of data, respectively.

Using Olex2[70], the structure was solved with the ShelXT[71] structure solution program using Direct Methods and refined with the ShelXL[72] by a full-matrix least-squares technique on F^2. All non-hydrogen atoms were refined anisotropically. The hydrogen atoms in the compound were added to the structure in idealized positions, with the exception of the atom involved with the formation of a zwitterionic structure in tzpy (more discussion on item 2.3.1), and further refined according to the riding model; molecular graphics: *OLEX2*[70]; software was used to prepare material for publication.

Searches in the Cambridge Structure Database (CSD), version 5.36, were performed using the Conquest software (version 1.17) and R < 0.1 and no powder data as restraints.

2.3. Results and discussion

2.3.1. Crystallographic discussion

The chemical structures of the ligands solved by diffraction revealed the formation of either the imidazole or tetrazole rings, as seen in Figure 2.1. The crystallographic data is presented in Table 2.1.

All the three reported molecules crystallized in the monoclinic crystal system, in space groups *P* 2_1*/ c* for impz and tzpy and in *Cc* for ditzpy. The assymetric unit of impz and ditzpy is described by one molecule, whereas that of tzpy is described by two, with no solvent molecule present in any of the structures. All bond lengths observed in the three ligands are in agreement with those found for the

corresponding pyrazine, pyridine, imidazole and tetrazole rings, as evaluated from the CSD.[73,74]

Some of the important bond lengths and angles can be found in Tables A.1 to A.3 of Appendix A. An analysis of the angles between the planes of the rings indicate they are almost coplanar in the crystals of all ligands, as reported in Table 2.2.

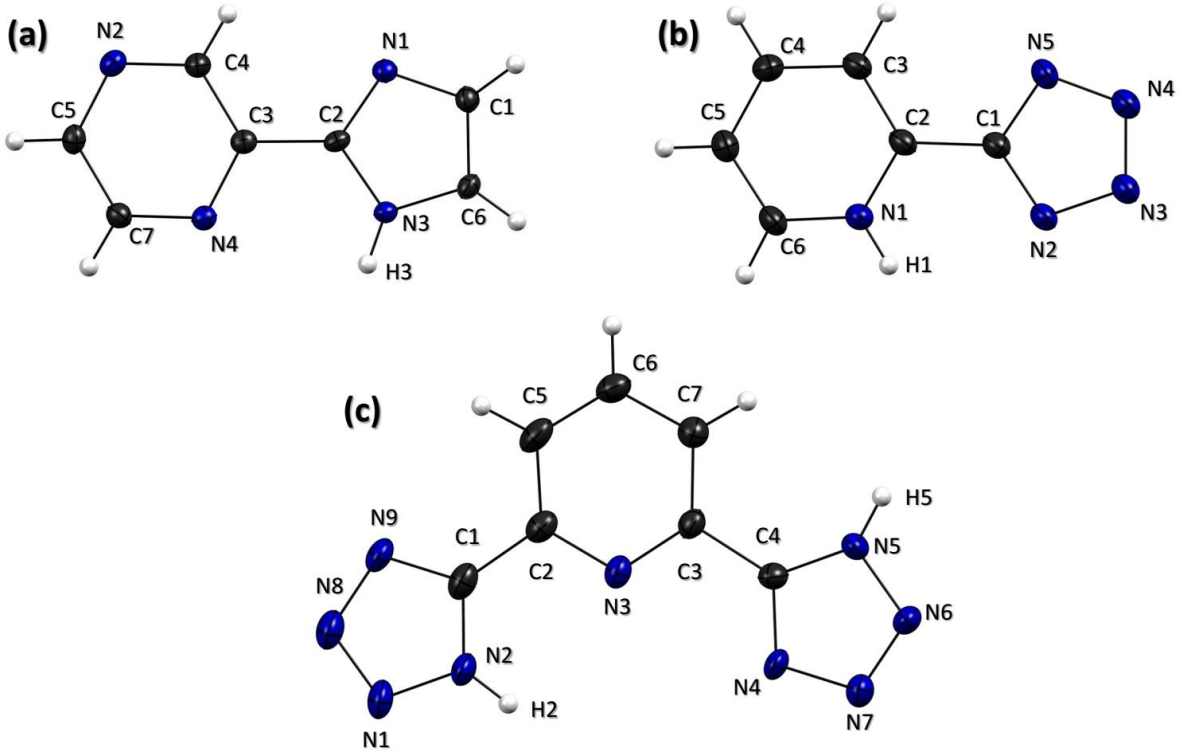

Figure 2.1. View of (a) impz, (b) one of the two tzpy molecules that describe its assymetric unit and (c) ditzpy. Atomic displacement ellipsoids are at the 50% probability level. Hydrogen atoms are represented by white spheres and only those bound to nitrogen atoms are labeled, for clarity.

The solved tzpy structure (Figure 2.1 (b)) shows that it is a zwitterion, because both tetrazolate and pyridinium ions are present within the same structure. This fact was attested by the presence of electronic density matching a hydrogen atom H1 nearer N1 from the pyridine ring during refinement, though it is seen that H1 is involved in an intramolecular hydrogen bonding with the N2 atom from the tetrazole ring (see Figure 2.2). Moreover, the tzpy zwitterion is involved in strong intermolecular hydrogen bonding between two molecules, which leads to the

formation of dimers and probably to easier packing in the crystal, as also shown in Figure 2.2.

Table 2.1. Crystallographic data of impz, tzpy and ditzpy structures.

Compound	impz	tzpy	ditzpy
Empirical formula	$C_7H_6N_4$	$C_6H_5N_5$	$C_7H_5N_9$
Molecular weight ($g \cdot mol^{-1}$)	146.16	147.15	215.20
Temperature (K)	296	150	150
Wavelength (Å)	Mo - K_α 0.71073	Cu - K_α 1.54178	Mo - K_α 0.71073
Crystal system	Monoclinic	Monoclinic	Monoclinic
Space Group	*P 2₁/ c*	*P 2₁/ c*	*Cc*
a (Å)	7.2269 (18)	9.4676 (6)	8.532(3)
b (Å)	9.650(2)	13.1565(8)	14.172(5)
c (Å)	9.864(3)	10.1173(6)	7.507(5)
α (^{o})	90	90	90
β (^{o})	91.481(5)	97.107(4)	103.503(5)
γ (^{o})	90	90	90
V ($Å^{-3}$)	687.7(7)	1250.5(1)	882.6(7)
Z	4	8	4
$\rho_{calcd.}$ ($g\ cm^{-3}$)	1.412	1.563	1.620
F(000)	304.0	440.0	608.0
μ (mm^{-1})	0.095	0.901	0.118
θ range (^{o})	3.52 - 26.82	5.54 - 68.26	2.84 - 26.07
Data/ restraints/ parameters	1143/0/100	1802/0/199	1499/ 2/ 151
R_1,wR_2 [$I > 2\sigma(I)$]	0.0363, 0.0947	0.0463, 0.1346	0.0366, 0.0946
Diff. peak and hole ($e/Å^{-3}$)	0.19 and -0.23	0.41 and -0.24	0.20 and -0.25
Goodness-of-fit on F^2	1.039	1.030	1.081

The formation of this zwitterionic species for the tzpy molecule was not reported before in the literature, as the ligand characterization is usually performed only by spectroscopic techniques.[57,67] Another example of a pyridinium-tetrazolate zwitterion from the literature is the 1-methyl-4-(tetrazol-5-ate)pyridinium ion. However, this reported compound has an imposed pyridinium formation due to its methylation and it does not involve a proton.[75,76]

Table 2.2. Angles between the least-squares adjusted planes of the rings.

Angle in impz (^{o})	Angle in tzpy (^{o})	Angles in ditzpy (^{o})
7.38(7)	3.74(9)	6.8(2)[a] and 7.0(2)[b]

a = between the planes of the C1-N2-N1-N-9-N8 and C2-N3-C3-C7-C6-C5 rings;

b = between the planes of the C2-N3-C3-C7-C6-C5 and C4-N4-N7-N6-N5 rings.

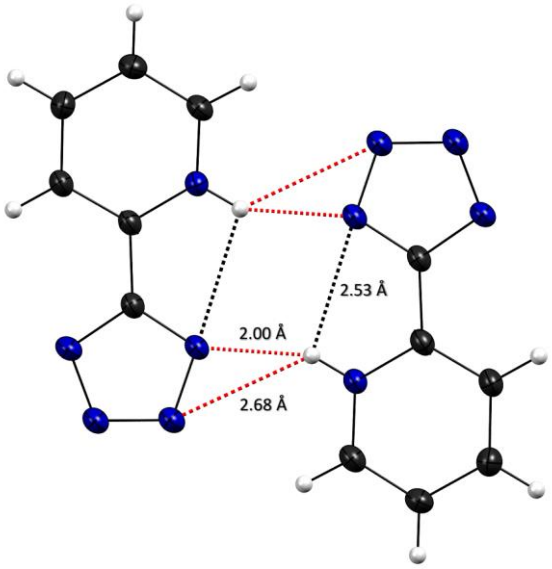

Figure 2.2. Intra (black dashed line) and intermolecular (red dashed line) hydrogen bonding in tzpy which leads to the formation of dimers in this crystal structure.

2.3.2. Supramolecular interactions

The supramolecular structure of impz involves the formation of a one-dimensional network of strong[77] hydrogen bonding involving imidazole atoms N3-H3···N1^{i} [H···A 2.01 Å, A···D 2.8257(18) Å, < (DHA) 158.0˚ (i = x, 1/2 - y, 1/2 + z)], as shown in Figure 2.3. Weaker and longer interactions[78] involving carbon atoms from imidazole and nitrogen atoms from pyrazine contribute to the formation of the three-dimensional array of the crystal, as described by: C1-H1···N4^{ii} [H···A 2.62 Å, A···D 3.407(2) Å, < (DHA) 142˚ (ii = 2 - x, 1/2 + y, 1/2 - z)], C6-H6···N2^{iii} [H···A 2.53 Å, A···D 3.429(2) Å, < (DHA) 162.0˚ (iii = 1 + x, 1/2 - y, 1/2 + z)] and C4-H4···N4^{iv} [H···A 2.57 Å, A···D 3.417(2) Å, < (DHA) 152˚ (iv = x, 1/2 - y, - 1/2 + z)] (see Figure 2.3). Hydrogen bonds are of fundamental importance in the chemistry of imidazoles and tetrazoles. As an example, the substitution of the hydrogen atom from the amino group by a methyl group lowers the melting point of free imidazole by almost 100 ^{o}C.[48]

Another important intermolecular interaction present in impz involves a “point-to-face” π interaction.[69] From Figure 2.3, it can be seen that the imidazole ring acts as electron donor to an electron-deficient hydrogen atom H5 from an adjacent pyrazine ring. This interaction can be described by symmetry as C5-H5···CG^{v}

[H···CG 2.51 Å (v = 1 - x, - 1/2 + y, 1/2 - z)], where CG is the center of gravity of the imidazole ring.

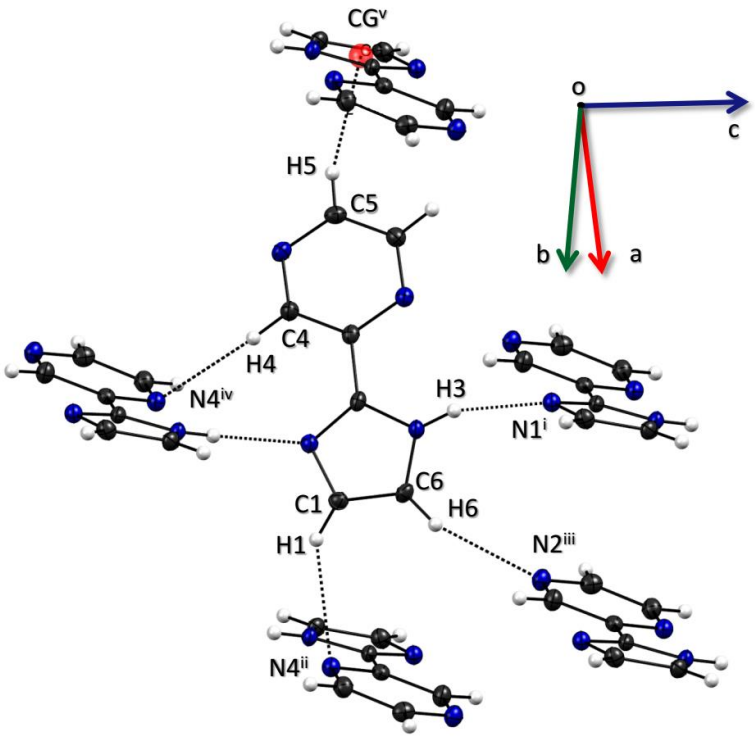

Figure 2.3. Intermolecular interactions present in impz crystal structure. The description of symmetry labels is given in the text.

All nitrogen atoms from the tetrazolic ring in tzpy are involved in either C-H···N[78] or N-H···N interactions. Since two tzpy molecules describe the assymetric unit of the structure, the hydrogen bonds that form the dimers are not equivalent, but are described by the same symmetry operation: N1-H1···N7^{vi} [H···A 2.00 Å, A···D 2.810(2) Å, < (DHA) 153˚ (vi = 1 - x, 1 - y, -z)] and N6-H(6A)···N2^{vi} [H···A 1.99 Å, A···D 2.808(2) Å, < (DHA) 153˚]. These hydrogen bonds were shown in Figure 2.2.

As opposite to impz, no point-to-face π interaction is observed in tzpy, which might indicate the pyrazine hydrogen H5 has a greater partial positive charge than the hydrogen atoms in the pyridine ring. However, the interactions described as offset π··· π[69] are present (see Figure 2.4) and are responsible for the stacking of the molecules.

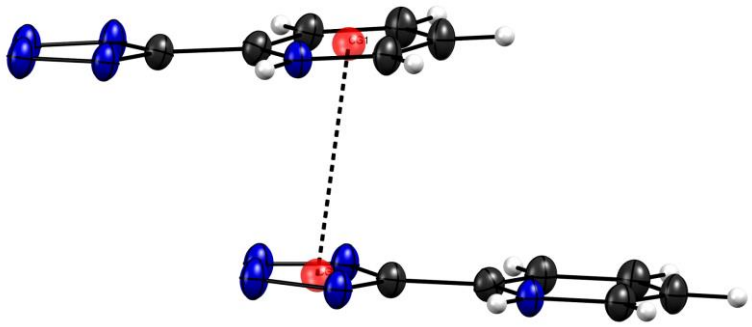

Figure 2.4. Representation of offset π··· π interactions in tzpy molecule.

An infinite one-dimensional chain of ditzpy molecules is created by two strong hydrogen bonds: N2-H2···N6^{vii} [H···A 1.98 Å, A···D 2.810(4) Å, < (DHA) 164˚ (vii = 1/2 + x, 1/2 - y, 1/2 + z)] and N5-H5···N4^{viii} [H···A 2.54 Å, A···D 2.832(5) Å, < (DHA) 175˚ (viii = -1/2 + x, 1/2 - y, -1/2 + z)] (see Figure 2.5).

Two weaker[78] C-H···N interaction involving the carbon atoms from the pyridine ring contribute to the expansion of the lattice, as described by C5-H5(A)···N8^{ix} [H···A 2.41 Å, A···D 3.288(5) Å, < (DHA) 154˚ (ix = -1/2 + x, 3/2 - y, -1/2 + z)] and C7-H7···N7^{viii} [H···A 2.53 Å, A···D 3.463(5) Å, < (DHA) 166˚] (Figure 2.5). As observed in tzpy, offset π···π interactions are responsible for the formation of the three-dimensional crystal structure of ditzpy.

No deviations of bond length or angle was observed in the three structures. However, some tendencies must be highlighted. The ring planarity is quite relevant for the molecular packing, probably due to the directional character of the π···π interactions observed in the ligands. Moreover, in both imidazole and tetrazole molecules, hydrogen bonding is essential for the network formation, which can be further explored in the design of new ligands and supramolecular systems.

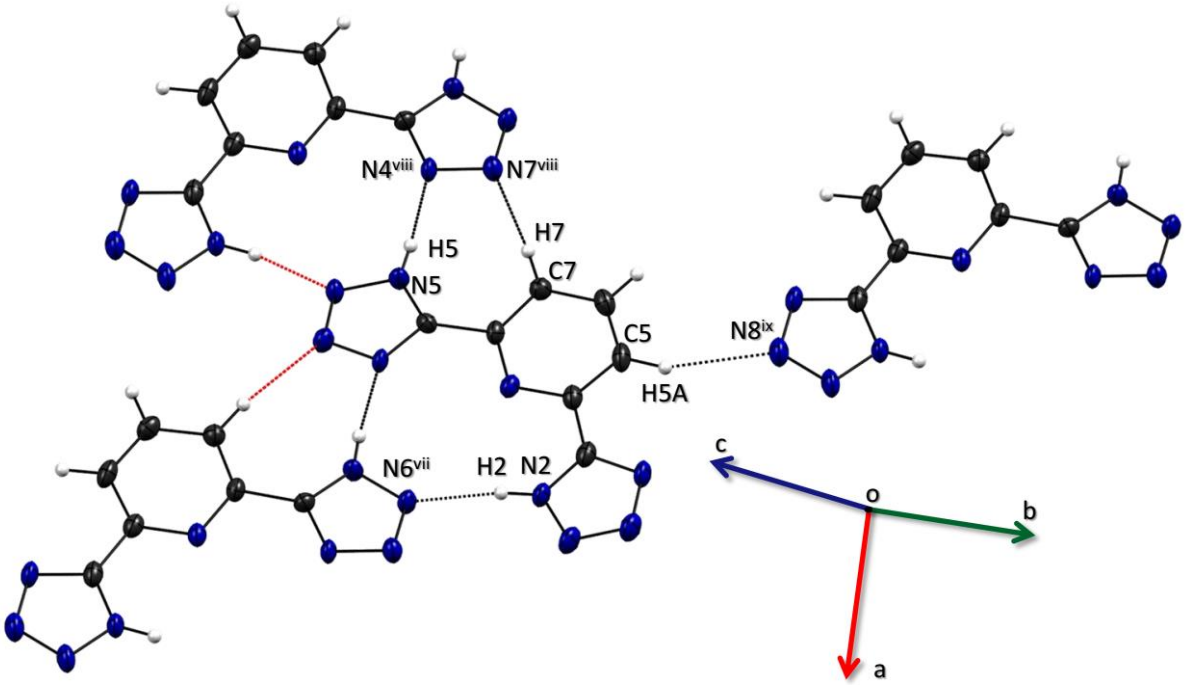

Figure 2.5. Intermolecular interactions present in ditzpy. The description of the symmetry labels is given in the text. Red dashed lines represent interactions already described from the central molecule.

2.4. Partial conclusions

Three N-heterocyclic molecules have been synthesized and characterized. X-ray single crystal diffraction provided a detailed set of data about these compounds, which cannot be usually attained by routine spectroscopic and chemical techniques, as reported in the literature.

The supramolecular structures of all ligands have strong N-H···N hydrogen bonds between either imidazole or tetrazole rings as major factors of network formation. Weaker C-H···N interactions show a minor contribution for the lattice formation. The type of π interactions was different in the structures. The imidazolic ligand impz had a point-to-face interaction, as opposite to the more frequent offset stacking observed in the tetrazolic ligands.

Chapter 3

A copper(II) complex with 2,2-thiophen-yl-imidazole: synthesis, spectroscopic characterization, X-ray crystallographic studies, interactions with calf-thymus DNA and antifungal activity

The content of this chapter is an **adaptation** of the article entitled “Copper(II), palladium(II) and platinum(II) complexes with 2,2-thiophen-yl-imidazole: synthesis, spectroscopic characterization, X-ray crystallographic studies and interactions with calf-thymus DNA” by Nina T. Zanvettor, Douglas H. Nakahata, Raphael E. F. de Paiva, Marcos A. Ribeiro, Alexandre Cuin, Pedro P. Corbi and André L. B. Formiga. This content was **reprinted with permission from *Inorganica Chimica Acta*. Copyright 2016. Elsevier Limited**. The license to use this article (full paper) in this dissertation is found in Appendix D.

Reference: *Inorg. Chim. Acta* **2016**, 443, 304-315.

My contribution to this work was in the synthesis and characterization of the copper(II) complex, participation on the biophysical experiments of interaction of the compounds with calf-thymus DNA and partial writing of the publication. The antifungal activity assay was not included in the published article.

3.1. Introduction

Metal ions have been explored in medicine for a long time. According to the literature, the vast application of metals in medicine includes antimicrobial and anticancer compounds, antiarthritic agents, enzymatic inhibitors, and others.[79,80] Nowadays, the platinum compounds, such as cisplatin (*cis*-$[PtCl_2(NH_3)_2]$), constitute one of the most widely used anticancer drugs.[79,81,82] Silver compounds, on the other hand, have been applied in the treatment of bacterial infections in burns and wounds, and also in other medical applications, including dental work and catheters[14,83], while gold complexes, such as auranofin and miochrisine, have been extensively used for the treatment of rheumatoid arthritis.[79]

Cisplatin was one of the first metallodrugs broadly employed in medicine. It was approved in 1978 by the FDA (Food and Drug Administration, USA) for cancer treatment. The first pharmacological activities of cisplatin were reported by Rosenberg *et al.*[2,3] In the late of the 1960's, Rosenberg evaluated the activity of this compound over Sarcoma 180 solid tumors implanted in mice[3], which resulted in a high cure rate. Today, cisplatin is still considered one of the most effective antitumor agents, especially for testicular cancer, for which the cure rate exceeds 90%.[84] Cisplatin is also considered in the treatment of head and neck, lung, colorectal and ovarian cancers.[81]

Nevertheless, cisplatin is also known for its renal and gastrointestinal toxicities.[7] Besides the side effects, the inherent or acquired resistance of some tumors to cisplatin also restricts its use.[84] These effects stimulated the search for new platinum-based chemotherapeutic drugs, which resulted in the approval of carboplatin in 1989 by FDA.[84] This drug has shown to have reduced collateral effects, mainly concerning its nephrotoxicity, neurotoxicity and ototoxicity.[84]

The search of new chemotherapeutic agents based on platinum led to the approval of oxaliplatin (worldwide), nedaplatin (China) and lobaplatin (Japan).[84] These platinum complexes derived from cisplatin are all of *cis*- geometry with two stable amine ligands and two labile ones. When these compounds enter inside the cells they are first hydrolyzed losing the labile ligands, and thus bind to DNA through the imidazole group of adjacent guanines. The interaction with DNA forms an intrastrand crosslink, which alters DNA structure blocking cell replication.[84]

Copper(II) complexes have also been investigated for their biological properties assuming that, since it is an endogenous element, it may be less toxic to normal cells. Copper(II) ions and their complexes are generally associated to redox processes. Copper enzymes, such as superoxide dismutase, are examples of copper compounds in the human body that act in redox reactions.[18] The coordination chemistry of copper(II) is quite distinct from palladium(II) and platinum(II), giving rise to different modes of action.[18]

In the field of medicinal chemistry, copper(II) complexes have received great attention due to their antitumor[18,40,41] and antibacterial activities.[37,85] However, the complete elucidation of their mechanisms of action is still in progress.[18] Both covalent and non-covalent (intercalation, groove binding or electrostatic) modes of interaction with DNA have been reported for copper(II) complexes in the literature.[35,85] Copper complexes with modulated redox potential can also be related to the generation of reactive oxygen species (ROS), which can further damage DNA and blockage cell proliferation.[18,41]

Imidazole is a five-membered aromatic heterocyclic diazole. It is found in several biomolecules, such as histamine, vitamin B_{12}, DNA, proteins and hemoglobin.[86] Imidazole exists in two tautomeric forms and exhibits a considerable Lewis basicity. It also participates in intermolecular interactions such as hydrogen bonding.[86] Due to these characteristics, several compounds based on imidazole are used as drugs, such as antitumoral, antibacterial, anti-fungal, antiparasitic, antihistaminic, antineuropathic and antihypertensive agents.[86]

Copper(II) complexes with imidazole derivatives that present pharmacological activity are under investigation.[87–90] Copper(II) complexes with benzimidazole derivatives have shown to interact with DNA and proteins and induce a significant cytotoxicity against cervical cancer cells.[87]

Thiophene is a five-membered, sulfur-containing heteroaromatic ring with remarkable pharmacological application. The biological activities of thiophene derivatives were more recently investigated, as this group is not usually found in living organisms with rare exceptions.[91] Nowadays, it is used as a building block in many drugs.[55,92] Examples of drugs with thiophene moieties are the antimicrobial cefoxitin, the anticancer raltitrexed, the anti-inflammatory tenoxicam and the antihypertensive tiamenidine.[92] Novel thiophene derived compounds with biological

activities are under investigation and new compounds with anticancer,[55,91] anti-inflammatory[93] and antimalarial activity[94] were recently synthesized.

Here we describe the synthesis, structural characterization and studies of interaction with calf-thymus DNA of a new copper(II) complex with the 2,2-thiophen-yl imidazole (thim) ligand.

3.2. Experimental Section

3.2.1. Materials and methods

2 –thiophenecarbonitrile 99%, aminoacetaldehyde dimethyl acetal 99 % and DNA sodium salt from calf-thymus type I 42% of guanine-citosine were purchased from Sigma-Aldrich Laboratories. $CuCl_2 \cdot 2H_2O$ 99% and $NaClO_4 \cdot H_2O$ 98.0 – 102.0 were purchased from Vetec – Sigma (Brazil). HCl 36.5 – 38 %, NaOH 97 %, glacial acetic acid, ethanol and methanol 99.8 % were purchased from Synth (Brazil). Metallic sodium was purchased from Riedel-de Haen. All other reagents and solvents were used as received, without further purification. Elemental analyses were performed on a Perkin Elmer 2400 CHNS/O Analyzer. Electronic spectra in the 190-1100 nm range were acquired by using a 1.0 cm quartz cuvette in a diode array HP8453 UV/Visible absorption spectrophotometer. Infrared spectroscopy measurements were performed on an Agilent Cary 630 FTIR spectrometer, using the Attenuated Total Reflectance (ATR) method, with a diamond cell. Spectra were recorded from 4000-400 cm^{-1}, with 64 scans and resolution of 4 cm^{-1}. The ^1H NMR spectra of thim was recorded in a Bruker Avance III 500 MHz (11.7 T) spectrometer. Electrospray ionization mass spectrometry (ESI-MS) measurements were carried out using a Waters Quattro Micro API. Samples were evaluated in the positive mode. $[CuCl_2(thim)_2]$ was analyzed in a 1:1 acetonitrile:water with 0.10% (v/v) formic acid. Each solution was directly infused into the instrument's ESI source and analysed in the positive mode, with capillary potential of 3 kV, trap potential of 2 kV, source temperature of 150 ^oC and nitrogen gas for desolvation. Fluorescence measurements were performed on a Cary Eclipse fluorescence spectrophotometer. Excitation and emission slits were of 5 nm and scanning speed was set to medium. A quartz cuvette of four clear windows and optical path length of 1 cm was used. Excitation wavelength was set as 525 nm and

emission window was from 540 to 750 nm. Circular dichroism measurements were performed in a Jasco J-720 spectrophotometer, from 200 to 260 nm, in quartz cuvettes of 0.5 cm of optical path length. Single crystal X-ray diffraction was performed with a Bruker Apex II CCD diffractometer with graphite monochromated Mo - K_α (λ = 0.71703 Å) radiation. More information about refinement and data treatment can be found in **Chapter 2** – subitem 2.2.3. All crystallographic data for this paper are deposited with the Cambridge Crystallographic Data Centre #1403268, #1406385 and #1406386.

3.2.2. Synthesis

thim: The synthesis of the ligand was carried out following a reported method in the literature.[59] This is a one-pot method for the preparation of heteroaryl-2-imidazoles from nitriles. Yield (Calcd. from the aminoacetal): 0.701 g, 58 %. Anal. Calcd. for $C_7H_6N_2S$ (%): C, 55.97; H, 4.03; N, 18.65. Found (%): C, 56.42; H, 4.18; N, 18.66. ^{1}H NMR (500 MHz, DMSO-d_6): δ 6.9 and 7.1 (br, 2H), 7.107 (dd, 1H, J = 3.6, 4.8 Hz), 7.488 (dd, 1.2, 4.2 Hz), 7.507 (dd, 1H, J = 1.2, 3.6 Hz), 12.5 (br, 1H) (for the spectrum, see Appendix B, Figure B.1). MS (ESI-(+)) (*m/z*): calcd for $C_7H_6N_2S$ $[M+H^+]^+$: 151.0, found: 151.1. This ligand is soluble in acid aqueous medium, methanol, ethanol, DMSO and DMF.

$[CuCl_2(thim)_2]$: The copper(II) complex was synthesized by the reaction of an ethanolic $CuCl_2{\cdot}2H_2O$ solution ($5.0{\cdot}10^{-4}$ mol, 10 mL) with an ethanolic solution of Thim ($1.0{\cdot}10^{-3}$ mol, 10 mL). The synthesis was carried out with stirring at room temperature. A reddish-brown solid slowly precipitated. After 4 hours of constant stirring the solid was collected by filtration, washed with a small amount of cold ethanol and dried in vacuum. Yield: 0.125 g, 58 %. Anal. Calcd. for $[CuCl_2C_{14}H_{12}N_4S_2]$ (%): C, 38.70; H, 2.78; N, 12.88. Found: C, 38.70; H, 2.96; N, 12.83. MS (ESI-(+)) (*m/z*): calcd for $[Cu(C_7H_6N_2S)_2]^+$: 363.0, found: 363.3. The complex is quite soluble in methanol, DMSO and DMF. After 4 days of slow concentration of the ethanolic filtrate, single crystals suitable for X-ray diffraction were formed.

3.2.3. DFT calculations

All calculations were performed with the hybrid PBE0 functional[95] with the ORCA package (version 3.0.3)[96] using the RIJCOSX method[97] to calculate the exchange energy. Densities were optimized with a 10^{-8} au convergence criterion for the energy and a 10^{-5} gradient for the KS orbitals. The def2-TZVP basis set[98,99] was used for all atoms. Geometry optimizations were performed without symmetry constrains using a conjugate gradient with a 5 x 10^{-6} au convergence criterion for the energy and a 10^{-4} criterion for the RMS of the gradient. Geometries were confirmed as minima of the PES by calculation of the Hessian showing no imaginary frequencies. Harmonic frequencies were scaled using a factor of 0.9593[100] and vibrational spectra were simulated using lorentzian functions with 20 cm^{-1} full widths at half heights.

3.2.4. DNA dialysis

Appropriate amount of calf-thymus (CT) DNA was dissolved in deionized water. It was dialyzed for 24 hours, using a membrane of 30000 Da cutoff in a 10 mM of $NaClO_4$ aqueous solution. The nucleic acid concentration was determined using UV-Vis spectroscopy, by considering a molar extinction coefficient of CT-DNA at 260 nm of 6600 $L \cdot mol^{-1} \cdot cm^{-1}$. The DNA concentration in this stock solution was determined as 450 μM.

3.2.5. Binding properties of compounds with DNA using UV-Vis spectroscopy

Solutions of compounds were dissolved in methanol and further diluted in a 10 mM $NaClO_4$ aqueous solution (final methanol volume was 4%) for an initial concentration of 20 μM. CT-DNA in 10 mM $NaClO_4$ aqueous solution was added to the solutions of the compounds for different [DNA]/ [compound] ratios, ranging from 0 to 7.0.

3.2.6 Competitive binding with ethidium bromide (ETBr) using fluorescence spectroscopy

Samples of CT-DNA (100 μM in 10 mM $NaClO_4$ aqueous solution) were incubated with thim and $[CuCl_2(thim)_2]$ with molar ratios r_i = 0.10 and 0.20 for 24 hours, at 37 ^oC. The spectra were recorded after successive additions of 2 μL aliquots of ethidium bromide (initial concentration of 0.50 $mg \cdot mL^{-1}$) prepared in 10 mM $NaClO_4$ aqueous solution. Spectra of pure CT-DNA with increasing concentration of ETBr and of pure ETBr were also recorded. Data were compared by taking the average of fluorescence intensity at 606 nm of three independent measurements as a function of ETBr concentration.

3.2.7. Circular Dichroism (CD) spectroscopy

The compounds (methanolic stock solutions) were added to DNA solutions (100 μM, in 10 mM $NaClO_4$ aqueous solution) for different [compound]/[DNA] ratios, from 0 to 0.30, and incubated at 37 ^oC for 24 hours. A CD spectrum of a sample with methanol at ratio = 0.30 was also prepared for control. The spectra were recorded with a scanning speed of 20 $nm \cdot min^{-1}$ and 8 accumulations.

3.2.8. CT-DNA thermal denaturation – melting point determination

Samples of CT-DNA (100 μM, in 10 mM $NaClO_4$ aqueous solution) were incubated with thim and $[CuCl_2(thim)_2]$ (molar ratio of compound/ CT-DNA of 0.10; methanolic stock solutions) for 24 hours at 37 ^oC. The absorbance at 260 nm of each sample was recorded as a function of temperature in the range 30 ^oC - 94 ^oC. The temperature was controlled with a thermostated water bath, using a 2 $^oC \cdot min^{-1}$ heating rate. The spectra were recorded after 1 minute of thermal equilibrium at each temperature. All measurements were performed in triplicate.

3.2.9. Antifungal activity assay

Antifungal activities of $[CuCl_2(thim)_2]$ were evaluated using the agar diffusion method. The tested yeasts were: *Candida albicans*: ATCC 26790, *Fusarium moniliforme*: ATCC 38159 and *Trichophyton mentagrophytes*: ATCC 11481. The base layer was obtained by addition of 20 mL of Agar Sabouraud (Difco) in Petri dishes of 20 x 150 mm. After solidification of this layer, 5 mL of saline solution with a concentration of 1 x 10^8 CFU·mL^{-1} (colony forming units) of the strains were added to obtain the seed layer. Wells of 5.0 mm of diameter were made in the agar, 20 μL of the treatment solutions (1 mg·mL^{-1}) were placed in the wells. Amphotericin was used as positive control whereas ethanol/water (1:1 EtOH/H_2O) solution was used as negative control. The dishes were incubated for 24 h at 37°C and the inhibition zones were measured (diameter and the space between the ring of the well and the beginning of fungi growth in millimeters). These experiments were performed in collaboration with Professor Dr. Marcelo Lancelloti and his research group (LABIOTEC) from the Biology Institute of UNICAMP.

3.3. Results and Discussion

3.3.1. Crystal structure of the Cu(II) complex

$[CuCl_2(thim)_2]$ crystallizes in the monoclinic space group *P2$_1$/c* with an asymmetric unit corresponding to half of the coordination formula $[CuCl_2(C_7H_6N_2S)_2]$. The $[CuCl_2(thim)_2]$ molecule is shown in Figure 3.1 and crystallographic data are presented in Table 3.1. The copper ion lies over the special position (1 1 0) with half occupancy. It is tetracoordinated by two imidazole nitrogens and two chlorides, resulting in a neutral complex. The Cu1-N10 bond distance, 1.9487(16) Å, is slightly shorter than the average value 1.970(17) Å found in CSD[74] for Cu-N in imidazole moieties, whereas the Cu1-Cl1 bond distance of 2.3036(5) Å is longer than those found in CSD for tetracoordinated copper(II) complexes (2.242(31) Å). The copper ion is perfectly located in the least square plane (rms=0 Å) defined by N10, N10^i, Cl1 e Cl1^i (I = -x, -y, -z). The long distance between Cu1 and S1 (3.0419(8) Å) is far from the average bond distance for a Cu-S (2.278(20) Å)[73] bond.

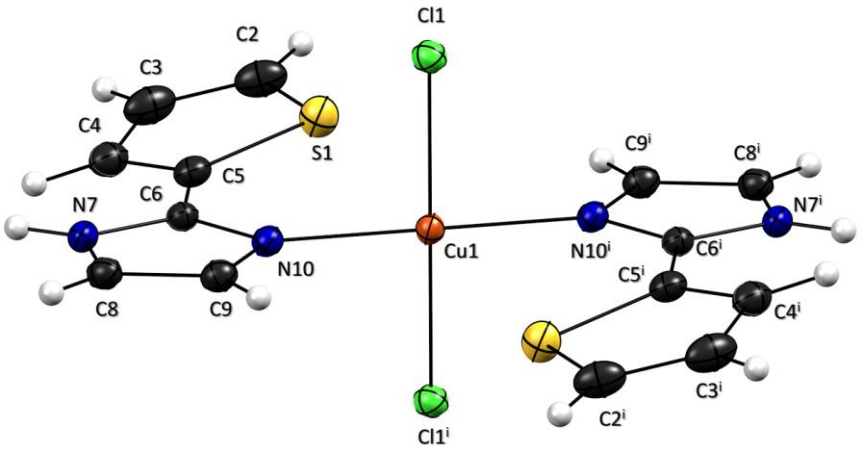

Figure 3.1. View of compound $[CuCl_2(thim)_2]$. Atomic displacement ellipsoids are at the 50% level. Hydrogen atoms are represented by open circles.

These observations are also in agreement with those found for a similar copper(II) complex containing benzimidazole.[101] When compared to the free imidazole ring[73] no significant differences were found, with the values varying within the experimental errors. Specifically, the C6-N10 bond (1.331(2) Å) has more double bond character than N7-C6 (1.347(2) Å). The bond distances in thiophene ring are in accordance with the related distances found in CSD. Moreover, both rings showed to be planar with least squares planes of 0.0041 Å and 0.0037 Å for thiophene and imidazole, respectively, where the planes deviated 14.03(12)˚ from each other. Bond distances and angles for $[CuCl_2(thim)_2]$ are shown in Appendix B, Table B.1.

Short hydrogen bonds connect the coordination compounds, forming an infinite 2D chain motif through N7-H7···Cl1^{ii} (H···A 2.33 Å, A···D 3.1728(17) Å, <(DHA) 165.1˚ (ii = -x, -1/2 + y, 1/2 - z). Two intermediate interactions arise between C8-H8···Cl1^{iii} (H···A 2.82 Å, A···D 3.639(2) Å, < (DHA) 147.0˚, iii = x, -1/2 - y, -1/2 + z) and C2-H2$^{\cdots}$ Cl1^{iv} (iv = -1 + x, y, z) forming a 2D infinite chain, as shown in Figure 3.2. The latter could be responsible to hold the thiophene group almost coplanar to the imidazole group. Distances between ring centroids are in the upper limit defined for $\pi\cdots\pi$ interactions (usually in the range 3.3 – 3.8 Å)[69], thus they are less relevant for the packing. The separation between the centroid defined by S1-C2-C3-C4-C5 and N7-C6-N10-C9-C8 rings is 3.7106(13) Å and the ring planes are almost coplanar with 6.95(10)˚ from each other.

Table 3.1. Crystallographic data for $[CuCl_2(thim)_2]$ crystal structure.

Empirical formula	$C_{14}H_{12}Cl_2CuN_4S_2$
Coordination formula	$[CuCl_2(C_7H_6N_2S)_2]$
Molecular weight ($g \cdot mol^{-1}$)	434.84
Temperature (K)	100(2)
Wavelength (Å)	Mo K_α – 0.71073
Crystal system	Monoclinic
Space Group	$P2_1/c$
a (Å)	8.7424(13)
b (Å)	12.9798(19)
c (Å)	8.0922(12)
α (^{o})	90
β (^{o})	111.374(3)
γ (^{o})	90
V ($Å^{-3}$)	855.1(2)
Z	2
$\rho_{calcd.}$ ($g\ cm^{-3}$)	1.697
F(000)	442
μ (mm^{-1})	1.836
θ range (^{o})	2.50 - 30.02
Reflections collected/ independent	13224/ 2504 (R_{int} = 0.0412)
Data/ restraints/ parameters	2504 / 0 / 106
R_1,wR_2 [I > 2σ (I)]	0.030, 0.067
Diff. peak and hole ($e/Å^{-3}$)	0.43 and -0.29
Goodness-of-fit on F^2	1.01
CCDC number	1406385

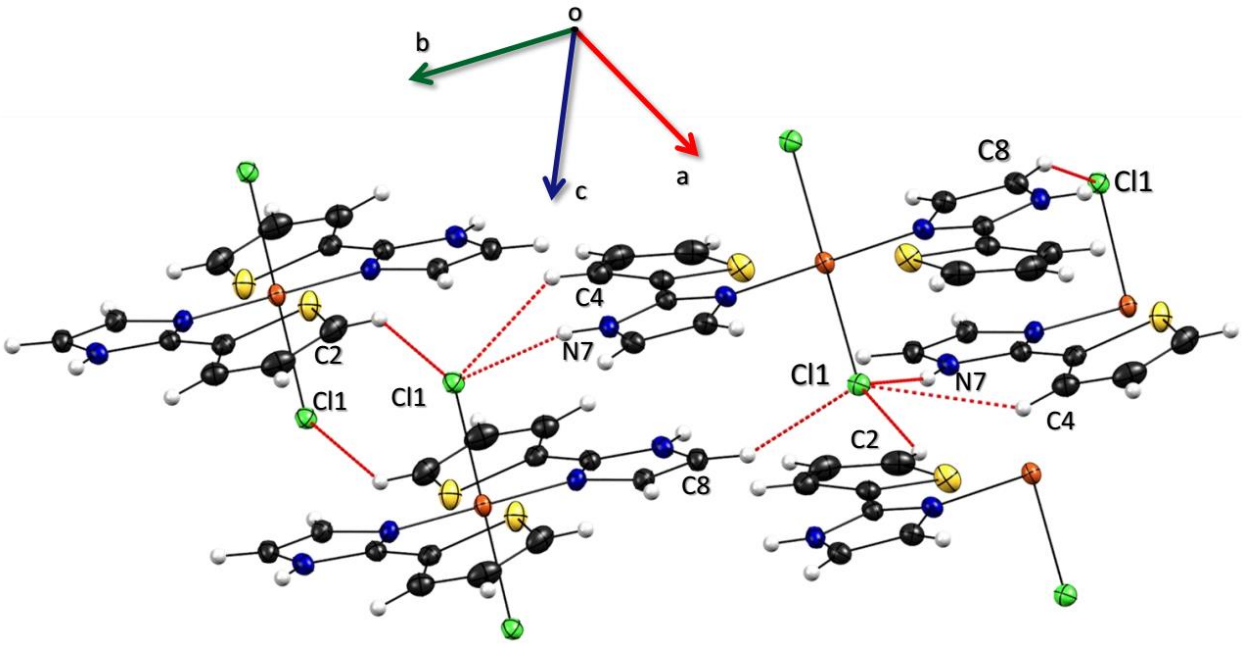

Figure 3.2. Hydrogen bonding pattern in $[CuCl_2(thim)_2]$.

3.3.2. Molecular modeling

The geometries of the Cu(II) complex was optimized using DFT with the hybrid PBE0 functional and a basis set of triple zeta quality for all atoms. Comparison between crystallographic data and DFT results show that geometries are well reproduced. Figure 3.3 shows the equilibrium geometry and Table 3.2 reports a comparison between experimental and calculated bond distances and angles.

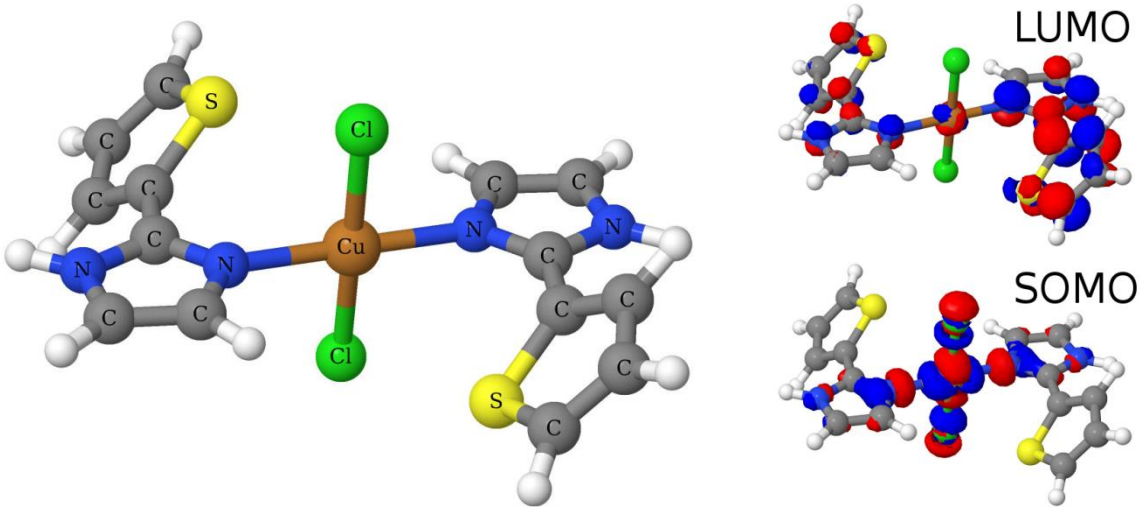

Figure 3.3. Equilibrium geometry and frontier Kohn-Sham orbitals obtained for $[CuCl_2(thim)_2]$ by DFT calculations with PBE0/def2-TZVP.

Table 3.2. Optimized bond lengths and angles of $[CuCl_2(thim)_2]$ and comparison with experimental values.

Bond length (Å) or angle (º)	**$[CuCl_2(thim)_2]$ (experimental)**
Cu-N	2.0256 (1.9487(16))
Cu-Cl	2.2595 (2.3036(5))
N-Cu-N	179.33 (180.00)
Cl-Cu-Cl	179.56 (180.00)
S1-C5-C6-N10	42.4 (-13.8(2))

The main difference between crystal and DFT structures is the rotation of the thiophene rings in the complex. The S1-C5-C6-N10 torsion angles in the crystal structures is -13.8(2)º while it is predicted to be around -42º by DFT, thus a difference

of almost 30°. This can be explained by the absence of intermolecular interactions between two asymmetric units in the gas phase simulation. Moreover, this observation reinforces the previous one based on XRD that the long range Cu(II)···S interaction is not relevant.

Frontier Kohn-Sham orbitals for $[CuCl_2(thim)_2]$ can be seen in Figure 3.3. As expected for a square planar d^9 complex, the SOMO (Singly Occupied Molecular Orbital) has a contribution from the $3d_{x^2-y^2}$ orbital from copper. The LUMO is mainly a combination of the π^* system of both thiophene ligands.

3.3.3. FTIR spectroscopy

Powdered samples of thim and $[CuCl_2(thim)_2]$ were analyzed by attenuated total reflectance Fourier-transform infrared spectroscopy (ATR-FTIR) and the full spectra can be found in Appendix B, Figure B.2. The band assignments were performed with the aid of DFT calculations for all species and the complete simulated spectra can also be found in Appendix B, Figure B.3.

The presence of a N-H···N hydrogen bond network in thim results in the large broadening of bands from approximately 3010 to 2500 cm^{-1}.[59,102] The broadening of this band is not present in the spectra of the complexes, because this type of interaction does not occur in these molecules, as seen in the crystal structures for $[CuCl_2(thim)_2]$. The band at 3176 cm^{-1} in the spectum of $[CuCl_2(thim)_2]$ is assigned as the N-H stretching mode.

The most important differences between the spectra of free ligand and complexes can be found in the range 1600-1380 cm^{-1}, where C=C and C=N stretching can be observed.[102] Figure 3.4 shows a comparison between experimental and simulated spectra in this region.

Calculations show that the band at 1431 cm^{-1} for thim corresponds to the asymmetric stretching of the N=C-N bonds of the imidazole rings. After coordination the band shifts to higher wavenumbers for the complex. The shift is +22 cm^{-1} for $[CuCl_2(thim)_2]$ and theoretical results predict shifts of +29 cm^{-1}, being in an excelent agreement with experimental values.

The bands at 1518 and 1589 cm^{-1} for thim correspond, respectively, to the C=C stretching of the thiophene ring and the C-C stretching mode of the atoms that

connect the rings. Theoretical results predict that upon coordination their relative intensities are reversed as can be seen in Figure 3.4 (b). The same tendency is observed in the experimental spectra of $[CuCl_2(thim)_2]$. The predicted shift to higher wavenumbers for the C-C stretching mode of the atoms that connect the rings is not observed experimentally. This band appears in the spectra of the complex at 1585 cm^{-1} and the small differences are probably due to the packing observed in the crystal structure which was not taken into account in calculations.

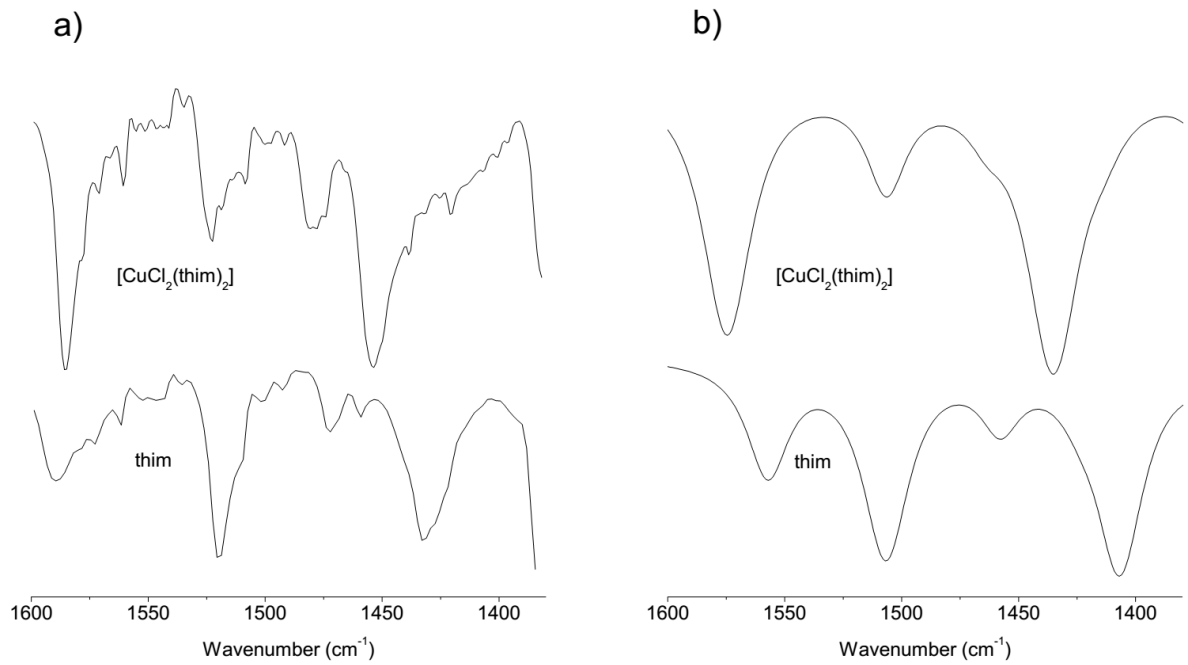

Figure 3.4. Partial **a)** Experimental ATR-FTIR and **b)** simulated PBE0/def2-TZVP spectra of thim and $[CuCl_2(thim)_2]$.

The C-S stetching mode is observed at 846 cm^{-1} in the ligand[102] and it is observed at 848 cm^{-1} in the spectrum of $[CuCl_2(thim)_2]$ (see Figure B.1, Appendix B). This assignment was confirmed by DFT, which predicted the band to be at 839 cm^{-1} for thim and at 843 cm^{-1} for the complex. The minor changes observed confirm that the sulfur atom of the thiophene ring is not involved in coordination, as it can be seen in the single crystal XRD structures.

3.3.4. Mass spectrometry

The mass spectrum of $[CuCl_2(thim)_2]$ given in Figure 3.5 shows the signal of the protonated ligand at *m/z* 151.1 and also the species $[Cu(I)(C_7H_6N_2S)_2]^+$ at *m/z* 363.3, whith matching isotopic pattern. Metal reduction is a widely occurring phenomenon in the electrospray process, especially for Cu(II) and Fe(III).[103,104] One hypothesis to explain Cu(II) reduction is that gaseous electrons produced by an electric discharge between the ESI capillary and the sampling cone can either reduce the metal ions on the surface of a droplet, or in the gas phase.[104]

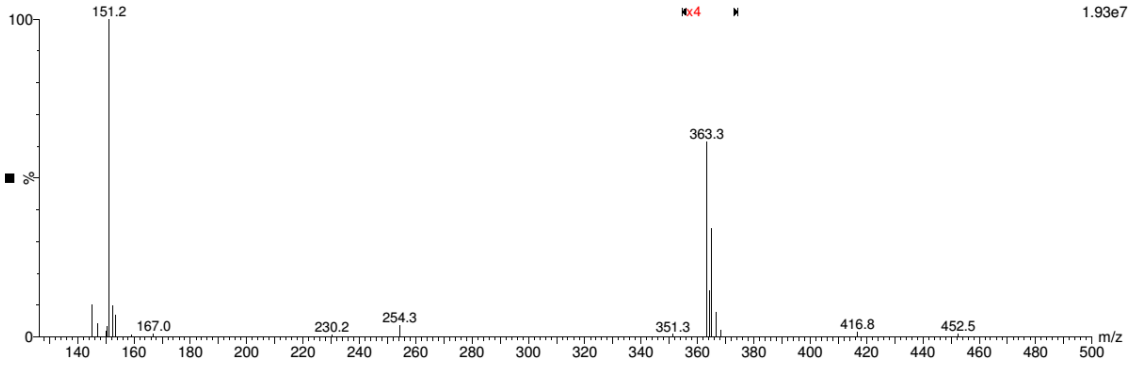

Figure 3.5. Mass spectrum of $[CuCl_2(thim)_2]$.

Neither $[Cu(II)Cl(C_7H_6N_2S)_2]^+$ (calculated *m/z* 398.9) nor $[Cu(II)Cl_2(C_7H_6N_2S)_2 + H]^+$ (calculated *m/z* 433.9) species were observed. The fact that thim acts as a monodentate ligand and does not chelate the metal ion probably contributes to the ease of metal reduction and chloride loss is favored in a water/ acetronitrile solution. Conductivity measurements of $[CuCl_2(thim)_2]$ in pure methanol do indicate that this complex undergoes partial solvolysis, with the molar conductivity value (95.2 $S \cdot cm^2 \cdot mol^{-1}$) within the range of 1:1 electrolytes in this solvent.[105] Both methanol and water have a similar donor number (around 18)[106], so the behavior of the complex in both aqueous solution (used in mass spectrometry experiment) and in methanolic solution (for conductivity measurements) should be similar.

3.3.5. UV – Visible spectroscopy and DNA interaction

The electronic spectra of a concentrated $[CuCl_2(thim)_2]$ methanolic solution is given in Figure 3.6. The d-d transition of $[CuCl_2(thim)_2]$ is observed as a broad band,

with low intensity and maximum at 768 nm. This is consistent with the fact that d-d transitions are prohibited by the Laporte selection rule. The blue-shift of the maximum observed for the d-d band when compared to $CuCl_2 \cdot 2H_2O$ dissolved in pure methanol (887 nm) is consistent with the stronger field induced by the ligand coordination.

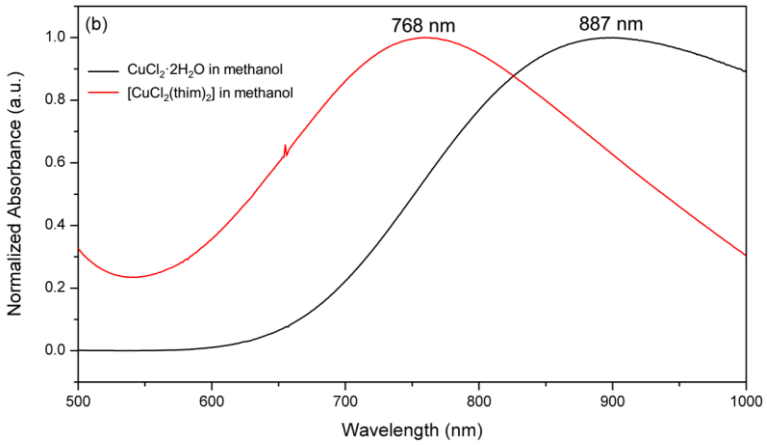

Figure 3.6. Normalized electronic spectra of methanolic $[CuCl_2(thim)_2]$ and $CuCl_2 \cdot 2H_2O$ solutions.

The UV-Visible spectrum of $[CuCl_2(thim)_2]$ was also recorded in the presence of increasing amounts of calf-thymus DNA (shown in Figure 3.7) as a first tool to evaluate its possible mode of interaction with DNA.[107–109] Bands in the range 200 - 400 nm of the spectrum without added DNA are assigned to $\pi \rightarrow \pi^*$ or $n \rightarrow \pi^*$ transitions of the ligand.

If an intercalative binding mode were in action, both hypochromism and batochromism should be observed. Batochromism would result from the coupling of π orbitals from the ligand with π orbitals from the DNA base pairs, therefore decreasing the $\pi \rightarrow \pi^*$ transition energy. However, the coupling orbital was already filled by electrons, so there is also a decrease in transition probabilities, so a concomitant hypochromism should be observed.[108,109] Neither of these phenomena were observed, which led us to exclude this type of interaction.

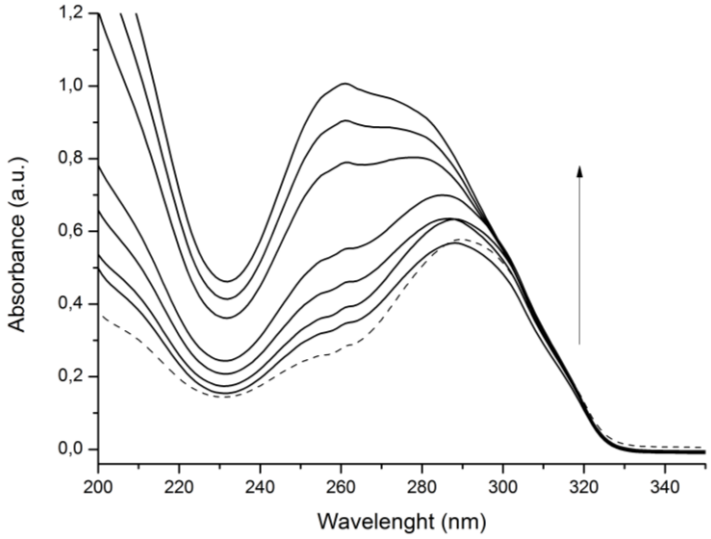

Figure 3.7. Electronic spectra of $[CuCl_2(thim)_2]$ (20 μmol·L^{-1}) with increasing amounts of an aqueous solution of CT-DNA (10 μmol·L^{-1}). The dashed line corresponds to the spectrum without DNA and solid lines are the spectra after DNA addition.

3.3.6. Fluorescence Studies with Ethidium Bromide

Ethidium bromide (ETBr) is a fluorescent compound known to intercalate with DNA, with enhancement of its fluorescence.[107] The fluorescence at 606 nm of solutions containing the compounds and DNA in two molar ratios ([compound]/[DNA]) were evaluated with increasing concentrations of ETBr in a 10 mmol·L^{-1} $NaClO_4$ solution.

From Figure 3.8, it can be observed that the highest fluorescence intensity (FI) is seen for the solution containing ETBr and DNA and the lowest FI is seen for the solution with only ETBr and none of the compounds. This behavior is expected as ETBr has a much higher FI when it interacts with DNA due to decreased quenching of its excited state by water after intercalating into the hydrophobic environment of the DNA molecule.[110]

All the compounds studied showed a reduced FI than the pure DNA solution with ETBr and a higher FI than the pure ETBr solution. Thim shows a higher FI than the complex. Also, thim does not show any considerable difference between the two molar ratios, indicating that the DNA is already saturated with thim in the low molar ratio.

The results show that thim and its Cu(II) complex interact with DNA considerably. Since the UV-Vis analyses indicated that the compounds do not intercalate with DNA, they probably have a mode of interaction that blocks the interaction of ETBr with DNA, but with no intercalation. Also, since thim shows the minor FI difference from pure DNA with ETBr, we could infer that the interaction of Thim with DNA is weaker than of the complex.

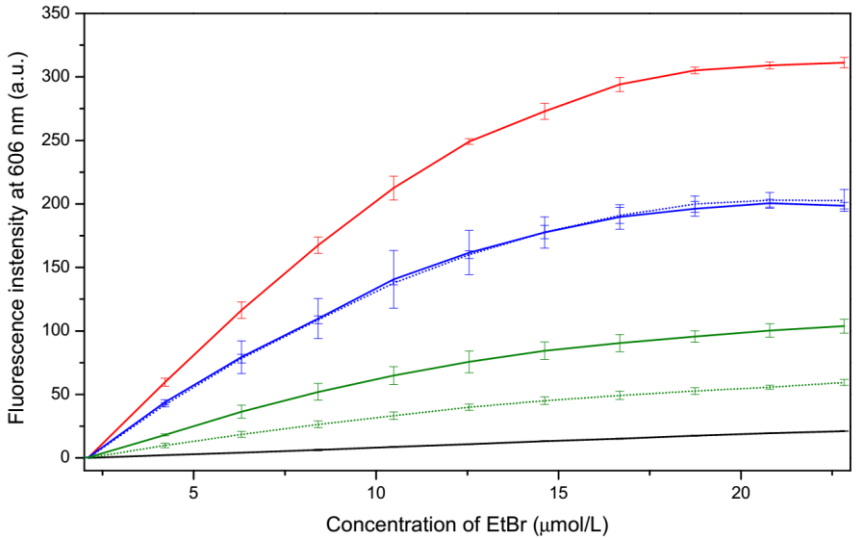

Figure 3.8. Fluorescence intensity of solutions containing the compounds studied and DNA with increasing concentrations of ETBr. The labels are: black: EtBr only; red: EtBr + CT–DNA; blue: thim; green: $[CuCl_2(thim)_2]$. Solid line: molar ratio (compound/DNA) of 0.1. Dotted line: molar ratio of 0.2.

3.3.7. Circular Dichroism (CD) of DNA

CD spectroscopy is a useful technique for evaluating DNA secondary structure and the changes in its conformation due to interaction with other molecules. According to the literature, the CD spectrum of DNA in B form consists of a negative band at 245 nm, due to right-handed helicity, and a positive band at 275 nm (not evaluated in our experiments) is related to base stacking.[111,112] In the calf-thymus DNA a positive band at 220 nm is also observed.[113]

Samples of CT-DNA were incubated with the compounds in 10 $mmol \cdot L^{-1}$ $NaClO_4$ aqueous solution at different molar ratios and the resulting spectra are shown in Figure 3.9.

Electrostatic and simple groove binding of small molecules to DNA do not usually lead to major distortions of the CD spectrum of CT-DNA, whereas intercalation leads to stabilization of the B-form of DNA, thus increasing the intensity of the helicity (245 nm) and stacking (275 nm) bands.[87,114]

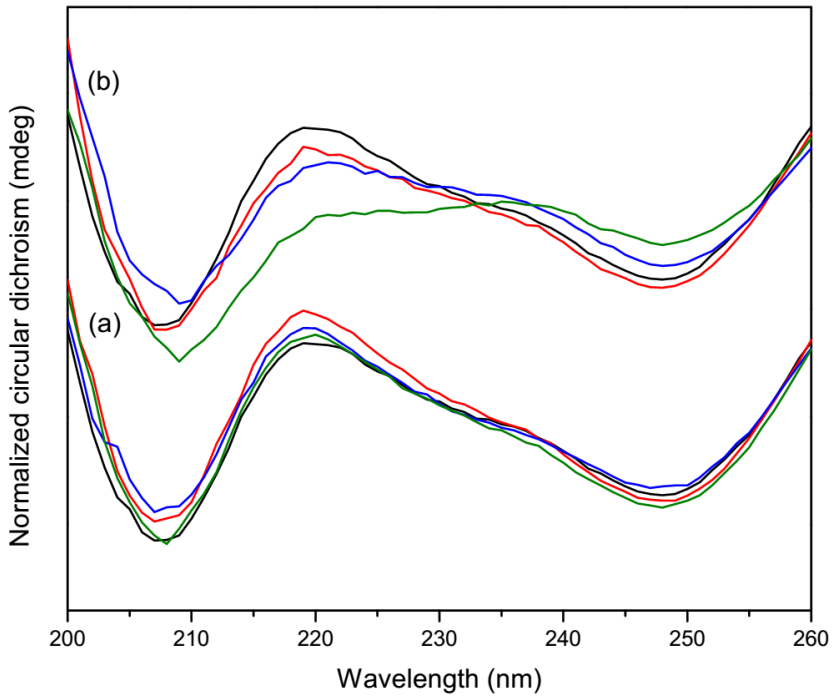

Figure 3.9. Circular Dichroism of CT-DNA (100 μM) samples in $NaClO_4$ aqueous solution (10 mM) incubated with (a) thim and (b) $[CuCl_2(thim)_2]$ (Labels are: black (DNA only), red (r_i = 0.10), blue (r_i = 0.20), green (r_i = 0.30).

It was observed that thim did not induce significant changes in the CD spectrum of CT-DNA in any molar ratio, so it may interact with DNA in a non-intercalative way. The Cu(II) complex, however, resulted in significant changes in the CD spectra even at low molar ratios. The band at 220 nm showed a significant decrease in intensity and bathochromic shifts for both complexes. The intensity of the CT-DNA band at 245 nm also decreased with increasing complex concentration, which indicates that the complex modify DNA helicity. Since major distortions and decreasing on the intensity of the band at 245 nm are observed for both complexes, non-covalent interactions can be ruled out for $[CuCl_2(thim)_2]$.

Isodichroic points are observed for the $[CuCl_2(thim)_2]$ complex around 230 nm, which is an indicative of more than one DNA conformation present in solution.[115]

This partial loss of B conformation of the DNA molecule may impede ETBr intercalation with DNA and lead to its fluorescence decrease, described previously.

3.3.8. Thermal denaturation of DNA

The thermal denaturation or melting temperature (T_m) of DNA is defined as the temperature when half of the total base pairs are unpaired.[116] It is the temperature in mid-transition from the folded to the unfolded forms of DNA.[117] This experiment is commonly used to study interactions of small molecules to DNA, since an increase in T_m indicates preferential binding to the folded form compared to the unfolded form.[117]

The results of thermal denaturation are shown in Table 3.3. The denaturation temperature was determined as the temperature in which the second derivative of the obtained curve is zero in the 60-80 ^oC interval (inflection point of the sigmoidal curve).

Table 3.3. Denaturation temperatures of DNA for free DNA, thim, $[CuCl_2(thim)_2]$ and Pd-Thim.

Compounds	Results	Δ(comp – DNA)
DNA	67.9 ± 0.9	0.0
thim	65.8 ± 0.7	-2.1
$[CuCl_2(thim)_2]$	68.5 ± 0.4	0.6

When a compound intercalates with DNA a high increase (between 8 to 13 °C) in T_m occurs.[116,118] Since only minor changes in T_m are observed for the tested compounds an intercalation mode of action is not probable to exist, as it was already seen in UV-Vis and CD studies previously discussed. In Table 3.3, it can be seen that thim promotes a stabilization of the unfolded form of DNA, as it decreases its T_m by approximately 2.1 °C.

It is known that imidazoles can interact with DNA nucleobases through hydrogen bonds.[119,120] It was shown by CD that thim interaction with DNA is not sufficiently strong to change conformation of DNA. CD and UV-Vis analysis showed that this compound does not intercalate. So, we propose that thim is binding to DNA through hydrogen bonds, causing the observed effect on T_m and partially impedes the intercalation of ETBr to DNA.

Table 3.3 also shows that the T_m for DNA incubated with $[CuCl_2(thim)_2]$ did not change, since the observed result is within the error. The previous CD analysis shows that $[CuCl_2(thim)_2]$ does not interact with DNA via non-covalent interactions. Long-range stabilization of the unfolded form can be compensated by local destabilization at sites of interstrand crosslinks.[121] $[CuCl_2(thim)_2]$ may then be binding to DNA via covalent bonds with no preferential mode between intrastrand and interstrand.

3.3.9. Antifungal activity assay

The disc diffusion method was used to evaluate the possible antifungal activity of $[CuCl_2(thim)_2]$. This compound was found to be active over the *Trichophyton mentagrophytes* strain, with an inhibition zone of 0.6 cm, which is smaller than the control compound amphotericin, which showed an inhibition zone of 2.6 cm. However, $[CuCl_2(thim)_2]$ was found to be inactive over *Fusarium moniliforme* and *Candida albicans*. *T. mentagrophytes* is one of the major organisms involved in dermathophytosis, the infection of keratinized tissues in humans and other animals.[122] The free ligand thim was inactive over all three tested fungi, which highlights the effect of complexation on the biological properties of the molecule.

3.4. Partial conclusions

A novel Cu(II) complex with thim was synthesized and fully characterized. Elemental and mass spectrometric measurements showed that the complex has the composition 1:2:2 metal/ligand/chloride. The structure of $[CuCl_2(thim)_2]$ was solved by single crystal XRD. The complex showed the coordination of thim to the metal ions by the imine nitrogen of the imidazole group in a *trans* geometry, with an increase in the torsion angle between the rings. The DNA interaction of thim and $[CuCl_2(thim)_2]$ was evaluated by different techniques. The biophysics studies indicate that thim interacts mainly via hydrogen bonding with CT-DNA, while the Cu(II) complex may form covalent bonds with CT-DNA, which is consistent due to the presence of coordinating atoms from the nucleobases, especially nitrogen. However, the ability of this complex to induce DNA cleavage in the absence and in the presence of a reducing agent was

not evaluated. Moreover, [$CuCl_2(thim)_2$] showed antifungal activity over *Trichophyton mentagrophytes,* but with an inhibition zone much lower than the control amphotericin.

Chapter 4

Synthesis, characterization and preliminary antimicrobial assays of copper(II) complexes with 2-(imidazole-2-yl)heteroaryl ligands

The content of this chapter is an adaptation of an article in preparation entitled “Synthesis, characterization and preliminary antimicrobial assays of copper(II) complexes with 2-(imidazole-2-yl)heteroaryl ligands”.

The introduction of this chapter was not included since it is an adaption of the content already presented in Chapter 1. My contribution to this work was in the syntheses and characterization of the copper(II) complexes and partial writing of the publication.

4.1. Experimental Section

4.1.1. Materials and Methods

2-Pyridinecarbonitrile (99%), 2-pyrazinecarbonitrile (99%), 2-pyrimidinecarbonitrile (97%), aminoacetaldehyde dimethyl acetal 99 % were purchased from Sigma Aldrich. $CuCl_2 \cdot 2H_2O$ (99%) was purchased from Vetec – Sigma (Brazil). Metallic sodium was purchased from Riedel-de Haen. All other reagents and solvents were used as received, without further purification.

Elemental analyses were performed on a Perkin Elmer 2400 CHNS/O Analyzer. Conductivity measurements were performed using a LAB1000 conductivity meter. The solutions were prepared in deionized water, with concentrations of 1.10^{-3} $mol \cdot L^{-1}$.

Electronic spectra in the 190-1100 nm range were acquired by using a 1.0 cm quartz cuvette in a diode array HP8453 UV/Visible absorption spectrophotometer.

Infrared spectroscopy measurements were performed on an Agilent Cary 630 FTIR spectrometer, using the Attenuated Total Reflectance (ATR) method, with a diamond cell. Spectra were recorded from 4000-400 cm^{-1}, with 64 scans and resolution of 4 cm^{-1}. Raman spectra were recorded using a Jobin-Yvon T64000 single spectrometer system, equipped with a confocal microscope and a nitrogen-cooled change coupled device (CCD) detector. The spectra were collected using a 632 nm (2 mW) laser at room temperature and with solid samples.

The ^1H NMR spectra of the ligands were recorded in DMSO-d6, in a Bruker Avance III 500 MHz (11.7 T) spectrometer.

Electrospray ionization quadrupole time-of-flight mass spectrometric (ESI-QTOF-MS) measurements were carried out in a Waters Xevo Q-TOF instrument. The samples were analyzed in a 1:1 methanol:water solution with addition of 0.10% (v/v) formic acid. Each solution was directly infused into the instrument's ESI source and analysed in the positive mode, with capillary potential of 3.00 kV, source temperature of 120 ^oC and nitrogen gas for desolvation.

X-Ray Powder Diffraction analyses were performed with a Shimadzu XRD7000 diffractometer, with a copper tube operating at 40 kV and 30 mA. The divergence and scatter slits were of 1.0^o and the receiving slit was of 0.30 mm. The

scanning was performed in the continuous mode, from 5 to 50^{o} and scan speed of 2^{o}·min^{-1}. Data collection for [$CuCl_2$(impm)] single crystals was performed with a Bruker Apex II CCD diffractometer with graphite monochromated Mo - Kα (λ = 0.71703 Å) radiation. More information about refinement and data treatment can be found in **Chapter 2** – subitem 2.2.3.

Molecular modeling calculations were performed according to details presented in **Chapter 3** – subitem 3.2.3.

4.1.2. Syntheses of the ligands

The ligands were synthesized in accordance to a reported method for the preparation of 2-substituted imidazoles.[59]

2-(Imidazol-2-yl)pyridine (impy) 2.60 g (25 mmol) of 2-pyridinecarbonitrile, 10 mL MeOH and 0.47 mL (2.5 mmol) of a 30 % solution of NaOMe in MeOH were added to a 100 mL round-bottom flask,. The mixture was stirred for 1 hour at 40 °C. 2.72 mL (25 mmol) of aminoacetaldehyde dimethyl acetal, followed by 2.75 mL of AcOH were added dropwise to the mixture and heated under reflux for 30 min. After the mixture was left to cool at room temperature, 15 mL of MeOH and 12.5 mL of HCl 6 mol·L^{-1} were added and the reaction was heated under reflux for 4.5 h. After that, the solution was evaporated to dryness and 27.5 a freshly prepared warm 1 g·mL^{-1} solution of K_2CO_3 was added dropwise, to adjust the pH to 10. This resulted in a reddish suspension that, after cooled to room temperature, was filtered and the filtrate was extracted with 50 mL of CH_2Cl_2. The resulting red solution was evaporated to dryness and recrystallized in boiling ethyl acetate. The product was obtained as a dark yellow powder, which was dried under vacuum. Yield 60 %. Anal. Calc. for $C_8H_7N_3$ (%): C 66.19; H 4.86; N 28.95. Found: C 65.58; H 5.06; N 28.48. ^{1}H NMR (500 MHz, DMSO-d_6): δ 7.160 (s, 2H), 7.362 (ddd, 1H, J = 1.0, 5.0, 7.5 Hz), 7.888 (td, 1H, J = 1.5, 7.8 Hz), 8.044 (dt, 1H, J = 1.0, 8.0 Hz), 8.602 (ddd, 1H, J = 1.0, 1.5, 4.5 Hz), 12.770 (br) (for the spectrum, see Figure C.1). HRMS (ESI-(+)-TOF) (*m/z*): calcd for $C_8N_3H_8$ [M+H$^+$]$^+$: 146.07, found: 146.07.

2-(Imidazol-2-yl)pyrazine (impz) Experimental details for this molecule were reported in **Chapter 2** – subitem 2.2.2.

2-(Imidazol-2-yl)pyrimidine (impm) To a 100 mL flask were added 2.62 g (25 mmol) of 2-pyrimidinecarbonitrile, 10 mL of MeOH and 0.47 mL of a 30 % solution of NaOMe in MeOH. The mixture was kept under vigorous stirring at room temperature for 1.5 hour. Then, 1.63 mL (15 mmol) of aminoacetaldehyde dimethyl acetal was added, followed by dropwise addition of 2.75 mL of AcOH. The system was heated under reflux for 30 minutes. After cooling, 15 mL of MeOH and 12.5 mL of HCl 6 $mol \cdot L^{-1}$ were added and the system was heated under reflux for 5 hours. After the reaction time, the solvent was rotary evaporated and 27.5 mL of a warm K_2CO_3 1 $g \cdot mL^{-1}$ solution were carefully added, forming a yellowish suspension which after cooling, was filtrated in a Buchner funnel. This ligand was obtained as a pale yellow powder. Yield 68 %. Anal. Calc. for $C_7H_6N_4$ (%): C 57.53; H 4.14; N 38.34. Found: C 57.52; H 4.20; N 39.06. ^{1}H NMR (500 MHz, DMSO-d_6): δ 7.234 (s, 2H), 7.442 (t, 1H, J = 5.0 Hz), 8.875 (d, 2H, J = 5.0 Hz), 12.972 (br) (for the spectrum see Figure C.2). HRMS (ESI-(+)-TOF) (*m/z*): calcd for $C_7N_4H_7$ $[M+H^+]^+$: 147.07, found: 147.06.

4.1.3. Syntheses of the Cu(II) complexes

The three complexes were synthesized by the mixture of methanolic solutions of the ligands and methanolic solution of $CuCl_2 \cdot 2H_2O$, with 1:1 stoichiometry (metal:ligand), under stirring and at room temperature for four hours.

[$CuCl_2$(impy)] Starting solutions: 1.0 mmol in 10 mL. A light-green solid precipitated and the powder was collected by filtration, washed with a small amount of cold methanol and dried under vacuum. The yield was 52%. This complex is soluble in water and DMSO and slightly soluble in methanol and ethanol. Anal. Calc. for $CuCl_2C_8H_7N_3$ (%): C 34.36; H 2.52; N 15.02. Found: C 34.49; H 2.75; N 14.97. Molar conductivity in deionized water ($S \cdot cm^2 \cdot mol^{-1}$): 203.7.

[$CuCl_2$(impz)] Starting solutions: 0.5 mmol in 5 mL. A green solid precipitated and the powder was collected by filtration, washed with a small amount of cold methanol

and dried under vacuum. The yield was 38%. This complex is soluble in water, DMSO and DMF and slightly soluble in methanol and ethanol. Anal. Calc. for $CuCl_2C_7H_6N_4$ (%): C 29.96; H 2.16; N 19.97. Found: C 30.24; H 2.46; N 19.78. Molar conductivity in deionized water ($S \cdot cm^2 \cdot mol^{-1}$): 206.9.

[$CuCl_2$(impm)] Starting solutions: 0.5 mmol in 5 mL. After four hours of stirring, no precipitation occurred. The solution was rotaevaporated to dryness and the remaining green solid was thoroughly washed with cold ethanol and dried under vacuum. The yield was 33 %. This complex is soluble in water, methanol, DMSO and DMF. Anal. Calc. for $CuCl_2C_7H_6N_4$ (%): C 29.96; H 2.16; N 19.97. Found: C 29.58; H 2.32; N 19.66. Molar conductivity in deionized water ($S \cdot cm^2 \cdot mol^{-1}$): 288.2. Single crystals of Cuimpm were obtained after slow concentration of a methanolic solution of this complex.

4.1.4. Antimicrobial assays

The Minimal Inhibitory Concentration (MIC) of impy, impz and impm and their corresponding Cu(II) complexes was evaluated over the Gram-positive *S. aureus* (ATCC 25923) and the Gram-negative *E. coli* (ATCC 25922) bacterial strains, according to standard procedures.[123]

The stock solutions of the ligands were prepared in DMSO and of the complexes in water. The strains were inoculated in tubes containing 2.0 mL of Brain Heart Infusion (BHI) and incubated for 18 hours at 35-37 ^oC. Sufficient inoculum of each bacterial suspension was added to new tubes of sterile BHI up to the value of 1.0 turbidity on the McFarland nephelometric scale (~ 3.0 x 10^8 $CFU \cdot mL^{-1}$). 100 µL of the samples (stock solutions of concentration 20 $\mu g \cdot \mu L^{-1}$) were added to different wells of a 96 well multiplate. Afterwards, 100 µL of the bacterial suspensions were added to serial dilution, up to a 0.5 McFarland nephelometric scale (~ 3.0 x 10^8 $CFU \cdot mL^{-1}$) and a final volume of 200 $\mu L \cdot well^{-1}$. The microplates were incubated for 18 h at 35-37 ^oC. After the incubation time, 15 µL of a 0.01 % resazurin solution (in sterile water) were added to each well. After 4 hours of reincubation, the measurement was performed. These experiments were performed in collaboration

with Professor Dr. Wilton Rogério Lustri and his research group (QUIMMERA) from UNIARA.

Antifungal activity assays were performed as reported in **Chapter 3**, subitem 3.2.9.

4.2. Results and discussion

4.2.1. Synthesis

The ligands were synthesized according to a procedure[59] for the preparation of 2-substituted imidazoles and the characterization results are consistent with the reported data. Elemental analyses of the prepared copper(II) compounds matched the proposed composition of one copper, one 2-(Imidazol-2-yl)heteroaryl ligand and two chlorides, resulting in a net zero charge for the complexes.

However, conductivity measurements of the Cu(II) compounds in deionized water (values reported in Experimental Section) showed that they behave as 1:2 electrolytes[124,125], so the chlorides are readily hydrolyzed in aqueous solution, and possibly lead to the formation of a charged $[Cu(OH_2)_2(impx)]^{2+}$ (x = y, z or m) complex. This is consistent with the behavior of the analogous copper complex with bipyridine in water.[126]

Mass spectrometry results showed the $[Cu(II)Cl(impx)]^+$ ion for all complexes and the $[Cu(I)(impx)]^+$ ion resultant from the loss of the second chloride and concomitant copper reduction, though no adducts with water were easily identified. Copper(II) reduction is a common process in mass spectrometry experiments.[103] The mass spectra of all complexes are given in Appendix C (Figures C.3 to C.5).

4.2.2. X-ray diffraction

The crystalline structure of $[CuCl_2(impy)]$ has already been solved in the literature[61] by X-Ray Powder Diffraction and refined using Rietveld analysis and the assymetric unit of this compound is given in Figure 4.1 (a). The pattern from the synthesized $[CuCl_2(impy)]$ (Appendix C, Figure C.6) is in agreement with the one already reported, thus indicating that the samples have similar structures. Each

copper center interacts axially with a chloride from an adjacent molecule with length that may be considered a weak bond, characteristic of Jahn-Teller distortions for the Cu(II) electronic configuration.[22]

Even though several attempts of obtaining single crystals from [$CuCl_2$(impz)] did not yield any suitable for diffraction, its powder diffractogram was recorded and is shown with the one recorded from impz in Appendix C, Figure C.5. [$CuCl_2$(impz)] has a low cristallinity profile, while the corresponding ligand impz is much more crystalline, as proved by the greater signal intensity (the data were normalized for better comparison) and shorter peak width. It is hypothesized that the three complexes may adopt similar structures and this is supported from their chemical similarity ,as seen from the data of other characterization techniques.

Single crystals of [$CuCl_2$(impm)] suitable for diffraction were obtained after slow evaporation of a methanolic solution. This molecule crystallized in the orthorrhombic crystal system, space group $P2_12_12_1$. The copper ion is coordinated to nitrogen atoms from the pyrimidine and imidazole rings and to two chlorides. The calculated τ_4 geometry index[127] for this complex was 0.09, which indicates a slightly distorted square planar geometry, as seen in Figure 4.1 (b). The angle between the planes of the imidazole and pyrimidine rings show that they are almost coplanar in this complex (angle = 1.27(15)^o). Crystallographic information of [$CuCl_2$(impm)] can be found in Table 4.1.

When comparing the bond lengths reported for [$CuCl_2$(impy)][61] to the values in [$CuCl_2$(impm)], the Cu-N_{imid} values are of the same magnitude (1.951(5) Å and 1.975(5) Å, respectively). The Cu-$N_{pyridine}$ bond length (2.117(5) Å) is longer than Cu-$N_{pyrimidine}$ (2.078(2) Å). However, both Cu-N bond lengths are within the average values found in CSD[74] for Cu-N (1.970(17)) Å in imidazole moieties and 2.061(50) Å for pyrimidine moieties) in tetracoordinated copper(II) complexes. The Cu-Cl1 and Cu-Cl2 bond lengths are 2.2489(6) and 2.2425(6) Å, respectively. These values are also in agreement with those found in the CSD (2.242(31) Å) for the average Cu-Cl distance in a tetracoordinate environment.

Table 4.1. Crystallographic data of $[CuCl_2(impm)]$ structure.

Empirical formula	$C_7H_6Cl_2CuN_4$
Coordination formula	$[CuCl_2(C_7H_6N_4)]$
Molecular weight ($g \cdot mol^{-1}$)	280.61
Temperature (K)	296
Wavelength (Å)	Mo - K_α 0.71073
Crystal system	Orthorrhombic
Space Group	$P2_12_12_1$
a (Å)	6.3102(6)
b (Å)	8.5236(8)
c (Å)	17.3125(17)
α (^{o})	90
β (^{o})	90
γ (^{o})	90
V ($Å^{-3}$)	931.16(15)
Z	4
$\rho_{calcd.}$ ($g\ cm^{-3}$)	2.002
F(000)	556
μ (mm^{-1})	2.878
θ range (^{o})	2.664 – 30.508
Reflections collected/ independent	13620/ 2607 (R_{int}= 0.0280)
Data/ restraints/ parameters	2607/ 0/ 137
R_1,wR_2 [I > 2σ (I)]	0.0203, 0.0457
Diff. peak and hole ($e/Å^{-3}$)	0.39 and -0.28
Goodness-of-fit on F^2	1.037
CCDC number	1441825

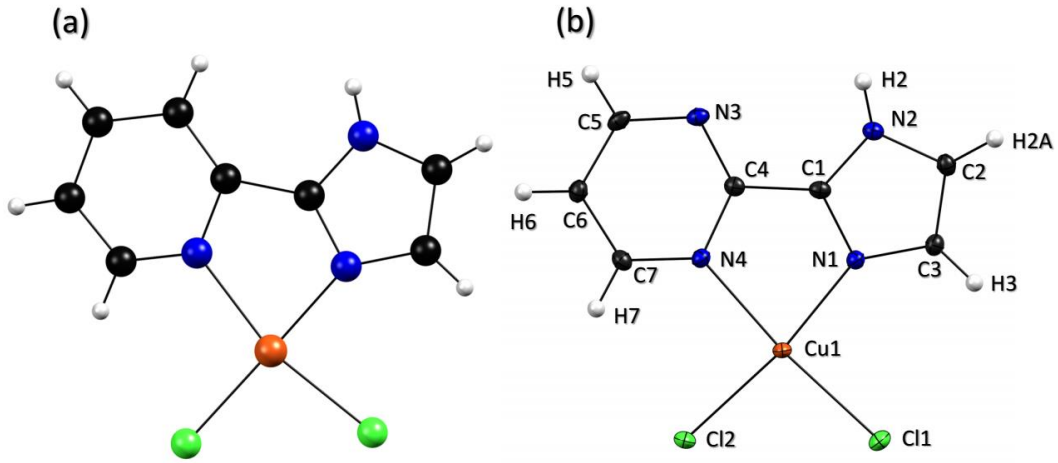

Figure 4.1. Comparison of the structures of **(a)** $[CuCl_2(impy)]$ and **(b)** $[CuCl_2(impm)]$. $[CuCl_2(impy)]$ was adapted from the CIF from reference [61] and represented by full circles due to powder diffraction measurements. Atomic displacement ellipsoids of $[CuCl_2(impm)]$ are at the 50% probability level. Hydrogen atoms are represented by white spheres.

In the crystal structure of [$CuCl_2$(impm)], there is no significant axial bonding nor interaction of a copper center to chlorides from adjacent molecules (see Figure 4.2 (b)), though they do superimpose. The measured values of the hypothetic interactions of a copper center with chlorides located directly above and below it [Cu1···Cl2^{i} (i = ±1/2 + x, 3/2 - y, -z)] are 3.1587(10) and 3.1822(10) Å, respectively. In many Cu(II) structures there are some minor axial interactions, but the geometry around the copper center can be considered square planar if the axial distances are greater than 3.0 Å.[22] As mentioned before, [$CuCl_2$(impy)] shows a Cu-Cl axial interaction (Figure 4.2 (a)), with value 2.847(5) Å[61], thus showing the difference in packing between the two complexes.

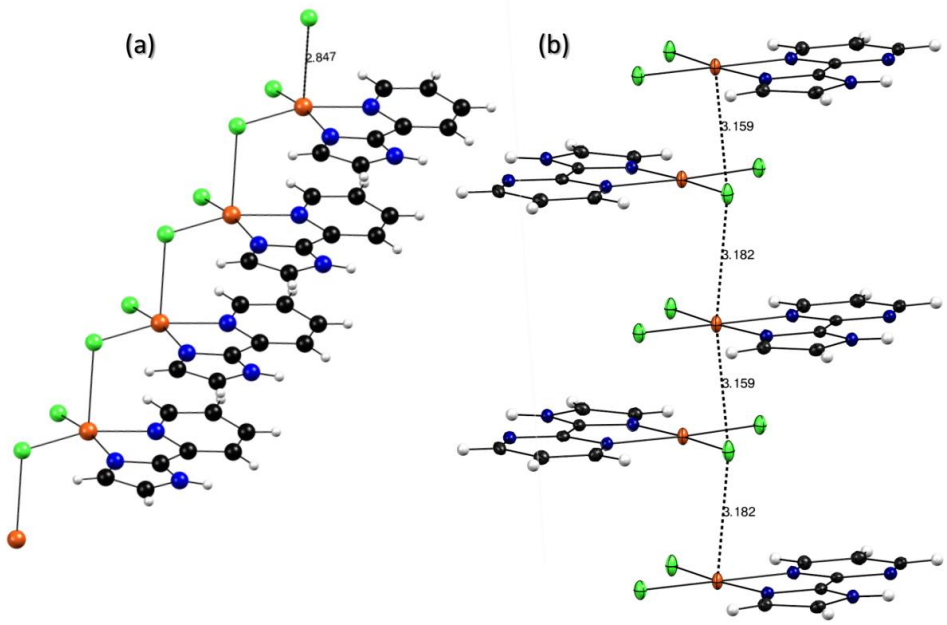

Figure 4.2. Representations of **(a)** Cu–Cl···Cu in [$CuCl_2$(impy)] and **(b)** Cu···Cl···Cu in [$CuCl_2$(impm)]. [$CuCl_2$(impy)] was adapted from the CIF from reference [61].

Short[77] hydrogen bonds connect the [$CuCl_2$(impm)] molecules, forming an infinite 2D chain motif through N2-H2···Cl2^{ii} [H···A 2.32 Å, A···D 3.1710(18) Å, < (DHA) 169.3˚ (ii = x, -1 + y, z)]. A weaker interaction[78] involves C3-H3···Cl1^{iii} [H···A 2.87 Å, A···D 3.444(2) Å, < (DHA) 120.9˚ (iii = 1 - x, -1/2 + y, -1/2 - z)] (Figure 4.3). π···π offset interactions contribute to the stacking of [$CuCl_2$(impm)] molecules and the centroid···centroid average distance is of 3.6 Å, which is within the values usually found for N-heterocycles (3.3. to 3.8 Å).[69]

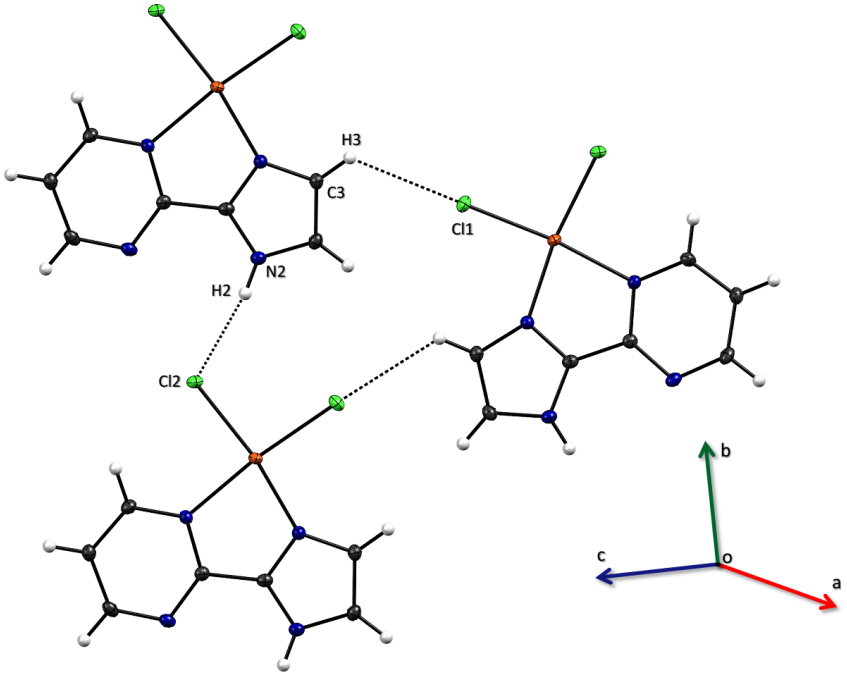

Figure 4.3. Molecular interactions in [$CuCl_2$(impm)].

4.2.3. Molecular modeling

Since the structure of [$CuCl_2$(impz)] was not solved by diffraction, molecular modeling was performed to obtain information about this compound. The equilibrium geometry of [$CuCl_2$(impz)] is shown in Figure 4.4, along with its frontier Kohn-Sham orbitals.

It can be seen that in the equilibrium geometry, this complex adopts the same coordination as [$CuCl_2$(impy)] and [$CuCl_2$(impm)], with bonding of Cu(II) to the nitrogens of the pyrazine and imidazole rings and to two chlorides, in a square planar geometry. The values of important bond lengths and angles of [$CuCl_2$(impz)] can be found in Table 4.2. No major differences are found between the calculated values for the three different complexes, which is consistent with their similarity in chemical composition and geometry.

The SOMO (α orbital) of [$CuCl_2$(impz)] has a contribution of the $3d_{x^2-y^2}$ metal orbital, as expected for a d^9 configuration in a square planar geometry. The LUMO (α and β) consist mainly of the π^* system of the impz ligand, with a contribution from Cu(II).

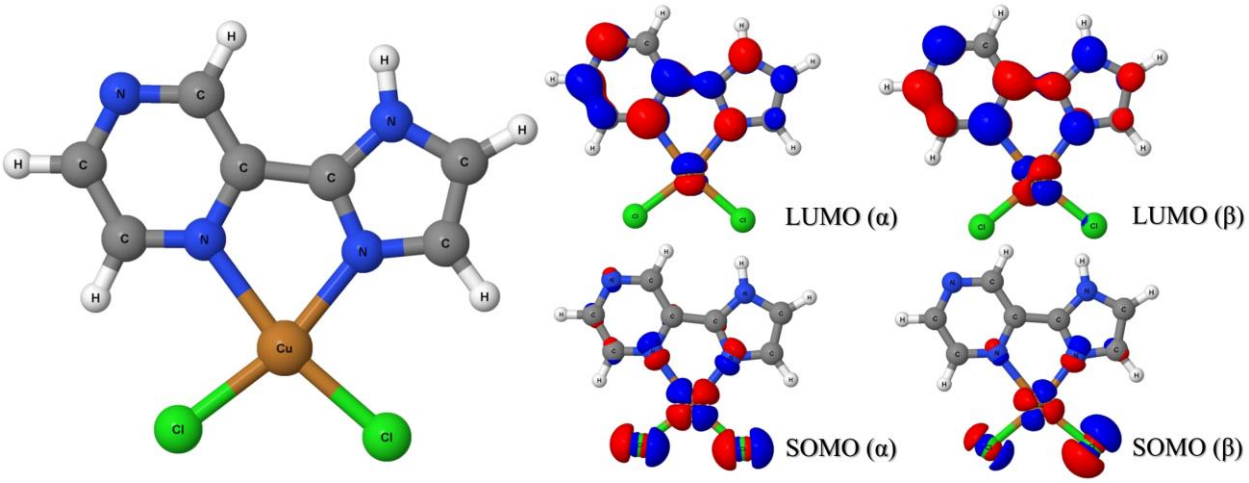

Figure 4.4. Equilibrium geometry and frontier Kohn-Sham orbitals obtained for [$CuCl_2$(impz)] by DFT calculations with PBE0/def2-TZVP.

The optimized geometries of [$CuCl_2$(impy)] and [$CuCl_2$(impm)] (see Appendix C, Figures C.8 and C.9, respectively) are in agreement with those found experimentally, as shown in the bond lengths and angles values from Table 4.2. The main deviations are the overestimations of Cu-N bond lengths and the Cl-Cu-Cl bond angle. The latter can be explained because of the existence of hydrogen bonding involving the chloride ions in the solid state, which are not taken into account in the calculations.

The Kohn-Sham orbitals for these compounds (Figures C.8 and C.9) show some differences which highlight the effect of increasing the number of nitrogen atoms (or changing its position) on the electronic structure of the complexes. This can be seen from the frontier orbitals of either [$CuCl_2$(impm)] or [$CuCl_2$(impz)] compared to [$CuCl_2$(impy)]. The first two complexes have an extra nitrogen atom which shows contribution for the frontier orbitals, as opposite to the corresponding carbon atom in [$CuCl_2$(impy)].

Table 4.2. Optimized bond lengths and angles of the copper(II) complexes.

Bond length (Å) or angle (°)	**[$CuCl_2$(impy)] (experimental)***	**[$CuCl_2$(impz)]**	**[$CuCl_2$(impm)] (experimental)**
Cu-N_{imid}	2.036 (1.951(5))	2.036	2.042 (1.9750(17))
Cu-N_{pyr}**	2.199 (2.119(5))	2.222	2.216 (2.0779(16))
Cu-$Cl_{t,\ imid}$***	2.197 (2.195(5))	2.191	2.196 (2.2425(6))
Cu-$Cl_{t,\ pyr}$	2.220 (2.255(5))	2.214	2.212 (2.2489(7))
N-Cu-N	76.10 (78.72(19))	75.66	76.18 (80.48(7))
Cl-Cu-Cl	100.97 (92.70(18))	101.74	101.93 (94.67(2))

* from reference [61]

** pyr = pyridine, pyrazine or pyrimidine

*** Cl *trans* to imidazole ring

4.2.4. Vibrational spectroscopies

The full experimental and theoretical FTIR spectra of the compounds are shown in Appendix C, Figures C.10 and C.11. The N-H and C-H stretchings[128] were expected to not differ much in energy when comparing the complexes, as these do not change much in structure to alter these vibrations. The calculated values for these stretchings are very similar and above 3000 cm^{-1}. The experimental band pattern next to the 3000 cm^{-1} region is also quite similar for all complexes, as expected.

The region from 1700 to 1200 cm^{-1} shown in Figure 4.5, however, is quite distinct for the complexes. From 1600 to 1400 cm^{-1}, combinations of C-$C_{aromatic}$ and C-$N_{aromatic}$ vibrations from the rings are observed[128], which justifies the differences in the spectra, as the six-membered N-heterocyle change in each complex.

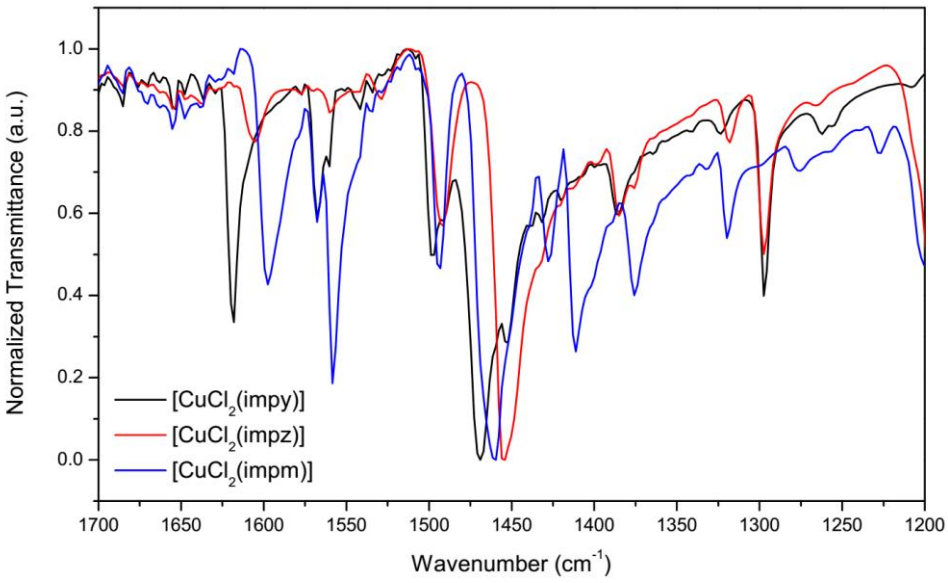

Figure 4.5. Partial ATR Infrared spectra of the copper(II) complexes.

Notably the bands observed at 1468, 1454 and 1459 cm^{-1}, for $[CuCl_2(impy)]$, $[CuCl_2(impz)]$ and $[CuCl_2(impm)]$, respectively, follow the trend of pKa values (defined from the equilibrium between the protonated and deprotonated N-heterocycles) of the free six-membered N-heterocycles (5.23, 0.65 and 1.21 for pyridine, pyrazine and pyrimidine, respectively)[129]. Results from molecular modelling showed that these vibrations have a component of streching of the C-N-$C_{aromatic}$ group (from the six-membered ring) involved in coordination to copper(II) and components from imidazole vibrations as well. An attempt to rationalize this energy order is indirectly relate it to the strength of the Cu-N bond. A stronger bond to Cu(II) (as in $[CuCl_2(impy)]$) would hamper the C-N-$C_{aromatic}$ stretching energy, thus leading to an increase of the energy required for such vibration to occur.

In order to investigate metal-ligand vibrations, the Raman spectra of the solid complexes were recorded from 100 to 600 cm^{-1} and are shown in Figure 4.6.

The attribution of copper-N and copper-Cl vibrations in imidazole[130], bipyridine and phenantroline[131,132] complexes has been studied in the past. However, exact attribution of the bands is misleading, as both vibrations tend to fall within the 200 – 300 cm^{-1} region, as opposite to Cu-N from exclusive σ donors, as ammonia and ethylenediamine[133], which fall well-above 300 cm^{-1}.

In the $[CuCl_2(bipy)]$ complex[131], two infrared bands were attributed to Cu-Cl stretching vibrations at 259 and 304 cm^{-1} and one band was assigned as Cu-N at 292 cm^{-1}. For the corresponding $[CuCl_2(phen)]$ complex, the Cu-Cl stretching was

assigned to two bands at 281 (shoulder) and 288, while Cu-N was assigned at 313 cm^{-1}. These attributions were made by comparing similar complexes with varying counterions.[131] Similarly, a $[CuCl_2(imidazole)_2]$ complex (polymeric, O_h symmetry) also showed two bands assigned to Cu-Cl at 276 and 245 cm^{-1} and one Cu-N at 306 cm^{-1}. The attributions in this paper were made by studying isotope substitution (^{63}Cu and ^{65}Cu).[130]

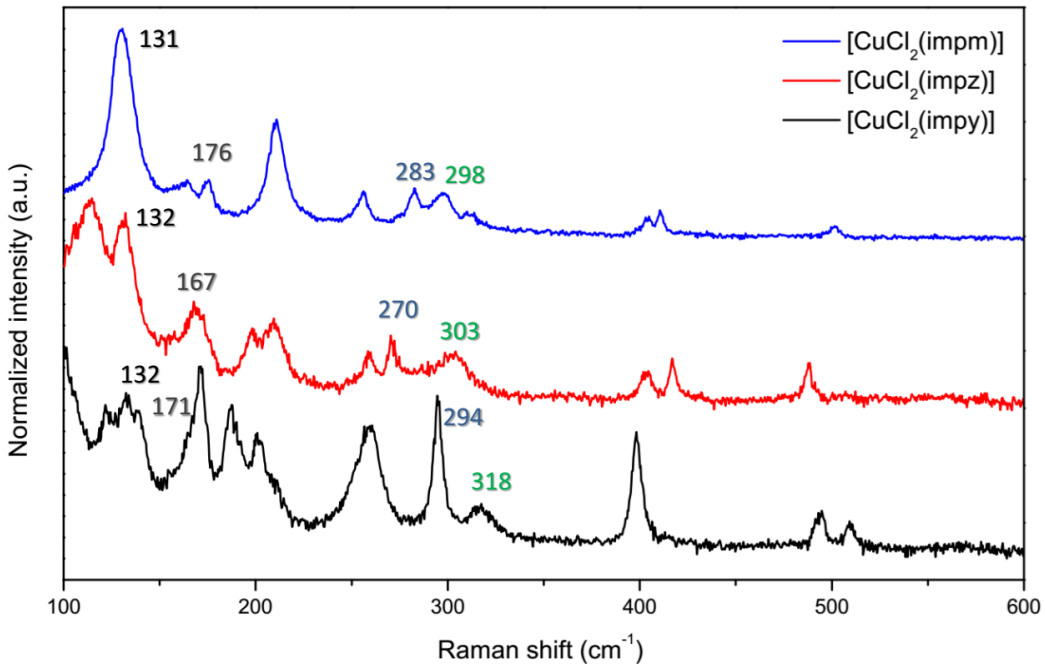

Figure 4.6. Raman spectra of the $[CuCl_2(impx)]$ complexes. Values reported in cm^{-1}.

The infrared calculations performed in this work predicted that there should be two bands with a component of Cu-Cl stretching around 320 cm^{-1} for the bond *trans* to the six-membered ring and 345 cm^{-1} for Cu-Cl *trans* to the imidazole ring. Even though the intensity of these calculated (infrared) transitions cannot be directly compared to those observed in the Raman spectrum from Figure 4.6, the presence of bands within 250 and 350 cm^{-1} are strong evidences of Cu-Cl stretchings in all three molecules. An attempt of band assignment, along with calculated infrared values are given in Table 4.3.

Contrary to what was reported for Cu-N stretchings, calculations showed that these vibrations should occur at 140 cm^{-1} for the $Cu\text{-}N_{pyr}$ (pyr = pyridine, pyrazine and pyrimidine) bond and 180 cm^{-1} for the bond to imidazole. These data suggest that the bond strength is greater for imidazole than for the six-membered rings, but there was

no significant difference (see Table 4.3) in bond strength between the pyridine, pyrazine and pyrimidine rings. Calculations of Raman spectra would allow more direct comparison and are under progress.

Table 4.3. Cu-L stretching vibrations in $[CuCl_2(impx)]$ complexes.

Stretching vibration (cm^{-1})	**$[CuCl_2(impy)]$ (calculated)**	**$[CuCl_2(impz)]$ (calculated)**	**$[CuCl_2(impm)]$ (calculated)**
υ Cu-N_{imid}	171 (184)	168 (183)	176 (180)
υ Cu-N_{pyr*}	132 (142)	132 (139)	131 (136)
υ Cu-$Cl_{t,\ imid**}$	318 (343)	303 (347)	298 (343)
υ Cu-$Cl_{t,\ pyr}$	294 (319)	270 (321)	283 (322)

* pyr = pyridine, pyrazine or pyrimidine

** Cl *trans* to imidazole ring

It must be highlighted that the three spectra have similar patterns, which is a spectroscopic evidence that supports the hypothesis these compounds do adopt similar geometries in the solid state. The axial Cu-Cl bond present in $[CuCl_2(impy)]$ (as discussed in diffraction section) and the fact that it is the complex with only one nitrogen atom in the six-membered ring may be the reasons of the observed differences.

4.2.5. Electronic spectroscopy

Electronic spectra of the concentrated copper(II) complexes solutions were recorded in order to observe d-d transitions of low absorptivity (Figure 4.7 and Table 4.4), whereas diluted solutions were studied to obtain insights on the intraligand transitions (Figure 4.8). It must be highlighted, however, that, as seen from conductivity measurements, the structures determined by crystallography are not maintained in aqueous solutions, as the chlorides are readily hydrolized. In order to maintain a high chloride concentration, the spectra were recorded in aqueous KCl 0.1 $mol \cdot L^{-1}$.

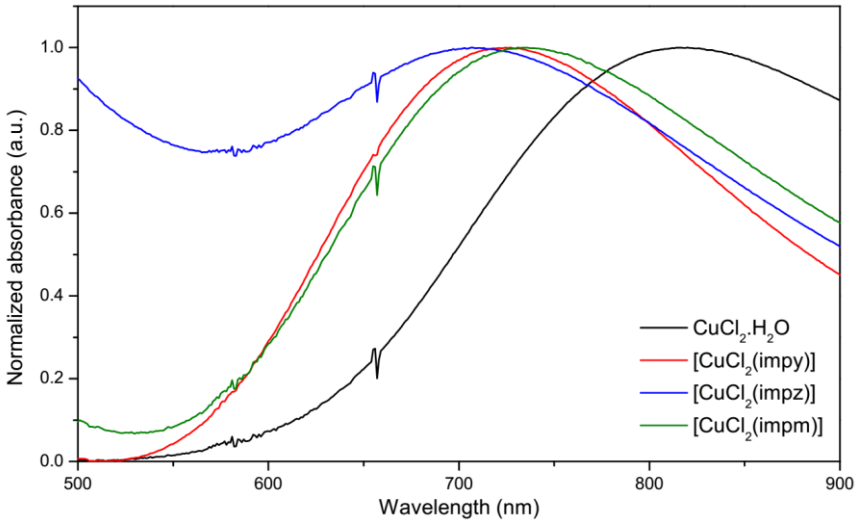

Figure 4.7. Electronic spectra of concentrated [$CuCl_2$(impx)] complexes solutions in aqueous KCl 0.1 mol·L^{-1}.

Figure 4.7 shows that all complexes had d-d transitions with absorption maxima blue-shifted in comparison to $CuCl_2 \cdot 2H_2O$ (λ_{max} = 820 nm), which is consistent with the stronger fields induced by the imidazolic ligands. The molar absorptivity coefficients of such d-d transitions were only estimated because of the baseline not being zero at these concentrations due to light scattering by partially undissolved complex particles.

The order of band maxima observed in the spectra is [$CuCl_2$(impz)] < [$CuCl_2$(impy)] < [$CuCl_2$(impm)]. The difference of this observed order from what was expected from the pKa values of the corresponding six-membered N-heterocycles (5.23, 0.65 and 1.21 for pyridine, pyrazine and pyrimidine, respectively)[129] is [$CuCl_2$(impz)], which should give the lowest blue-shift assuming σ-donation is the major effect from the heterocycles.

The ligand impy shows two bands above 250 nm and one more at higher energies (below 220 nm). Upon Cu(II) coordination, the band at 292 nm undergoes a batochromic shift up to 308 nm. The absorption coefficients, which are related to transition probabilities, were not altered much.

Table 4.4. Wavelength maxima and molar absorption coefficients of electronic transitions of impx ligands and [$CuCl_2$(impx)] complexes in KCl 0.1 mol·L^{-1}. λ given in nm; ε given in L·mol^{-1}·cm^{-1}.

Compound	**λ_1/ ε**	**λ_2/ ε**	**λ_3/ ε**	**λ_4/ ε**	**d-d/ ε**
impy	-	263 ($6.9.10^3$)	-	292 ($10.4.10^3$)	-
[$CuCl_2$(impy)]	-	262 ($6.9.10^3$)	-	308 ($10.9.10^3$)	727 (32)
impz	230 ($5.4.10^3$)	273 ($10.2.10^3$)	296 ($11.1.10^3$)	319 ($12.8.10^3$)	-
[$CuCl_2$(impz)]	231 ($6.1.10^3$)	269 ($8.1.10^3$)	-	329 ($8.4.10^3$)	707 (46)
impm	-	284 ($10.1.10^3$)	-	-	-
[$CuCl_2$(impm)]	-	283 ($9.6.10^3$)	-	303 (sh) ($8.7.10^3$)	731 (21)

The ligand impz shows a more complex spectrum than impy, consisting of at least four bands. The addition of one nitrogen atom on the pyridine ring at position 4 (pyrazine) led to changes on the electronic properties of the ligand. The least energetic band of impz at 319 nm underwent the same batochromic shift observed for [$CuCl_2$(impy)], but of 10 nm. The observed band at 296 nm seen in impz is identified as a shoulder next to the band 269 nm in [$CuCl_2$(impz)]. This complex is the one that showed greatest differences between its spectrum and of the ligand, even in absorption coefficients. This indicates that coordination greatly affects the electronic properties of impz.

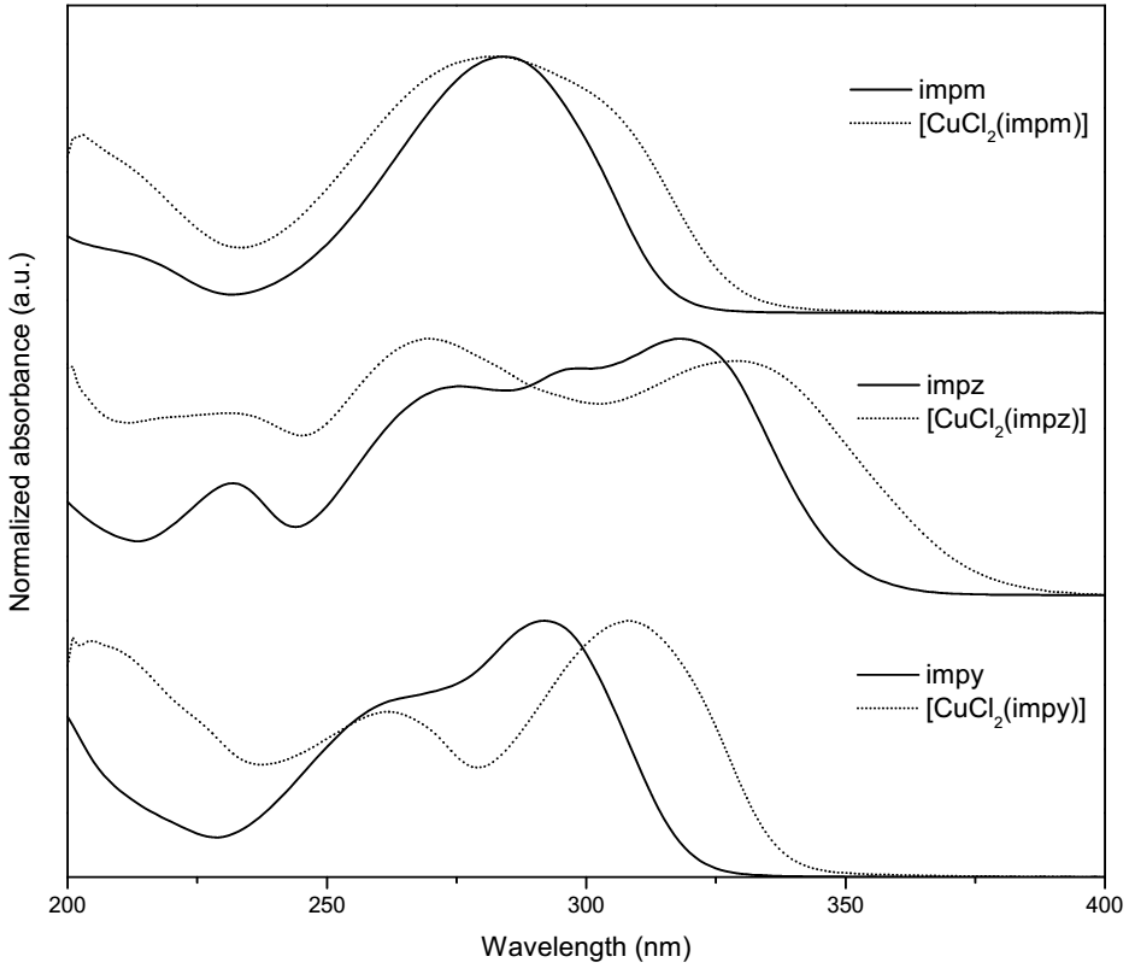

Figure 4.8. Electronic spectra of diluted impx ligands and [$CuCl_2$(impx)] complexes solutions in aqueous KCl 0.1 mol·L^{-1}. The spectra were normalized for better comparison.

By changing the position of the nitrogen atom on the heteroaryl ring from 4 (pyrazine) to 3 (pyrimidine), the spectrum of the corresponding pyrimidine ligand appears to be simpler. However, this single broad band became wider after coordination, which indicates it is actually a superposition of several electronic transitions. This was proved by the spectrum of [$CuCl_2$(impm)], which is even broader and a new transition can be identified as a shoulder at 303 nm. The trend of batochromic shift of the band observed for the other molecules was also seen for this complex.

The red shift observed for all complexes is an evidence of complexation and that the nature of this transition is the same for these molecules. However, identifying

the exact origin of batochromism is difficult, as coordination may influentiate the energies of the orbitals of the ground state, excited state or both at the same time.

4.2.6. Antimicrobial activity assays

The MIC values of the compounds over Gram-negative (*E. coli*) and Gram-positive (*S. aureus*) bacterial strains are shown in Table 4.5. It was found that both strains were resistant to all ligands. The copper complexes, however, showed activity over both strains, with values similar to $CuCl_2 \cdot 2H_2O$, which is known for its antibacterial and antifungal activities, though at high concentrations.[16] The close values to $CuCl_2 \cdot 2H_2O$ and no distinction between the MIC for the complexes may be an evidence that labilization of the impx ligands occurs in the tested conditions, even though mass spectrometry and electronic spectroscopy did not indicate this loss in diluted concentrations. The similar activity profile may also be due to the charge of the aquo species formed in solution (as observed from conductivity measurements), which may hamper cell uptake, which is a key step[16] in copper(II) activity, unless there is a membrane damage mechanism.

Table 4.5. MIC values of the Cu(II) complexes, in comparison to $CuCl_2 \cdot 2H_2O$.

Samples	*S. aureus* (MIC - $\mu mol \cdot mL^{-1}$)	*E. coli* (MIC - $\mu mol \cdot mL^{-1}$)
$CuCl_2 \cdot 2H_2O$	14.7	14.7
$[CuCl_2(impy)]$	17.8	17.8
$[CuCl_2(impm)]$	17.8	17.8
$[CuCl_2(impz)]$	17.8	17.8

The disc diffusion method of evaluating antifungal activity showed that the ligands and the complexes were not active over *Fusarium moniliforme, Candida albicans* and *Trichophyton mentagrophytes* under the tested conditions.

4.3. Partial conclusions

Two new Cu(II) complexes with the impz and impm ligands, of composition $[CuCl_2(impx)]$ were synthesized and had their properties compared to the already reported complex with impy. The crystal structure of $[CuCl_2(impm)]$ was solved by

single crystal XRD, which showed a slightly distorted square planar geometry, with no axial bonding to another chloride, as opposed to the reported [$CuCl_2$(impy)] structure. Molecular modeling and spectroscopic techniques indicated that the [$CuCl_2$(impz)] complex, which did not have its structure solved by diffraction, adopts a similar geometry to the other two compounds. The complexes showed antibacterial activity over *E. coli* and *S. aureus*, with MIC values similar to $CuCl_2 \cdot 2H_2O$, but showed no antifungal activity over the three tested strains under the tested conditions.

Chapter 5

Global discussion and conclusions

Several N-heterocycles containing either imidazole or tetrazole rings in their structures have been synthesized and characterized. Chapter 2 of this dissertation discusses about the crystal structure of some of the N-heterocyclic ligands of interest in our research group.

An important feature from the chemistry of imidazoles and tetrazoles is the proton tautomeric equilibrium[134] in solution between the amino and imino nitrogens, which could be verified by ^{1}H NMR spectroscopy (see the spectra in Appendices A to C)

The ^{1}H NMR spectra of impz (Appendix A) and thim (Appendix B) showed two broad separate signals from the hydrogens bound to the two carbon atoms from the imidazole ring. The spectra of impy and impm (Appendix C), however show only one broad signal with integration to two hydrogens. The proton equilibrium is facilitated in a protic solvent, such as water itself. Possibly, the water content present in the samples, the glassware or in DMSO – d6 contributed to the equilibrium in impy and impm, though sample preparation was the same for all ligands.

The crystallographic data from the tetrazolic ligand tzpy showed the presence of a zwitterion (pyridinium and tetrazolate ions) in the solid state, opposite to the usually reported neutral molecule. However, solution studies using NMR (appendix A) showed that the molecule indeed converts to the neutral form even in the aprotic solvent DMSO and thus it adopts the reported form.

^{1}H NMR was also useful to compare the chemistry of tetrazoles and imidazoles. The hydrogen directly bound to the tetrazolic ring is attributed (in the literature) to a signal around 3 ppm which is much more shielded than the corresponding hydrogen in imidazole (above 12 ppm). Moreover, mass spectrometry

experiments indirectly showed differences from chemical stabilities of the two rings (Appendix A), as the imidazolic ligands usually lost HCN fragments, whereas the tetrazolic ligand tzpy lost N_2.

The crystal structures from three of the studied ligands showed the importance of the hydrogen from imidazole and tetrazole in the determination of the supramolecular structure of such molecules. Identification of intermolecular interactions of a class of molecules is essential for the rational design of new structures in supramolecular chemistry.

About the bioactivity of azoles, it is interesting that the tested imidazolic ligands were not active over neither bacteria nor fungi. The structure of antifungal imidazolic compounds has an N-substituted imidazole.[50] So, from the obtained results, substitution of 2-substituted imidazoles with another aromatic ring, such as pyridine, does not lead to highly active antimicrobial compounds.

Chapters 3 and 4 describe the syntheses and characterization of the copper(II) complexes with the imidazolic N-heterocycles, that are different in both geometric configurations, mode of binding and number of ligands: $[CuCl_2(thim)_2]$ adopted *trans* configuration, monodentate coordination via imidazole and the stoichiometry of two ligands was set to maintain two nitrogen atoms bound to copper. In the $[CuCl_2(impx)]$ complexes, the ligands coordinated in a chelate bidentate mode by both the imidazole and the six-membered aromatic rings. It is only hypothesized that $[CuCl_2(thim)_2]$ adopted a *trans* configuration due to steric hindrance that a *cis* configuration would impose in the crystal packing.

Comparison of crystallographic data from the *trans* $[CuCl_2(thim)_2]$ and the $[CuCl_2(impm)]$ complexes showed that the former adopted a regular square planar geometry (τ_4 index[127] zero), whereas the latter was slightly distorted, with the copper ion located slightly out of the ligand plane (τ_4 index 0.09). No significant Cu–Cl axial bonding was identified for neither complexes, but hydrogen bonding involving chlorides was shown to be essential for crystal packing. The presence of these unconventional N-H···Cl hydrogen bonds may be one of the reasons why no solvent molecules were necessary for crystallization.

The Cu-N bond length for imidazole coordination (1.9750(17) Å) in $[CuCl_2(impm)]$ was shorter than the one for pyrimidine (2.0779(16) Å) and the same trend was observed in the reported $[CuCl_2(impy)]$[61] structure. Relating bond length to

bond strength can be misleading even with crystal data, unless the changes between the compared structures are really significant (for example changing the oxidation state of the metal). It has been stated that the difference between M-$N_{imidazole}$ and M-$N_{pyridine}$ bond lengths is probably more related to steric effects than to a stronger bond.[135]

Molecular modeling allowed the prediction of the equilibrium geometry of [$CuCl_2$(impz)], which did not have its structure solved by diffraction. It could be seen from the plotted Kohn – Shan orbitals that the presence of extra number of nitrogen atoms affects the electronic structure of the molecule. Molecular modeling did not predict any significant differences between the Cu-N (from pyridine, pyrazine and pyrimidine) bond lengths.

Some chemical differences between the complexes were observed and they could be directly related to their mode of coordination. For example, the copper(II) ion from the monodentate [$CuCl_2(thim)_2$] complex was easily reduced in mass spectrometry experiments, resulting in the loss of two chloride ions and only the $[Cu(I)(thim)_2]^+$ species was observed. However, for the [$CuCl_2$(impx)] complexes, the bidentate coordination of the ligands ensured greater stabilization of copper(II), so some $[Cu(II)Cl(impx)]^+$ ions survive in the gas phase, though $[Cu(I)(impx)]^+$ is still the dominant species. Chloride solvolysis was also proved by conductivity measurements.

Infrared spectroscopy, along with molecular modeling, was used to identify the vibrations that have contribution of imidazole stretching, which changed after coordination to Cu(II). Raman spectroscopy was used to evaluate the metal-ligand vibrations. All three complexes had similar spectra profiles, with small differences in band energies, which is consistent with a similar mode of coordination.

Electronic spectroscopy in solution showed a hypsochromic shift of the d-d band of the complexes compared to $CuCl_2 \cdot 2H_2O$, which is an indication of the stronger field of the N-heterocycles when compared to water. Moreover, in the [$CuCl_2$(impx)] complexes, some of the intraligand electronic transitions showed a batochromic shift, which is consistent with coordination. The fact that the intraligand bands of thim did not show a shift after coordination to Cu(II) may indicate that they are predominantly related to thiophene transitions, which is not involved in coordination, as proved by other techniques.

The complexes of the tetrazolic ligands with Cu(II) were not synthesized in this work, and studying them would add information about the effects of the five-membered ring on the properties of the complexes. The versatile nature of the Cu(II) ion also allows the obtention of bis and tris complexes with the studied ligands, which remain to be investigated.

The synthesized copper(II) complexes were tested over bacterial and fungal strains. The three $[CuCl_2(impx)]$ complexes were tested in relation to their antibacterial properties and they showed MIC values similar to $CuCl_2 \cdot 2H_2O$ over *E. coli* and *S. aureus*. However, the number and the position of the nitrogen atoms in the ligand did not influence the antibacterial activity of the complexes. This profile may be related to the dominant effect of high positive charge of the complexes, which may hinder their entrance in the cells.[16]

$[CuCl_2(thim)_2]$ was the only compound that showed antifungal activity over *Trichophyton mentagrophytes*. This shows the difference that stoichiometry and *trans* geometry played in the determination of bioactivity, as the $[CuCl_2(impx)]$ complexes were not active. The presence of thiophene was not the determinant factor of antifungal activity of $[CuCl_2(thim)_2]$, as the free ligand did not show an inhibition zone.

Even though the studied molecules in this work showed limited antimicrobial activity, the results showed that substitution of classical bipyridine and phenantroline by other classes of ligands, such as imidazole, may be promising for further tailoring of copper(II) complexes. Chemical modifications of the studied ligands, such as the obtention of lipophilic cations and substituting the labile chloride ligands by other bioactive ligands may lead to more active compounds.

Bibliography

[1] K. D. Mjos, C. Orvig, *Chem. Rev.* **2014**, *114*, 4540–63.

[2] B. Rosenberg, L. VanCamp, T. Krigas, *Nature* **1965**, *205*, 698–699.

[3] B. Rosenberg, L. VanCamp, J. E. Trosko, V. H. Mansour, *Nature* **1969**, *222*, 385–386.

[4] T. C. Johnstone, G. Y. Park, S. J. Lippard, *Anticancer Res.* **2014**, *34*, 471–476.

[5] M. Fanelli, M. Formica, V. Fusi, L. Giorgi, M. Micheloni, P. Paoli, *Coord. Chem. Rev.* **2016**, *310*, 41–79.

[6] S. Medici, M. Peana, V. M. Nurchi, J. I. Lachowicz, G. Crisponi, M. A. Zoroddu, *Coord. Chem. Rev.* **2015**, *284*, 329–350.

[7] L. Kelland, *Nat. Rev. Cancer* **2007**, *7*, 573–584.

[8] W. I. Sundquist, S. J. Lippard, *Coord. Chem. Rev.* **1990**, *100*, 293–322.

[9] D. Wang, S. J. Lippard, *Nat. Rev. Drug Discov.* **2005**, *4*, 307–320.

[10] D. Gaynor, D. M. Griffith, *Dalt. Trans.* **2012**, *41*, 13239.

[11] P. Bruijnincx, P. Sadler, *Curr. Opin. Chem. Biol.* **2008**, *12*, 197–206.

[12] C.-M. Che, R. W.-Y. Sun, W.-Y. Yu, C.-B. Ko, N. Zhu, H. Sun, *Chem. Commun. (Camb).* **2003**, 1718–1719.

[13] V. Milacic, D. Chen, L. Ronconi, K. R. Landis-Piwowar, D. Fregona, Q. P. Dou, *Cancer Res.* **2006**, *66*, 10478–86.

[14] W. K. Jung, H. C. Koo, K. W. Kim, S. Shin, S. H. Kim, Y. H. Park, *Appl. Environ. Microbiol.* **2008**, *74*, 2171–2178.

[15] C. N. Banti, S. K. Hadjikakou, *Metallomics* **2013**, *5*, 569.

[16] G. Borkow, J. Gabbay, *Curr. Med. Chem.* **2005**, *12*, 2163–2175.

[17] L. M. Gaetke, H. S. Chow-Johnson, C. K. Chow, *Arch. Toxicol.* **2014**, *88*, 1929–1938.

[18] C. Santini, M. Pellei, V. Gandin, M. Porchia, F. Tisato, C. Marzano, *Chem. Rev.* **2014**, *114*, 815–862.

[19] N. . Greenwood, A. Earnshaw, *Chemistry of the Elements*, Butterworth-Heinemann, Great Britain, **1997**.

[20] R. R. Conry, *Encyclopedia of Inorganic Chemistry. Copper: Inorganic & Coordination Chemistry*, John Wiley & Sons, Ltd, **2006**.

[21] K. S. Chaturvedi, J. P. Henderson, *Front. Cell. Infect. Microbiol.* **2014**, *4*, 1–12.

[22] B. J. Hathaway, *Comprehensive Coordination Chemistry, Volume 5: Late Transition Metals*, Pergamon Press, Great Britain, **1987**.

[23] F. Tisato, C. Marzano, M. Porchia, M. Pellei, C. Santini, *Med. Res. Rev.* **2009**, *30*, 708–749.

[24] M. A. Halcrow, *Dalt. Trans.* **2003**, *35*, 4375.

[25] J. J. R. Fraústo da Silva, R. J. P. Williams, *The Biological Chemistry of the Elements*, Oxford University Press, New York, **2001**.

[26] E. I. Solomon, D. E. Heppner, E. M. Johnston, J. W. Ginsbach, J. Cirera, M. Qayyum, M. T. Kieber-Emmons, C. H. Kjaergaard, R. G. Hadt, L. Tian, *Chem. Rev.* **2014**, *114*, 3659–3853.

[27] J. T. Rubino, K. J. Franz, *J. Inorg. Biochem.* **2012**, *107*, 129–143.

[28] J. M. McCord, I. Fridovich, *J. Biol. Chem.* **1969**, *244*, 6049–55.

[29] I. Laba, K. Hernadi, I. Pa, I. Fekete, L. Korecz, A. Rockenbauer, I. Szila, T. Kiss, *New J. Chem.* **2005**, *29*, 740–745.

[30] P. Verwilst, K. Sunwoo, J. S. Kim, *Chem. Commun.* **2015**, *51*, 5556–5571.

[31] A. K. Boal, A. C. Rosenzweig, *Chem. Rev.* **2009**, *109*, 4760–4779.

[32] T. D. Rae, P. J. Schimidt, R. A. Pufahl, V. C. Culotta, T. V. O´Halaran, *Science* **1999**, *284*, 805–808.

[33] J. A. Lemire, J. J. Harrison, R. J. Turner, *Nat. Rev. Microbiol.* **2013**, *11*, 371–384.

[34] G. Grass, C. Rensing, M. Solioz, *Appl. Environ. Microbiol.* **2011**, *77*, 1541–1547.

[35] G. Barone, A. Terenzi, A. Lauria, A. M. Almerico, J. M. Leal, N. Busto, B. García, *Coord. Chem. Rev.* **2013**, *257*, 2848–2862.

[36] K. Giannousi, G. Sarafidis, S. Mourdikoudis, A. Pantazaki, C. Dendrinou-Samara, *Inorg. Chem.* **2014**, *53*, 9657–9666.

[37] S. Rajalakshmi, A. Fathima, J. R. Rao, B. U. Nair, *RSC Adv.* **2014**, *4*, 32004.

[38] Z. Bin Ou, Y. H. Lu, Y. M. Lu, S. Chen, Y. H. Xiong, X. H. Zhou, Z. W. Mao, X. Y. Le, *J. Coord. Chem.* **2013**, *66*, 2152–2165.

[39] C. Duncan, A. R. White, *Metallomics* **2012**, *4*, 127–38.

[40] C. Marzano, M. Pellei, F. Tisato, C. Santini, *Anticancer. Agents Med. Chem.* **2009**, *9*, 185–211.

[41] L. Ruiz-Azuara, M. E. Bravo-Gómez, *Curr. Med. Chem.* **2010**, *17*, 3606–3615.

[42] I. Gracia-Mora, L. Ruiz-Ramírez, C. Gómez-Ruiz, M. Tinoco-Méndez, a Márquez-Quiñones, L. R. Lira, a Marín-Hernández, L. Macías-Rosales, M. E. Bravo-Gómez, *Met. Based. Drugs* **2001**, *8*, 19–28.

[43] L. Becco, A. Rodríguez, M. E. Bravo, M. J. Prieto, L. Ruiz-Azuara, B. Garat, V. Moreno, D. Gambino, *J. Inorg. Biochem.* **2012**, *109*, 49–56.

[44] C. Wende, C. Lüdtke, N. Kulak, *Eur. J. Inorg. Chem.* **2014**, 2597–2612.

[45] M. Pitié, C. Boldron, H. Gornitzka, C. Hemmert, B. Donnadieu, B. Meunier, *Eur. J. Inorg. Chem.* **2003**, 528–40.

[46] M. C. Rodríguez-Argüelles, E. C. López-Silva, J. Sanmartín, P. Pelagatti, F. Zani, *J. Inorg. Biochem.* **2005**, *99*, 2231–2239.

[47] A. A. Soayed, H. M. Refaat, D. a. Noor El-Din, *Inorganica Chim. Acta* **2013**, *406*, 230–240.

[48] K. Hofmann, *Chemistry of Heterocyclic Compounds, Volume 6: General Properties and Structure of the Imidazoles*, Interscience Publishers, **1953**.

[49] WHO, “No Title,” **n.d.**

[50] I. J. Sud, D. S. Feingold, *J. Invest. Dermatol.* **1981**, *76*, 438–441.

[51] E. Vitaku, D. T. Smith, J. T. Njardarson, *J. Med. Chem.* **2014**, *57*, 10257–10274.

[52] G. I. Koldobskii, V. A. Ostrovskii, V. S. Popavskii, *Chem. Heterocycl. Compd.* **1981**, *17*, 965–988.

[53] R. J. Herr, *Bioorg. Med. Chem.* **2002**, *10*, 3379–3393.

[54] J. B. Press, *Pharmacologically Active Compounds and Other Thiophene Derivatives*, John Wiley & Sons, Ltd, **1985**.

[55] D. Gramec, L. Peterlin Mašič, M. Sollner Dolenc, *Chem. Res. Toxicol.* **2014**, *27*, 1344–1358.

[56] D. Gil, L. F. García, M. Rojas, *Toxicol. Appl. Pharmacol.* **2003**, *190*, 111–9.

[57] A. D. Bond, A. Fleming, J. Gaire, F. Kelleher, J. McGinley, V. McKee, U. Sheridan, *Polyhedron* **2012**, *33*, 289–296.

[58] A. Fleming, J. Gaire, F. Kelleher, J. McGinley, V. McKee, *Tetrahedron* **2011**, *67*, 3260–3266.

[59] M. E. Voss, C. M. Beer, S. a. Mitchell, P. a. Blomgren, P. E. Zhichkin, *Tetrahedron* **2008**, *64*, 645–651.

[60] R. Singh, P. K. Bharadwaj, *Cryst. Growth Des.* **2013**, *13*, 3722–3733.

[61] E. Coronado, M. Giménez-Marqués, G. M. Espallargas, L. Brammer, *Nat. Commun.* **2012**, *3*, 828.

[62] Y. Chi, B. Tong, P. Chou, *Coord. Chem. Rev.* **2014**, *281*, 1–25.

[63] M. Serratrice, M. a. Cinellu, L. Maiore, M. Pilo, A. Zucca, C. Gabbiani, A. Guerri, I. Landini, S. Nobili, E. Mini, et al., *Inorg. Chem.* **2012**, *51*, 3161–3171.

[64] S.-L. Xiao, L. Liu, P.-J. Ma, G.-H. Cui, *Zeitschrift für Anorg. und Allg. Chemie* **2014**, *640*, 1484–1489.

[65] J. Roh, K. Vávrová, A. Hrabálek, *European J. Org. Chem.* **2012**, 6101–6118.

[66] W. G. Finnegan, R. A. Henry, R. Lofquist, *J. Am. Chem. Soc.* **1958**, *80*, 3908–3911.

[67] Z. P. Demko, K. B. Sharpless, *J. Org. Chem.* **2001**, *66*, 7945–7950.

[68] F. Himo, Z. P. Demko, L. Noodleman, K. B. Sharpless, *J. Am. Chem. Soc.* **2003**, *125*, 9983–9987.

[69] C. Janiak, *J. Chem. Soc. Dalt. Trans.* **2000**, 3885–3896.

[70] O. V. Dolomanov, L. J. Bourhis, R. J. Gildea, J. a K. Howard, H. Puschmann, *J. Appl. Crystallogr.* **2009**, *42*, 339–341.

[71] G. M. Sheldrick, *Acta Crystallogr. Sect. A Found. Adv.* **2014**, *71*, 3–8.

[72] G. M. Sheldrick, *Acta Crystallogr. Sect. A Found. Crystallogr.* **2007**, *64*, 112–122.

[73] F. H. Allen, D. G. Watson, L. Brammer, a. G. Orpen, R. Taylor, *Int. Tables Crystallogr. Vol. C Math. Phys. Chem. tables* **2004**, *C*, 790–811.

[74] F. H. Allen, *Acta Crystallogr. Sect. B Struct. Sci.* **2002**, *58*, 380–388.

[75] L. Beverina, A. Sanguineti, G. Battagliarin, R. Ruffo, D. Roberto, S. Righetto, R. Soave, L. Lo Presti, R. Ugo, G. a Pagani, *Chem. Commun. (Camb).* **2011**, *47*, 292–4.

[76] L. Beverina, G. a. Pagani, *Acc. Chem. Res.* **2014**, *47*, 319–329.

[77] G. Jeffrey, H. Maluszynska, J. Mitra, *Int. J. Biol. Macromol.* **1985**, *7*, 336–348.

[78] T. Steiner, *Crystallogr. Rev.* **1996**, *6*, 1–51.

[79] R. Bakhtiar, E. I. Ochiai, *Gen. Pharmacol.* **1999**, *32*, 525–540.

[80] W. F. Kean, L. Hart, W. W. Buchanan, *Br. J. Rheumatol.* **1997**, *36*, 560–572.

[81] L. Galluzzi, I. Vitale, J. Michels, C. Brenner, G. Szabadkai, a Harel-Bellan, M. Castedo, G. Kroemer, *Cell Death Dis.* **2014**, *5*, e1257.

[82] N. P. Farrell, *Chem. Soc. Rev.* **2015**, *44*, 8773–8785.

[83] B. S. Atiyeh, M. Costagliola, S. N. Hayek, S. A. Dibo, *Burns* **2007**, *33*, 139–148.

[84] C. Monneret, *Ann. Pharm. Fr.* **2011**, *69*, 286–295.

[85] B.-L. Fei, W. Li, W.-S. Xu, J.-Y. Long, Q.-B. Liu, W.-Y. Sun, C. E. Anson, A. K. Powell, *Eur. J. Inorg. Chem.* **2013**, *2013*, 5919–5927.

[86] L. Zhang, X.-M. Peng, G. L. V Damu, R.-X. Geng, C.-H. Zhou, *Med. Res. Rev.* **2014**, *34*, 340–437.

[87] R. Loganathan, S. Ramakrishnan, E. Suresh, A. Riyasdeen, M. A. Akbarsha, M. Palaniandavar, *Inorg. Chem.* **2012**, *51*, 5512–5532.

[88] X. Hou, X. Li, H. Hemit, H. A. Aisa, *J. Coord. Chem.* **2014**, *67*, 461–469.

[89] J. Al-Shuneigat, J. Q. Yu, P. Beale, K. Fisher, F. Huq, *Med. Chem.* **2010**, *6*, 321–328.

[90] X.-F. He, C. M. Vogels, A. Decken, S. a Westcott, *Can. J. Chem.* **2003**, *81*, 861–865.

[91] K. K. Jha, S. Kumar, I. Tomer, R. Mishra, *J. Pharm. Res.* **2012**, *5*, 560–566.

[92] R. Romagnoli, P. Giovanni, C. Lopez-cara, M. Kimatrai, D. Preti, M. Aghazadeh, J. Balzarini, P. Nussbaumer, M. Bassetto, A. Brancale, et al., *Bioorg. Med. Chem.* **2014**, *22*, 5097–5109.

[93] A. M. Isloor, B. Kalluraya, K. Sridhar Pai, *Eur. J. Med. Chem.* **2010**, *45*, 825–830.

[94] D. Caridha, A. K. Kathcart, D. Jirage, N. C. Waters, *Bioorganic Med. Chem. Lett.* **2010**, *20*, 3863–3867.

[95] C. Adamo, V. Barone, *J. Chem. Phys.* **1999**, *110*, 6158.

[96] F. Neese, *Wiley Interdiscip. Rev. Comput. Mol. Sci.* **2012**, *2*, 73–78.

[97] R. Izsák, F. Neese, *J. Chem. Phys.* **2011**, *135*, 144105.

[98] F. Weigend, M. Häser, H. Patzelt, R. Ahlrichs, *Chem. Phys. Lett.* **1998**, *294*, 143–152.

[99] F. Weigend, F. Furche, R. Ahlrichs, *J. Chem. Phys.* **2003**, *119*, 12753–12762.

[100] Y. Tantirungrotechai, K. Phanasant, S. Roddecha, P. Surawatanawong, V. Sutthikhum, J. Limtrakul, *J. Mol. Struct. THEOCHEM* **2006**, *760*, 189–192.

[101] M. F. Belicchi, G. F. Gasparri, C. Pelizzi, P. Tarasconi, *Transit. Met. Chem.* **1985**, *10*, 295–299.

[102] A. Ünal, B. Eren, *Spectrochim. Acta - Part A Mol. Biomol. Spectrosc.* **2013**, *114*, 129–136.

[103] M. Satterfield, J. S. Brodbelt, *Inorg. Chem.* **2001**, *40*, 5393–5400.

[104] W. Henderson, J. S. McIndoe, *Mass Spectrometry of Inorganic, Coordination and Organometallic Compounds: Tools - Techniques - Tips*, John Wiley & Sons, Ltd, Chichester, UK, **2005**.

[105] W. J. Geary, *Coord. Chem. Rev.* **1971**, *7*, 81–122.

[106] V. Gutmann, *Coord. Chem. Rev.* **1976**, *18*, 225–255.

[107] C. Qiao, S. Bi, Y. Sun, D. Song, H. Zhang, W. Zhou, *Spectrochim. Acta - Part A Mol. Biomol. Spectrosc.* **2008**, *70*, 136–143.

[108] L. Tabrizi, H. Chiniforoshan, H. Tavakol, *Spectrochim. Acta Part A Mol. Biomol. Spectrosc.* **2015**, *141*, 16–26.

[109] N. Shahabadi, S. Mohammadi, R. Alizadeh, *Bioinorg. Chem. Appl.* **2011**, *2011*, 1–8.

[110] J. Olmsted, D. R. Kearns, *Biochemistry* **1977**, *16*, 3647–3654.

[111] J. Kypr, I. Kejnovská, D. Renčiuk, M. Vorlíčková, *Nucleic Acids Res.* **2009**, *37*, 1713–1725.

[112] Z. Wang, D. Liu, S. Dong, *Biophys. Chem.* **2000**, *87*, 179–184.

[113] E. Zabost, A. M. Nowicka, M. Donten, Z. Stojek, *Phys. Chem. Chem. Phys.* **2009**, *11*, 8933.

[114] B. Nordén, F. Tjerneld, *Biopolymers* **1982**, *21*, 1713–1734.

[115] J.-P. Macquet, J.-L. Butour, *Biochimie* **1978**, *60*, 901–914.

[116] N. Shahabadi, S. Kashanian, M. Purfoulad, *Spectrochim. Acta. A. Mol. Biomol. Spectrosc.* **2009**, *72*, 757–761.

[117] J.-L. Mergny, L. Lacroix, *Oligonucleotides* **2003**, *13*, 515–537.

[118] M. Cusumano, M. L. Di Pietro, A. Giannetto, *Inorg. Chem.* **2006**, *45*, 230–235.

[119] P. B. Dervan, B. S. Edelson, *Curr. Opin. Struct. Biol.* **2003**, *13*, 284–299.

[120] K. Kissinger, K. Krowicki, J. C. Dabrowiak, J. W. Lown, *Biochemistry* **1987**, *26*, 5590–5595.

[121] E. N. Galyuk, A. S. Fridman, V. I. Vorob'ev, S. G. Haroutiunian, S. a Sargsyan, M. M. Hauruk, D. Y. Lando, *J. Biomol. Struct. Dyn.* **2008**, *25*, 407–417.

[122] K. Makimura, Y. Tamura, T. Mochizuki, a Hasegawa, Y. Tajiri, R. Hanazawa, K. Uchida, H. Saito, H. Yamaguchi, *J. Clin. Microbiol.* **1999**, *37*, 920–4.

[123] Clinical and Laboratory Standards Institute. *Performance Standards for Antimicrobial Susceptibility Testing; Twenty-Third Informational Supplement.*

CLSI document M100-S23. Clinical and Laboratory Standards Institute, 950 West Valley Road, Suite 2500, Wayne, Pennsylvania 19087 USA, 2013.

[124] H. Isci, W. R. Mason, *Inorg. Chem.* **1974**, *13*, 1175–1180.

[125] D.-D. Klaehn, H. Paulus, R. Grewe, H. Elias, *Inorg. Chem.* **1984**, *23*, 483–490.

[126] S. M. Barnett, K. I. Goldberg, J. M. Mayer, *Nat. Chem.* **2012**, *4*, 498–502.

[127] L. Yang, D. R. Powell, R. P. Houser, *Dalton Trans.* **2007**, 955–964.

[128] D. L. Pavia, G. M. Lampman, G. S. Kriz, *Introduction to Spectroscopy: A Guide for Students of Organic Chemistry.*, Cencage Learning, Belmont, **2009**.

[129] D. R. Lide, *CRC Handbook of Chemistry and Physics*, **2005**.

[130] B. C. Cornilsen, K. Nakamoto, *J. Inorg. Nucl. Chem.* **1974**, *36*, 2467–2471.

[131] R. E. Wilde, T. K. K. Srinivasan, S. N. Ghosh, *J. Inorg. Nucl. Chem.* **1973**, *35*, 1017–1021.

[132] Y. Saito, J. Takemoto, B. Hutchinson, K. Nakamoto, B. Y. Y. Saito, K. N. I, *Inorg. Chem.* **1972**, *11*, 2003–2011.

[133] A. B. P. Lever, E. Mantovani, *Inorg. Chem.* **1971**, *10*, 817–826.

[134] M. Tanokura, *Biochim. Biophys. Acta - Protein Struct. Mol. Enzymol.* **1983**, *742*, 586–596.

[135] A. Nimmermark, L. Öhrström, J. Reedijk, *Zeitschrift für Krist. - Cryst. Mater.* **2013**, *228*, 311–317.

Appendix A

Supplements to Chapter 2

A.1. Nuclear Magnetic Resonance spectra

The full spectroscopic characterization of the impz molecule had already been reported in a previous dissertation of our research group by M. Sc. Eduardo Guimarães Ratier de Arruda. The ^{1}H NMR spectrum of this molecule is given in Figure A.1 for informative purposes.

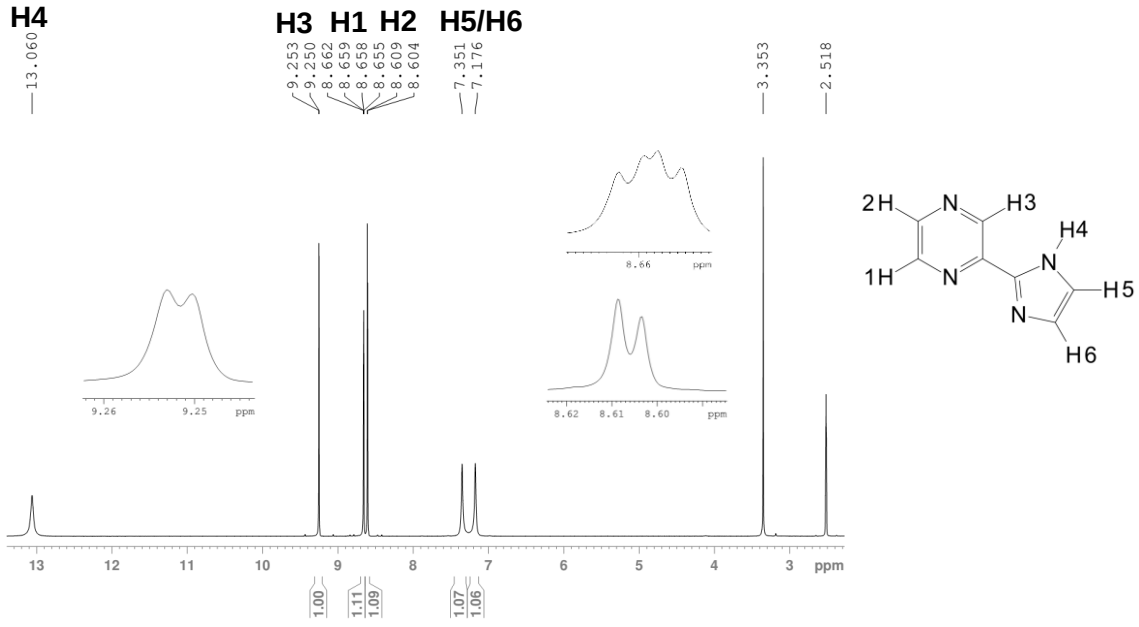

Figure A.1. ^{1}H NMR of impz in DMSO – d6.

Figures A.2 and A.3 shows the ^{1}H and ^{13}C NMR spectra of tzpy in DMSO – d6. The ^{1}H spectrum shows four signals, which all integrate to one, corresponding to

the four hydrogen atoms of the pyridine ring. The ^{1}H signal attribution (Figure A.2) was based on the chemical shifts and coupling constants (given in the main text – Experimental Section), which were in agreement with those found for 2-substituted pyridine rings.

A small and broad signal (not shown) around 3.2 ppm is present on the spectrum and it is usually assigned to the hydrogen atom bound to the tetrazole ring. As seen from the crystal structure, the hydrogen atom was closer to the pyridine ring. However, the hypothesis that this proton can be in equilibrium in solution cannot be excluded. Additional experimental evidence for this equilibrium was obtained using the {^{15}N, ^{1}H} HMBC NMR technique and the spectrum is given in Figure A.5.

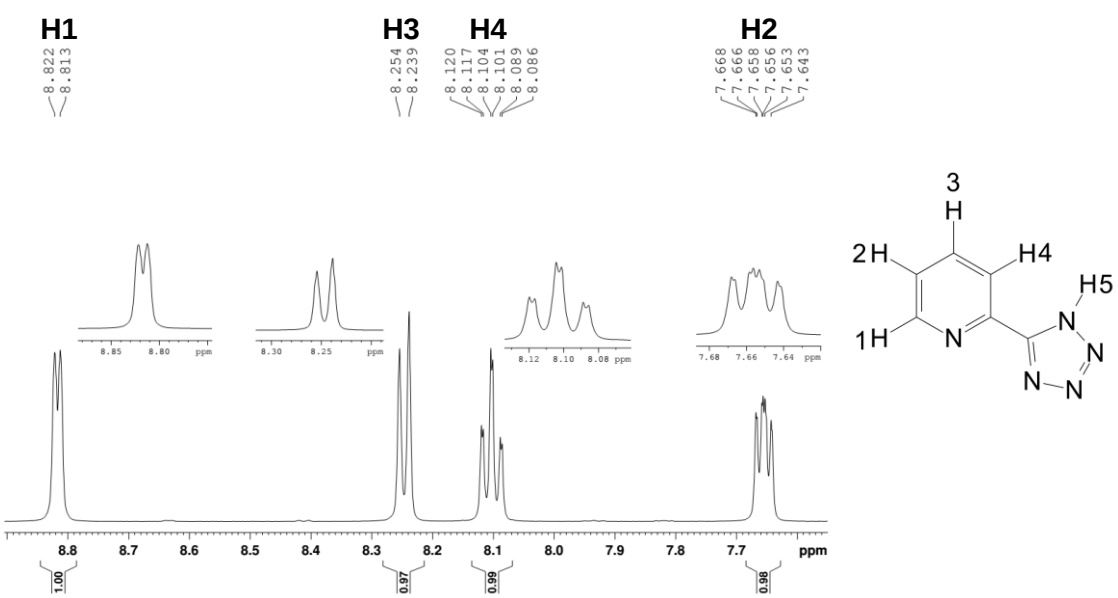

Figure A.2. ^{1}H NMR of tzpy in DMSO – d6.

The ^{13}C spectrum, shown in Figure A.2 shows six signals, which are in agreement with the chemical structure of the ligand. Two of them are of lower intensity, which is consistent with the presence of two quaternary carbons. Assignment of all carbon signals was achieved by {^{13}C, ^{1}H} HSQC and HMBC NMR techniques, shown in Figure A.4. The quaternary carbon of pyridine was identified due to the $^{2}J_{C5H4}$ coupling observed in the {^{13}C, ^{1}H} HMBC contour map in Figure A.4.

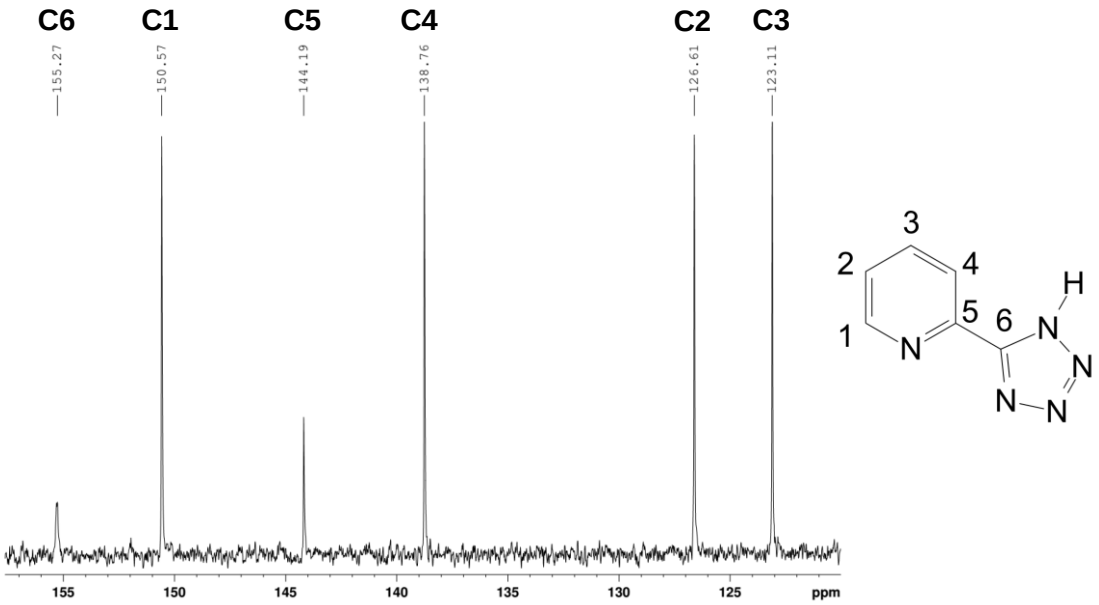

Figure A.3. ^{13}C NMR of tzpy in DMSO – d6.

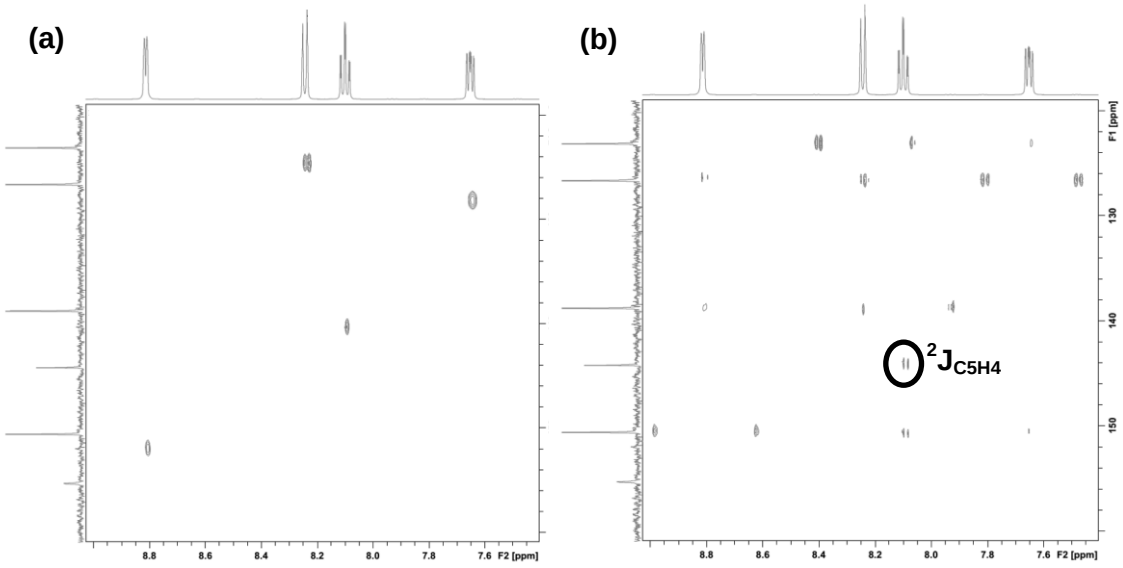

Figure A.4. {^{13}C, ^{1}H} (a) HSQC and (b) HMBC NMR contour maps of tzpy.

As seen from Figure A.5, the only nitrogen signal observed showed a correlation with H1, which is only possible if it were attributed to the nitrogen atom from pyridine, via a $^{2}J_{H1N1}$ coupling. No extra signals were observed, even using the {^{15}N, ^{1}H} HSQC experiment, which supports the hypothesis of equilibrium involving the proton of the tzpy molecule.

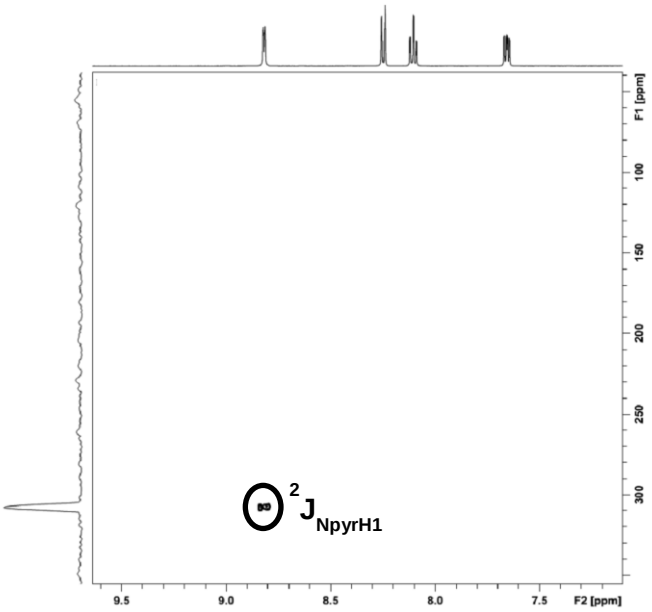

Figure A.5. {^{15}N, ^{1}H} HMBC NMR contour map of tzpy.

The ^{1}H NMR spectrum of ditzpy (Figure A.6) showed an unexpected broad and intense signal of δ at 8.348 ppm. From the chemical structure o ditzpy the pattern of signals should be a triplet and a doublet integrating to one and two hydrogens, respectively. However, even after purification, the spectrum remained the same. Curiously, no other compound involved in the synthesis should give such an intense signal (more intense than the solvent signal) or such a pattern. For this reason, ^{13}C NMR was not performed. Thus, chemical characterization of this ligand was achieved only by mass spectrometry (see Subsection A.2) and elemental analysis.

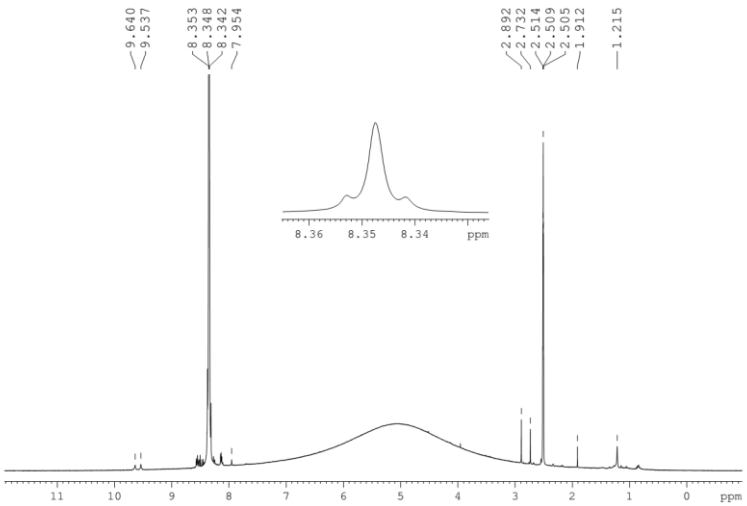

Figure A.6. ^{1}H NMR of ditzpy in DMSO – d6.

A.2. Mass spectra

Figures A.7 to A.9 show the mass spectra of the three ligands. In all spectra, the $[M+H]^+$ ion can be observed at m/z 147.1, 148.1 and 216.3 for impz, tzpy and ditzpy, respectively, which confirms the proposed compositions. Mass spectrometry of ditzpy, as opposed to ^{1}H NMR, resulted in the expected composition and no other major species indicative of contamination can be observed.

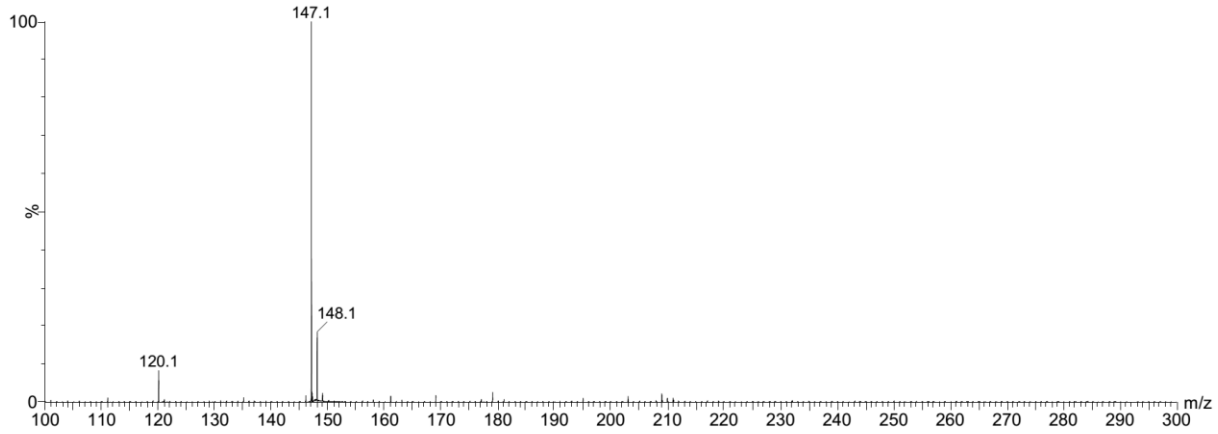

Figure A.7. Mass spectrum of impz.

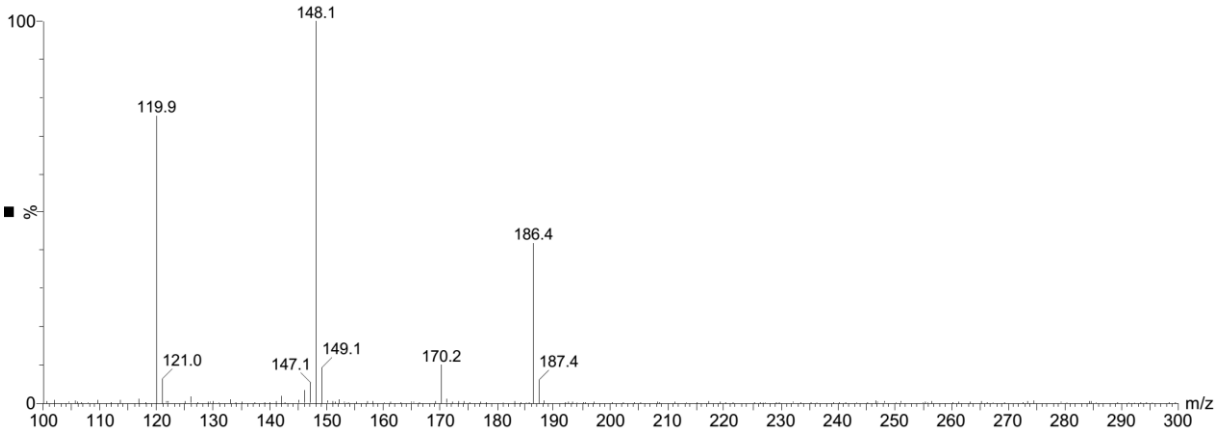

Figure A.8. Mass spectrum of tzpy.

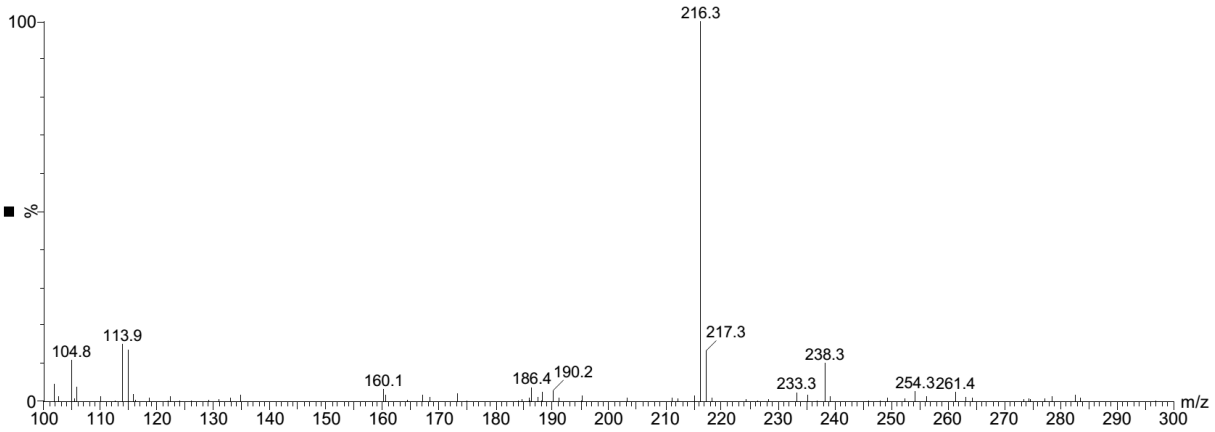

Figure A.9. Mass spectrum of ditzpy.

impz showed a second peak at m/z 120.1, which corresponds to the loss of HCN from the ligand, a common fragmentation of imidazole rings. tzpy showed a second peak at m/z 120.0, which can be attributed to the loss of N_2 from the ligand. ditzpy showed a second peak at m/z 238.0, which is 22 units above the mass of $[M+H]^+$, thus indicating the formation of the $[M+Na]^+$ adduct, not observed in the other ligands.

A.3. Crystal structures – bond lengths and angles

Table A.1. Bond lengths and angles of impz.

Bond or angle	Experimental value (Å or ^{o})
N(1)-C(1)	1.3707(19)
N(1)-C(2)	1.3284(19)
N(2)-C(4)	1.3292(19)
N(2)-C(5)	1.3362(19)
N(3)-C(2)	1.3525(18)
N(3)-C(6)	1.3644(18)
N(4)-C(3)	1.3428(19)
N(4)-C(7)	1.3366(19)
C(1)-C(6)	1.365(2)
C(2)-C(3)	1.461(2)
C(3)-C(4)	1.395(2)
C(5)-C(7)	1.384(2)
C(1)-N(1)-C(2)	105.27(12)
C(4)-N(2)-C(5)	116.01(12)
C(2)-N(3)-C(6)	107.45(11)
C(3)-N(4)-C(7)	115.84(12)
N(1)-C(1)-C(6)	110.13(12)
N(1)-C(2)-N(3)	111.19(12)
N(1)-C(2)-C(3)	124.74(12)
N(3)-C(2)-C(3)	123.94(12)
N(4)-C(3)-C(2)	117.87(12)
N(4)-C(3)-C(4)	121.41(13)
C(2)-C(3)-C(4)	120.70(13)
N(2)-C(4)-C(3)	122.39(13)
N(2)-C(5)-C(7)	121.99(13)
N(3)-C(6)-C(1)	105.96(12)
N(4)-C(7)-C(5)	122.33(13)
N(3)-C(2)-C(3)-N(4)	5.8(2)

Table A.2. Bond lengths and angles of tzpy. The values of only one of the molecules necessary to describe the assymetric unit are given.

Bond or angle	Experimental value (Å or ^{o})
N(1)-C(2)	1.347(2)
N(1)-C(6)	1.349(2)
N(2)-N(3)	1.347(2)
N(2)-C(1)	1.334(3)
N(3)-N(4)	1.317(2)
N(4)-N(5)	1.347(2)
N(5)-C(1)	1.343(2)
C(1)-C(2)	1.461(3)
C(2)-C(3)	1.381(3)
C(3)-C(4)	1.383(3)
C(4)-C(5)	1.390(3)
C(5)-C(6)	1.371(3)
C(2)-N(1)-C(6)	122.26(16)
N(3)-N(2)-C(1)	104.59(14)
N(2)-N(3)-N(4)	109.30(15)
N(3)-N(4)-N(5)	109.96(15)
N(4)-N(5)-C(1)	103.95(15)
N(2)-C(1)-N(5)	112.20(16)
N(2)-C(1)-C(2)	125.53(16)
N(5)-C(1)-C(2)	122.27(17)
N(1)-C(2)-C(1)	117.99(17)
N(1)-C(2)-C(3)	119.07(17)
C(1)-C(2)-C(3)	122.94(16)
C(2)-C(3)-C(4)	119.56(17)
C(3)-C(4)-C(5)	120.21(18)
C(4)-C(5)-C(6)	118.44(18)
N(1)-C(6)-C(5)	120.46(17)
N(2)-C(1)-C(2)-N(1)	1.4(3)

Table A.3. Bond lengths and angles of ditzpy.

Bond or angle	Experimental value (Å or ^{o})
N(1)-N(2)	1.345(4)
N(1)-N(8)	1.302(4)
N(2)-C(1)	1.336(5)
N(3)-C(2)	1.349(4)
N(3)-C(3)	1.342(5)
N(4)-N(7)	1.332(4)
N(4)-C(4)	1.339(5)
N(5)-N(6)	1.367(4)
N(5)-C(4)	1.323(5)
N(6)-N(7)	1.286(5)
N(8)-N(9)	1.358(5)
N(9)-C(1)	1.328(4)
C(1)-C(2)	1.455(5)
C(2)-C(5)	1.388(5)
C(3)-C(4)	1.467(4)
C(3)-C(7)	1.389(5)
C(5)-C(6)	1.381(6)
C(6)-C(7)	1.385(4)
N(2)-N(1)-N(8)	106.2(3)
N(1)-N(2)-C(1)	109.2(3)
C(2)-N(3)-C(3)	116.6(3)
N(7)-N(4)-C(4)	109.4(3)
N(6)-N(5)-C(4)	105.5(3)
N(5)-N(6)-N(7)	111.0(3)
N(4)-N(7)-N(6)	106.4(3)
N(1)-N(8)-N(9)	110.6(3)
N(8)-N(9)-C(1)	106.1(3)
N(2)-C(1)-N(9)	107.9(3)
N(2)-C(1)-C(2)	124.3(3)
N(9)-C(1)-C(2)	127.7(3)
N(3)-C(2)-C(1)	114.9(3)
N(3)-C(2)-C(5)	123.6(3)
C(1)-C(2)-C(5)	121.5(3)
N(3)-C(3)-C(4)	114.4(3)
N(3)-C(3)-C(7)	124.1(3)
C(4)-C(3)-C(7)	121.5(3)
N(4)-C(4)-N(5)	107.8(3)
N(4)-C(4)-C(3)	124.7(3)
N(5)-C(4)-C(3)	127.6(3)
C(2)-C(5)-C(6)	118.1(3)
C(5)-C(6)-C(7)	119.9(3)
C(3)-C(7)-C(6)	117.6(3)
N(2)-C(1)-C(2)-N(3)	-1.8(5)
N(3)-C(3)-C(4)-N(4)	-5.2(6)

Appendix B

Supplements to Chapter 3

B.1. ^{1}H NMR spectrum of thim

The spectroscopic characterization of thim can be found in the full paper Chapter 3 of this dissertation was based on. The ^{1}H NMR spectrum of this molecule is given in Figure B.1 for informative purposes.

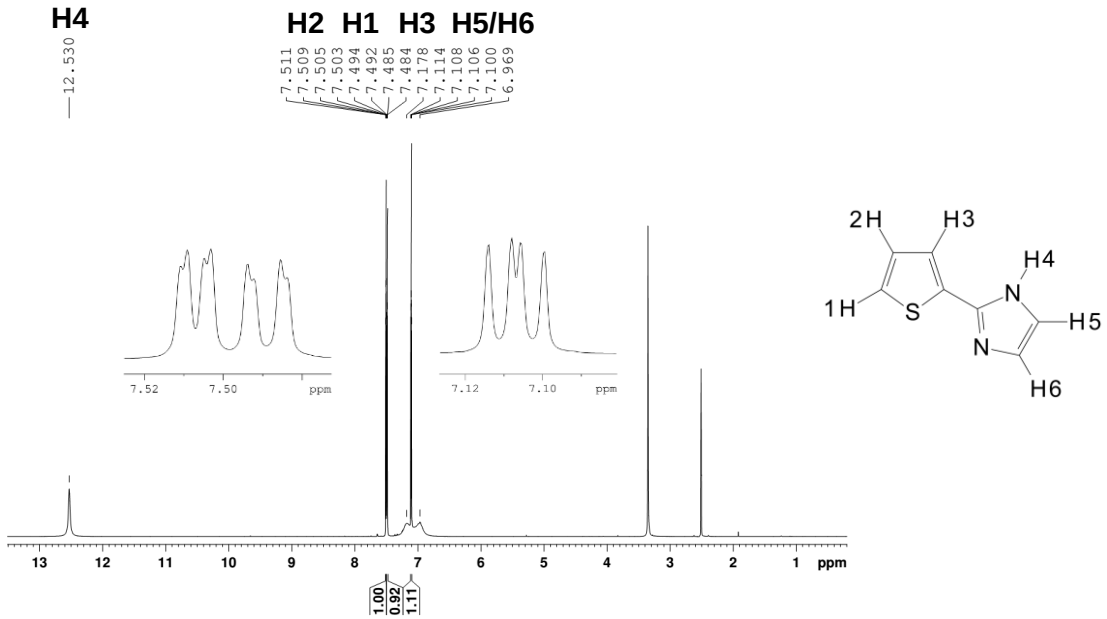

Figure B.1. ^{1}H NMR of thim in DMSO – d6.

The assignment of hydrogen atoms was based on coupling constants calculations (for the values, see Experimental Section of Chapter 3).

B.2. Crystal structure – bond lengths and angles

Table B.1. Bond lengths and angles of $[CuCl_2(thim)_2]$.

Bond or angle	Experimental value (Å or ^{o})
Cu(1)-Cl(1)	2.3036(6)
Cu(1)-N(10)	1.9487(16)
S(1)-C(5)	1.721(2)
S(1)-C(2)	1.704(3)
N(10)-C(10)	1.378(3)
N(10)-C(6)	1.331(3)
N(7)-C(8)	1.365(3)
N(7)-C(6)	1.347(3)
C(8)-C(9)	1.356(3)
C(5)-C(6)	1.448(3)
C(4)-C(5)	1.380(3)
C(2)-C(3)	1.348(3)
Cl(1)-Cu(1)-N(10)	88.95(5)
Cl(1)-Cu(1)-Cl(1)a	180
Cl(1)-Cu(1)-N(10)a	91.05(5)
N(10)-Cu(1)-N(10)a	180
C(2)-S(1)-C(5)	91.86(10)
Cu(1)-N(10)-C(9)	124.90(13)
Cu(1)-N(10)-C(6)	128.56(14)
C(9)-N(10)-C(6)	106.52(16)
C(8)-N(7)-C(6)	108.70(16)
N(10)-C(9)-C(8)	109.27(18)
N(7)-C(8)-C(9)	106.00(18)
N(10)-C(6)-N(7)	109.50(17)
N(10)-C(6)-C(5)	126.43(18)
N(7)-C(6)-C(5)	124.04(17)
S1-C5-C6-N10	-13.8(2)

B.3. FTIR spectra

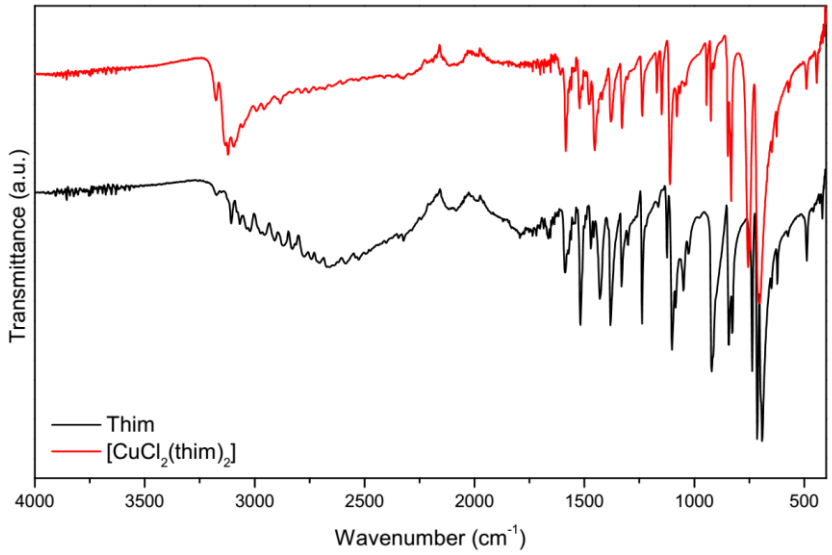

Figure B.2. Full experimental ATR infrared spectra of thim and $[CuCl_2(thim)_2]$.

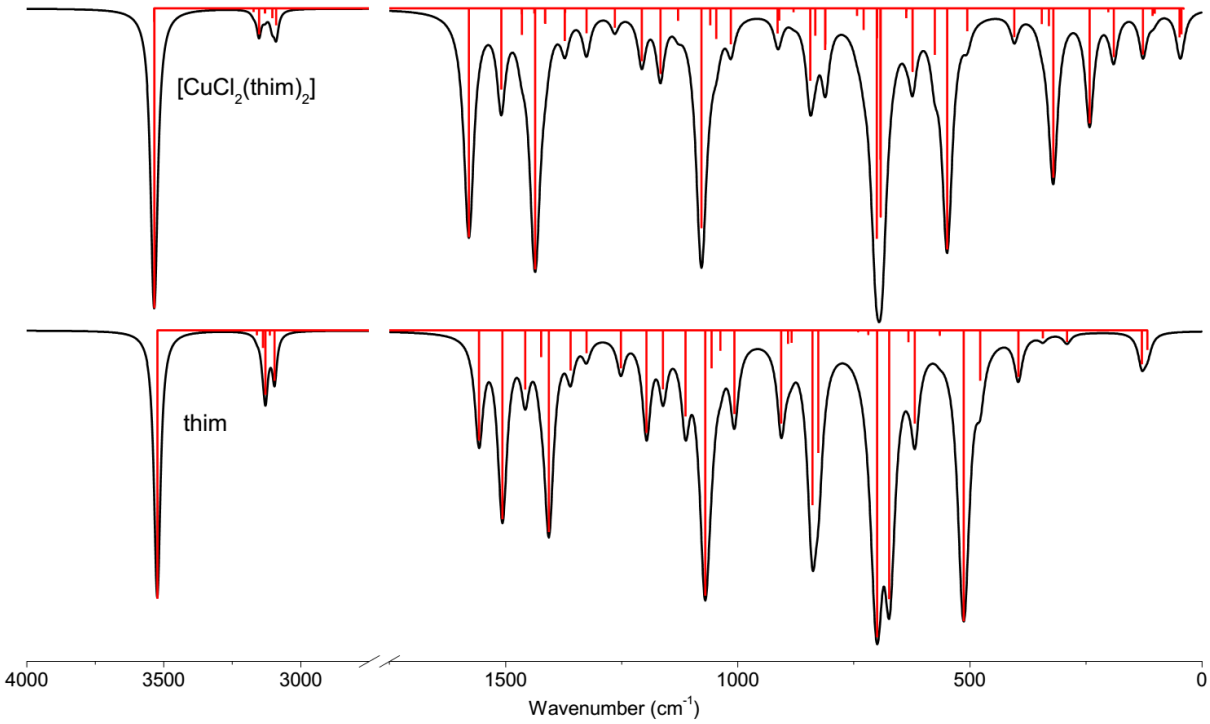

Figure B.3. Simulated infrared spectra based on DFT calculations with PBE0/def2-TZVP. Red lines indicate the position of the vibrational transitions.

Appendix C

Supplements to Chapter 4

C.1. ^{1}H NMR spectra

The full spectroscopic characterization of the impy and impm molecules had already been reported in a previous dissertation of our research group by M. Sc. Eduardo Guimarães Ratier de Arruda. The ^{1}H NMR spectra of these molecule are given in Figures C.1 and C.2 for informative purposes. Signal attribution was based on coupling constants (given in Experimental Section of **Chapter 4**).

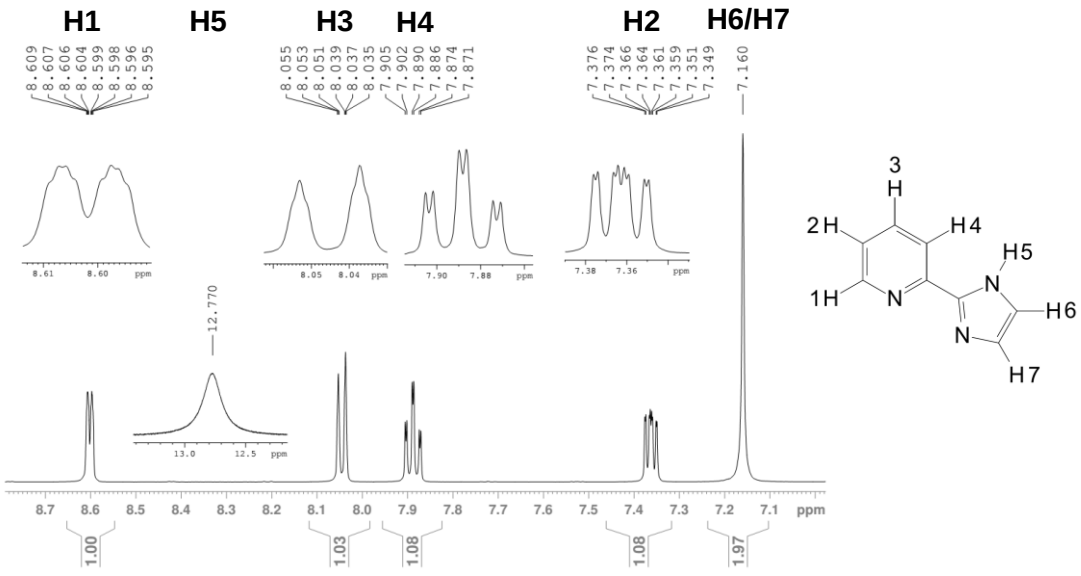

Figure C.1. ^{1}H NMR of impy in DMSO – d6.

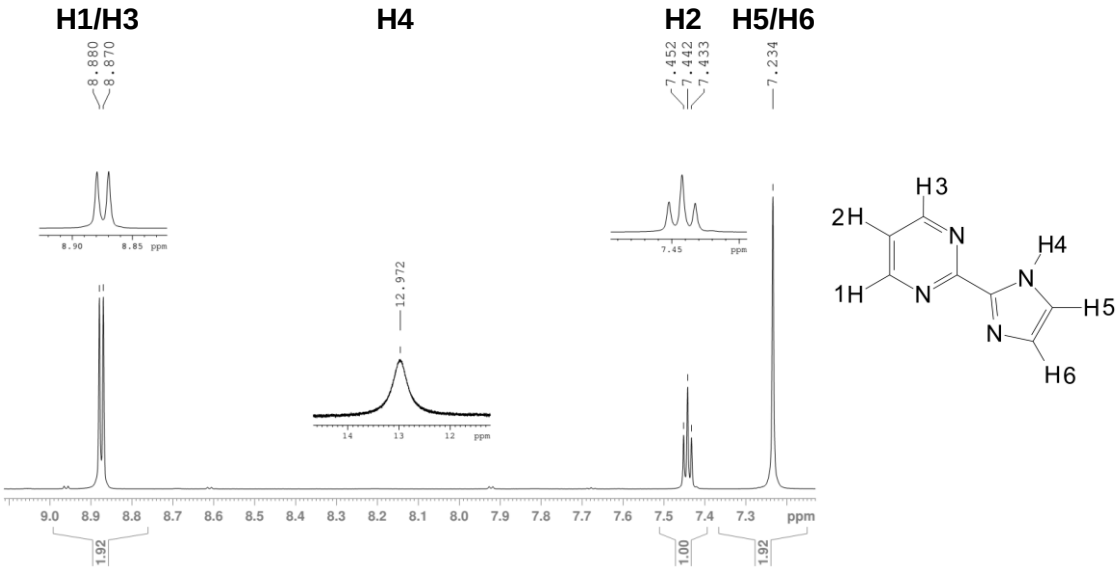

Figure C.2. ^{1}H NMR of impm in DMSO – d6.

C.2. Mass spectra of the copper(II) complexes

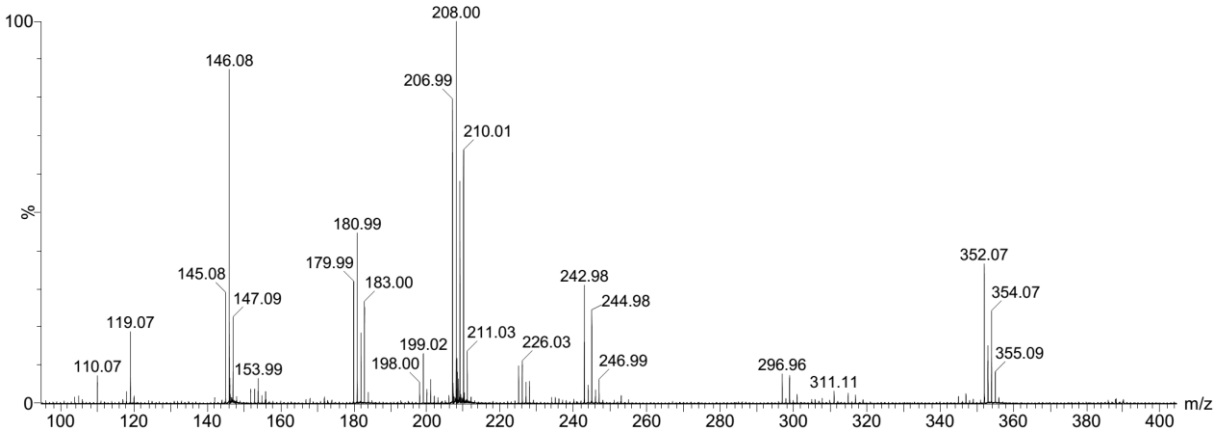

Figure C.3. Mass spectrum of [$CuCl_2$(impy)].

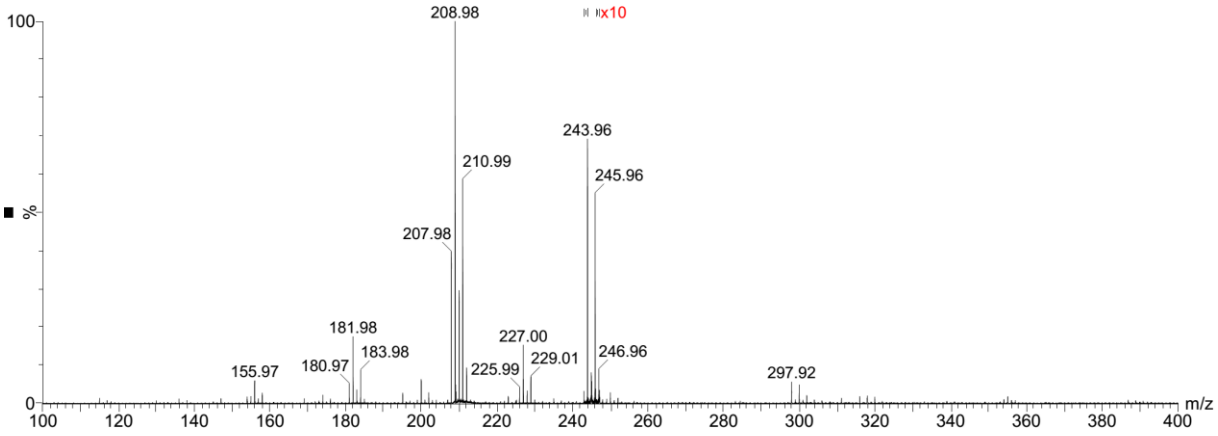

Figure C.4. Mass spectrum of [$CuCl_2$(impz)].

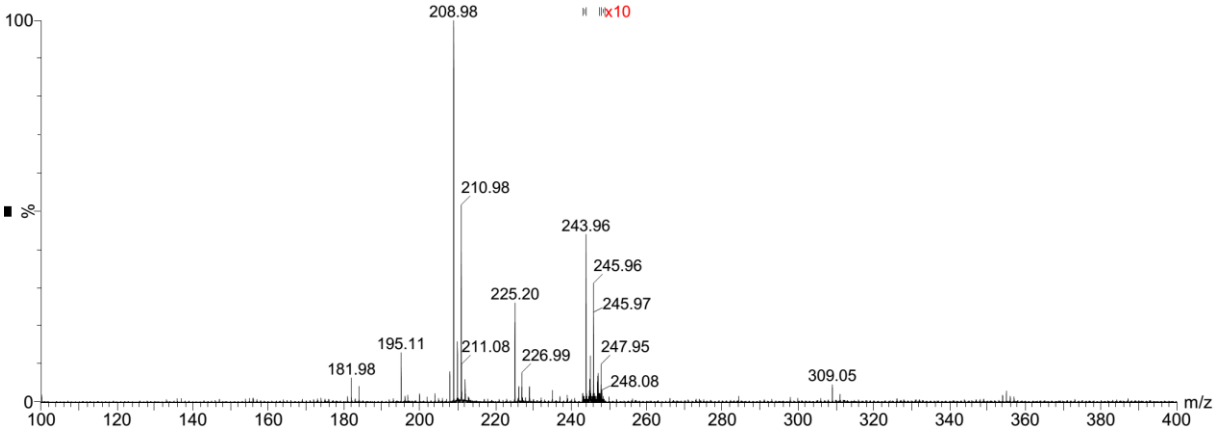

Figure C.5. Mass spectrum of [$CuCl_2$(impm)].

C.3. Powder diffractograms

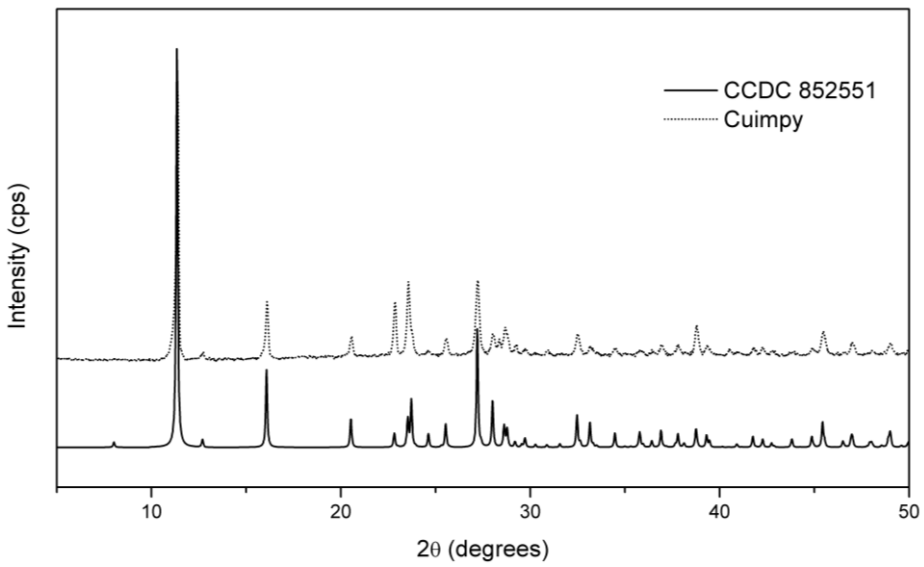

Figure C.6. X-ray powder diffractograms from the synthesized [$CuCl_2$(impy)] (dotted line) and the generated pattern from a reported CIF (full line).

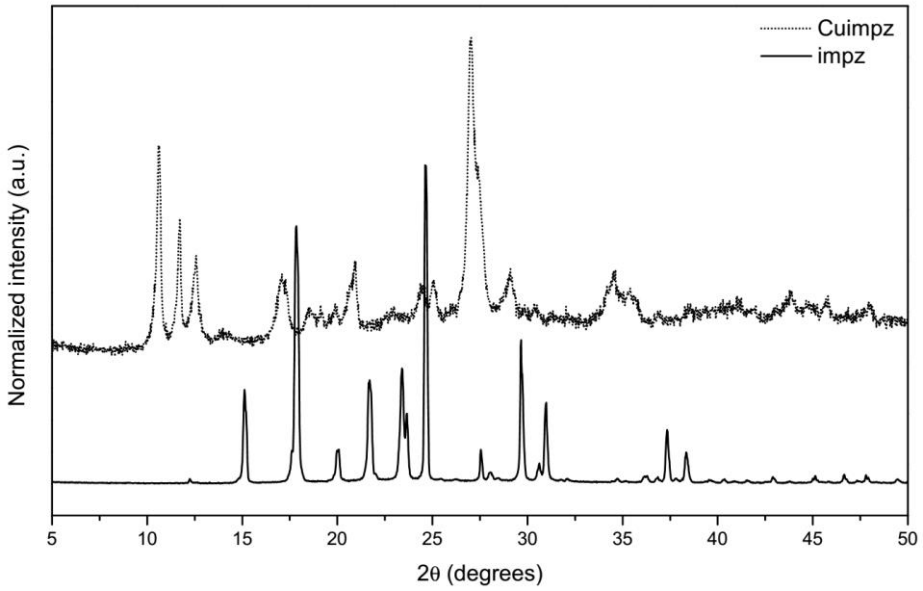

Figure C.7. X-ray powder diffractograms from the synthesized [$CuCl_2$(impz)] (dotted line) and of the free ligand impz (full line).

C.4. Molecular modeling

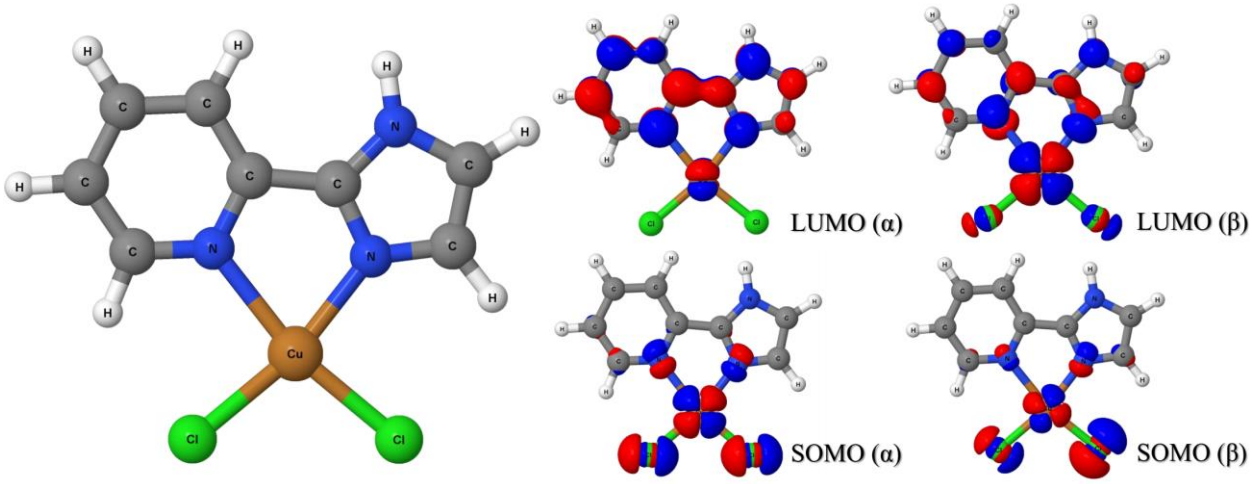

Figure C.8. Equilibrium geometry and frontier Kohn-Sham orbitals obtained for Cuimpy by DFT calculations with PBE0/def2-TZVP.

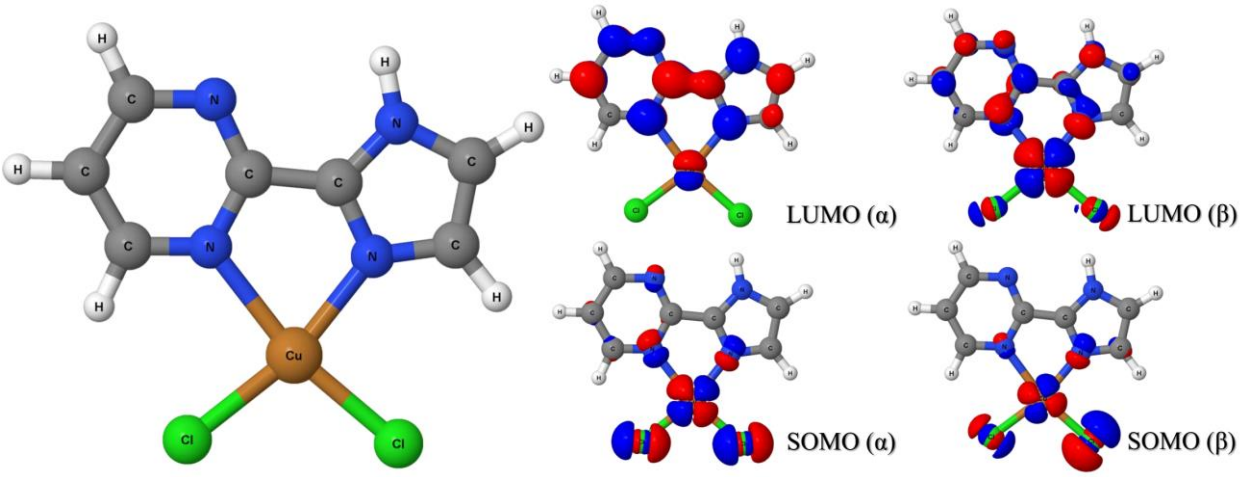

Figure C.9. Equilibrium geometry and frontier Kohn-Sham orbitals obtained for Cuimpm by DFT calculations with PBE0/def2-TZVP.

C.5. Infrared spectra

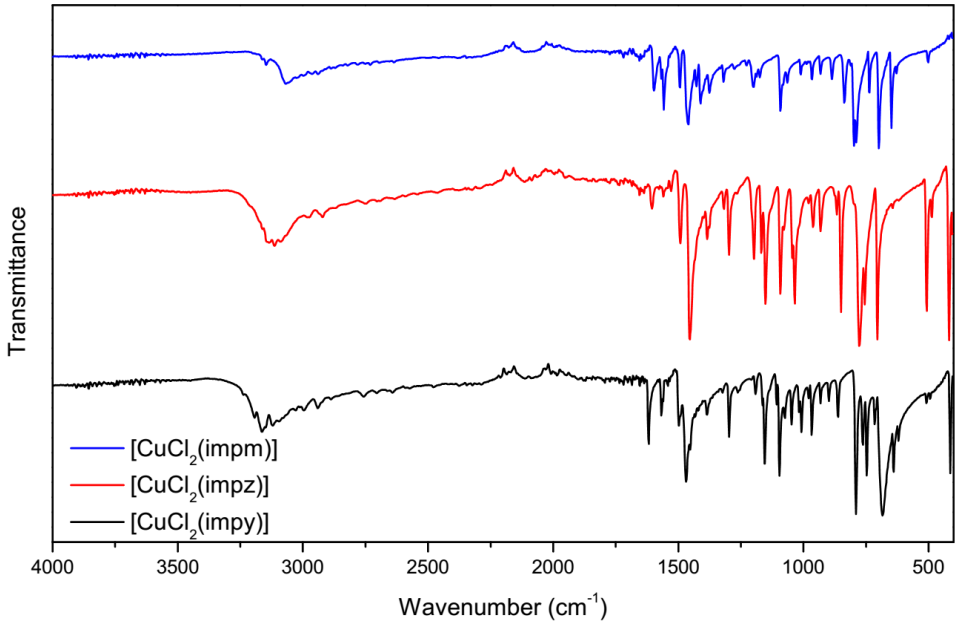

Figure C.10. Full ATR Infrared spectra of the copper(II) complexes.

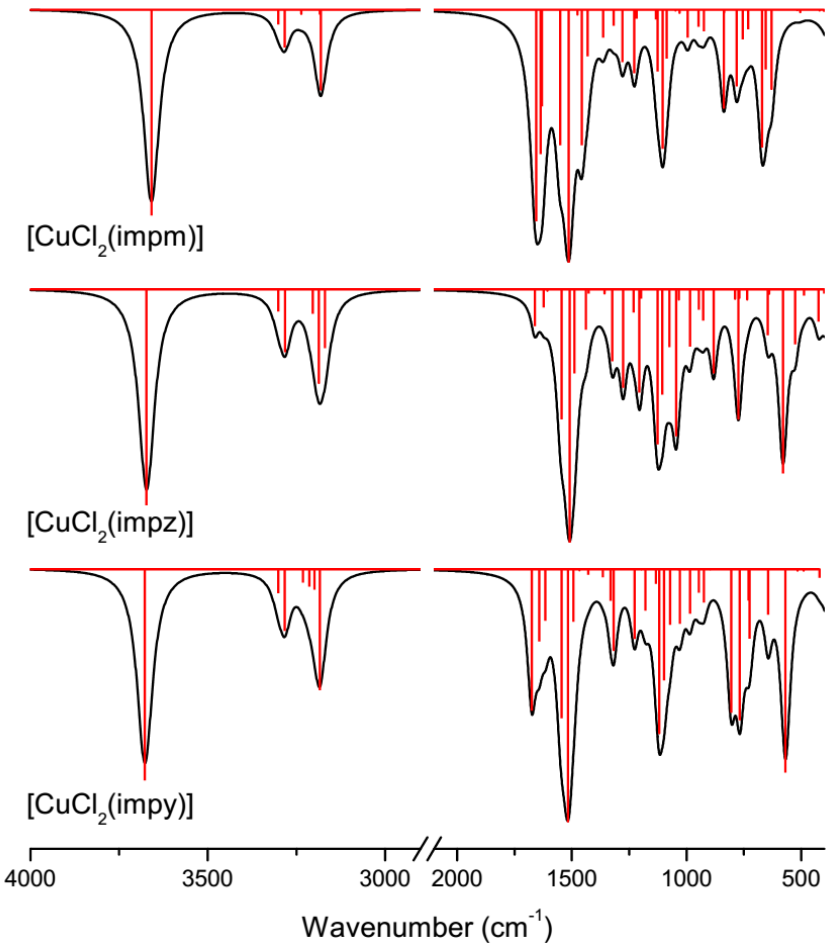

Figure C.11. Simulated infrared spectra of the copper(II) complexes based on DFT calculations with PBE0/def2-TZVP. Red lines indicate the position of the vibrational transitions.

Appendix D

Additional documents

De acordo com a Informação CCPG 001/2015 da Pró-Reitoria de Pós-Graduação da UNICAMP e a Norma para Encaminhamento de Dissertações e Teses da Pós-Graduação/IQ, faz-se necessária a seguinte declaração para a redação da Dissertação em formato alternativo ao já estabelecido:

DECLARAÇÃO

As cópias dos documentos de minha autoria ou de minha coautoria, já publicados ou submetidos para publicação em revistas científicas ou anais de congressos sujeitos a arbitragem, que constam da minha Dissertação de Mestrado intitulada “SYNTHESIS, CHARACTERIZATION AND BIOACTIVITY OF COPPER(II) COMPLEXES WITH N-HETEROCYCLES/ SÍNTESE, CARACTERIZAÇÃO E BIOATIVIDADE DE COMPLEXOS DE COBRE(II) COM N-HETEROCICLOS” não infringem os dispositivos da Lei n^{o} 9.610/98, nem o direito autoral de qualquer editora.

Campinas, 26 de Fevereiro de 2016.

Autor: Douglas Hideki Nakahata, R.G. n^{o} 7.853.732-9

Orientador: Prof. Dr. André Luiz Barboza Formiga, R.G. n^{o} 11455693-9

D.1. License to reproduce the content of Chapter 3

ELSEVIER LICENSE
TERMS AND CONDITIONS

Jan 13, 2016

This is a License Agreement between Douglas Nakahata ("You") and Elsevier ("Elsevier") provided by Copyright Clearance Center ("CCC"). The license consists of your order details, the terms and conditions provided by Elsevier, and the payment terms and conditions.

All payments must be made in full to CCC. For payment instructions, please see information listed at the bottom of this form.

Supplier	Elsevier Limited The Boulevard,Langford Lane Kidlington,Oxford,OX5 1GB,UK
Registered Company Number	1982084
Customer name	Douglas Nakahata
Customer address	Dr. Shigeo Mori street Campinas, 13083-770
License number	3786600073686
License date	Jan 11, 2016
Licensed content publisher	Elsevier
Licensed content publication	Inorganica Chimica Acta
Licensed content title	Copper(II), palladium(II) and platinum(II) complexes with 2,2-thiophen-yl-imidazole: synthesis, spectroscopic characterization, X-ray crystallographic studies and interactions with calf-thymus DNA
Licensed content author	Nina T. Zanvettor,Douglas H. Nakahata,Raphael E.F. de Paiva,Marcos A. Ribeiro,Alexandre Cuin,Pedro P. Corbi,André L.B. Formiga
Licensed content date	Available online 11 January 2016
Licensed content volume number	n/a
Licensed content issue number	n/a
Number of pages	1
Start Page	None
End Page	None
Type of Use	reuse in a thesis/dissertation
Portion	full article
Format	both print and electronic
Are you the author of this Elsevier article?	Yes
Will you be translating?	No
Title of your thesis/dissertation	SYNTHESIS, CHARACTERIZATION AND BIOACTIVITY OF COPPER(II) COMPLEXES WITH N-HETEROCYCLES

Expected completion date	Feb 2016
Estimated size (number of pages)	
Elsevier VAT number	GB 494 6272 12
Permissions price	0.00 USD
VAT/Local Sales Tax	0.00 USD / 0.00 GBP
Total	0.00 USD

Terms and Conditions

INTRODUCTION

1. The publisher for this copyrighted material is Elsevier. By clicking "accept" in connection with completing this licensing transaction, you agree that the following terms and conditions apply to this transaction (along with the Billing and Payment terms and conditions established by Copyright Clearance Center, Inc. ("CCC"), at the time that you opened your Rightslink account and that are available at any time at http://myaccount.copyright.com).

GENERAL TERMS

2. Elsevier hereby grants you permission to reproduce the aforementioned material subject to the terms and conditions indicated.
3. Acknowledgement: If any part of the material to be used (for example, figures) has appeared in our publication with credit or acknowledgement to another source, permission must also be sought from that source. If such permission is not obtained then that material may not be included in your publication/copies. Suitable acknowledgement to the source must be made, either as a footnote or in a reference list at the end of your publication, as follows:
"Reprinted from Publication title, Vol /edition number, Author(s), Title of article / title of chapter, Pages No., Copyright (Year), with permission from Elsevier [OR APPLICABLE SOCIETY COPYRIGHT OWNER]." Also Lancet special credit - "Reprinted from The Lancet, Vol. number, Author(s), Title of article, Pages No., Copyright (Year), with permission from Elsevier."
4. Reproduction of this material is confined to the purpose and/or media for which permission is hereby given.
5. Altering/Modifying Material: Not Permitted. However figures and illustrations may be altered/adapted minimally to serve your work. Any other abbreviations, additions, deletions and/or any other alterations shall be made only with prior written authorization of Elsevier Ltd. (Please contact Elsevier at permissions@elsevier.com)
6. If the permission fee for the requested use of our material is waived in this instance, please be advised that your future requests for Elsevier materials may attract a fee.
7. Reservation of Rights: Publisher reserves all rights not specifically granted in the combination of (i) the license details provided by you and accepted in the course of this licensing transaction, (ii) these terms and conditions and (iii) CCC's Billing and Payment terms and conditions.
8. License Contingent Upon Payment: While you may exercise the rights licensed immediately upon issuance of the license at the end of the licensing process for the transaction, provided that you have disclosed complete and accurate details of your proposed use, no license is finally effective unless and until full payment is received from you (either by publisher or by CCC) as provided in CCC's Billing and Payment terms and conditions. If full payment is not received on a timely basis, then any license preliminarily granted shall be deemed automatically revoked and shall be void as if never granted. Further, in the event

that you breach any of these terms and conditions or any of CCC's Billing and Payment terms and conditions, the license is automatically revoked and shall be void as if never granted. Use of materials as described in a revoked license, as well as any use of the materials beyond the scope of an unrevoked license, may constitute copyright infringement and publisher reserves the right to take any and all action to protect its copyright in the materials.

9. Warranties: Publisher makes no representations or warranties with respect to the licensed material.

10. Indemnity: You hereby indemnify and agree to hold harmless publisher and CCC, and their respective officers, directors, employees and agents, from and against any and all claims arising out of your use of the licensed material other than as specifically authorized pursuant to this license.

11. No Transfer of License: This license is personal to you and may not be sublicensed, assigned, or transferred by you to any other person without publisher's written permission.

12. No Amendment Except in Writing: This license may not be amended except in a writing signed by both parties (or, in the case of publisher, by CCC on publisher's behalf).

13. Objection to Contrary Terms: Publisher hereby objects to any terms contained in any purchase order, acknowledgment, check endorsement or other writing prepared by you, which terms are inconsistent with these terms and conditions or CCC's Billing and Payment terms and conditions. These terms and conditions, together with CCC's Billing and Payment terms and conditions (which are incorporated herein), comprise the entire agreement between you and publisher (and CCC) concerning this licensing transaction. In the event of any conflict between your obligations established by these terms and conditions and those established by CCC's Billing and Payment terms and conditions, these terms and conditions shall control.

14. Revocation: Elsevier or Copyright Clearance Center may deny the permissions described in this License at their sole discretion, for any reason or no reason, with a full refund payable to you. Notice of such denial will be made using the contact information provided by you. Failure to receive such notice will not alter or invalidate the denial. In no event will Elsevier or Copyright Clearance Center be responsible or liable for any costs, expenses or damage incurred by you as a result of a denial of your permission request, other than a refund of the amount(s) paid by you to Elsevier and/or Copyright Clearance Center for denied permissions.

LIMITED LICENSE

The following terms and conditions apply only to specific license types:

15. **Translation**: This permission is granted for non-exclusive world **English** rights only unless your license was granted for translation rights. If you licensed translation rights you may only translate this content into the languages you requested. A professional translator must perform all translations and reproduce the content word for word preserving the integrity of the article.

16. **Posting licensed content on any Website**: The following terms and conditions apply as follows: Licensing material from an Elsevier journal: All content posted to the web site must maintain the copyright information line on the bottom of each image; A hyper-text must be included to the Homepage of the journal from which you are licensing at http://www.sciencedirect.com/science/journal/xxxxx or the Elsevier homepage for books at http://www.elsevier.com; Central Storage: This license does not include permission for a scanned version of the material to be stored in a central repository such as that provided by Heron/XanEdu.

Licensing material from an Elsevier book: A hyper-text link must be included to the Elsevier homepage at http://www.elsevier.com . All content posted to the web site must maintain the

copyright information line on the bottom of each image.

Posting licensed content on Electronic reserve: In addition to the above the following clauses are applicable: The web site must be password-protected and made available only to bona fide students registered on a relevant course. This permission is granted for 1 year only. You may obtain a new license for future website posting.

17. **For journal authors:** the following clauses are applicable in addition to the above:

Preprints:

A preprint is an author's own write-up of research results and analysis, it has not been peer-reviewed, nor has it had any other value added to it by a publisher (such as formatting, copyright, technical enhancement etc.).

Authors can share their preprints anywhere at any time. Preprints should not be added to or enhanced in any way in order to appear more like, or to substitute for, the final versions of articles however authors can update their preprints on arXiv or RePEc with their Accepted Author Manuscript (see below).

If accepted for publication, we encourage authors to link from the preprint to their formal publication via its DOI. Millions of researchers have access to the formal publications on ScienceDirect, and so links will help users to find, access, cite and use the best available version. Please note that Cell Press, The Lancet and some society-owned have different preprint policies. Information on these policies is available on the journal homepage.

Accepted Author Manuscripts: An accepted author manuscript is the manuscript of an article that has been accepted for publication and which typically includes author-incorporated changes suggested during submission, peer review and editor-author communications.

Authors can share their accepted author manuscript:

- immediately
  - via their non-commercial person homepage or blog
  - by updating a preprint in arXiv or RePEc with the accepted manuscript
  - via their research institute or institutional repository for internal institutional uses or as part of an invitation-only research collaboration work-group
  - directly by providing copies to their students or to research collaborators for their personal use
  - for private scholarly sharing as part of an invitation-only work group on commercial sites with which Elsevier has an agreement
- after the embargo period
  - via non-commercial hosting platforms such as their institutional repository
  - via commercial sites with which Elsevier has an agreement

In all cases accepted manuscripts should:

- link to the formal publication via its DOI
- bear a CC-BY-NC-ND license - this is easy to do
- if aggregated with other manuscripts, for example in a repository or other site, be shared in alignment with our hosting policy not be added to or enhanced in any way to appear more like, or to substitute for, the published journal article.

Published journal article (JPA): A published journal article (PJA) is the definitive final record of published research that appears or will appear in the journal and embodies all value-adding publishing activities including peer review co-ordination, copy-editing,

formatting, (if relevant) pagination and online enrichment.
Policies for sharing publishing journal articles differ for subscription and gold open access articles:
Subscription Articles: If you are an author, please share a link to your article rather than the full-text. Millions of researchers have access to the formal publications on ScienceDirect, and so links will help your users to find, access, cite, and use the best available version.
Theses and dissertations which contain embedded PJAs as part of the formal submission can be posted publicly by the awarding institution with DOI links back to the formal publications on ScienceDirect.
If you are affiliated with a library that subscribes to ScienceDirect you have additional private sharing rights for others' research accessed under that agreement. This includes use for classroom teaching and internal training at the institution (including use in course packs and courseware programs), and inclusion of the article for grant funding purposes.
Gold Open Access Articles: May be shared according to the author-selected end-user license and should contain a CrossMark logo, the end user license, and a DOI link to the formal publication on ScienceDirect.
Please refer to Elsevier's posting policy for further information.
18. **For book authors** the following clauses are applicable in addition to the above:
Authors are permitted to place a brief summary of their work online only. You are not allowed to download and post the published electronic version of your chapter, nor may you scan the printed edition to create an electronic version. **Posting to a repository:** Authors are permitted to post a summary of their chapter only in their institution's repository.
19. **Thesis/Dissertation**: If your license is for use in a thesis/dissertation your thesis may be submitted to your institution in either print or electronic form. Should your thesis be published commercially, please reapply for permission. These requirements include permission for the Library and Archives of Canada to supply single copies, on demand, of the complete thesis and include permission for Proquest/UMI to supply single copies, on demand, of the complete thesis. Should your thesis be published commercially, please reapply for permission. Theses and dissertations which contain embedded PJAs as part of the formal submission can be posted publicly by the awarding institution with DOI links back to the formal publications on ScienceDirect.

Elsevier Open Access Terms and Conditions
You can publish open access with Elsevier in hundreds of open access journals or in nearly 2000 established subscription journals that support open access publishing. Permitted third party re-use of these open access articles is defined by the author's choice of Creative Commons user license. See our open access license policy for more information.
Terms & Conditions applicable to all Open Access articles published with Elsevier:
Any reuse of the article must not represent the author as endorsing the adaptation of the article nor should the article be modified in such a way as to damage the author's honour or reputation. If any changes have been made, such changes must be clearly indicated.
The author(s) must be appropriately credited and we ask that you include the end user license and a DOI link to the formal publication on ScienceDirect.
If any part of the material to be used (for example, figures) has appeared in our publication with credit or acknowledgement to another source it is the responsibility of the user to ensure their reuse complies with the terms and conditions determined by the rights holder.
Additional Terms & Conditions applicable to each Creative Commons user license:
CC BY: The CC-BY license allows users to copy, to create extracts, abstracts and new works from the Article, to alter and revise the Article and to make commercial use of the Article (including reuse and/or resale of the Article by commercial entities), provided the

user gives appropriate credit (with a link to the formal publication through the relevant DOI), provides a link to the license, indicates if changes were made and the licensor is not represented as endorsing the use made of the work. The full details of the license are available at http://creativecommons.org/licenses/by/4.0.

CC BY NC SA: The CC BY-NC-SA license allows users to copy, to create extracts, abstracts and new works from the Article, to alter and revise the Article, provided this is not done for commercial purposes, and that the user gives appropriate credit (with a link to the formal publication through the relevant DOI), provides a link to the license, indicates if changes were made and the licensor is not represented as endorsing the use made of the work. Further, any new works must be made available on the same conditions. The full details of the license are available at http://creativecommons.org/licenses/by-nc-sa/4.0.

CC BY NC ND: The CC BY-NC-ND license allows users to copy and distribute the Article, provided this is not done for commercial purposes and further does not permit distribution of the Article if it is changed or edited in any way, and provided the user gives appropriate credit (with a link to the formal publication through the relevant DOI), provides a link to the license, and that the licensor is not represented as endorsing the use made of the work. The full details of the license are available at http://creativecommons.org/licenses/by-nc-nd/4.0.

Any commercial reuse of Open Access articles published with a CC BY NC SA or CC BY NC ND license requires permission from Elsevier and will be subject to a fee.

Commercial reuse includes:

- Associating advertising with the full text of the Article
- Charging fees for document delivery or access
- Article aggregation
- Systematic distribution via e-mail lists or share buttons

Posting or linking by commercial companies for use by customers of those companies.

20. **Other Conditions**:

v1.8

Questions? customercare@copyright.com or +1-855-239-3415 (toll free in the US) or +1-978-646-2777.